E7.5-1 A large farm field is in the shape of a parallelogram. Two adjacent sides are defined by the vectors:

$$\vec{A} = (3000 \text{ ft})\vec{E} + (4000 \text{ ft})\vec{N} \quad \text{and} \quad \vec{B} = (10{,}000 \text{ ft})\vec{E}$$

where the directions are $\vec{E}$ = east and $\vec{N}$ = north. Use the vector cross product to determine how many acres of land are contained in the field. Note that 1 acre = 44,000 ft^2.

E7.7-1 **a.** A coaxial transmission line consists of an inner conductor of radius a and an outer conductor of radius b. Between these conductors is a dielectric having a relative dielectric constant of ε_R. Derive an expression for the capacitance per unit length of this line.

b. A certain model of this transmission line has an inner conductor diameter of 1 cm and an outer conductor inside diameter of 3.35 cm, with a relative dielectric constant between the conductors of 2.1. What is the capacitance per unit length of this transmission line?

E7.7-2 The energy stored in an electric field is given by

$$U_E = \frac{\varepsilon_0 \varepsilon_R}{2} \int\int_V |E|^2 \, dV$$

and for a capacitor it is also given by

$$U_E = \tfrac{1}{2} C V^2$$

Show that both of these expressions give the same result for U_E for a unit length of coaxial line L, where C is the capacitance/unit length examined in E7.7-1.

E7.8-1 A static electric potential function exists in a region described by a (x, y, z) coordinate system. The function is

$$\Phi = 3x^3 + 5(y^2 - y) + 17z + 6 \text{ volts}$$

Calculate the amount of energy required to move an electron from the origin to the point $(4, 5, 2)$.

E7.8-2 What is the gradient of the potential function

$$\Phi = 3x^3 + 5(y^2 - y) + 17z + 6 \text{ volts}$$

at the point $(4, 5, 2)$?

E7.10-1 Two straight parallel conductors are a distance D apart and carry currents +I and −I, respectively, "into and out of the paper." Find an expression for and graph the magnitude of the total H field in the plane of the paper as a function of position between and outside of the linear interval containing the conductors.

E7.11-1 Find the curl of the vector field

$$\vec{A} = (y^2z)\vec{x} + (x^3y)\vec{y} + (z^2xy)\vec{z}$$

E7.12-1 The circular path shown encloses a uniform magnetic field into the page. The radius of the path is $r = 0.2$ m and the magnetic flux density is given by $\vec{B} = 20(1 - e^{-t})$ teslas, where t is in seconds. (a) Calculate V and I at t = 1 s. (b) Graph B and V for $0 < t < 4$ s.

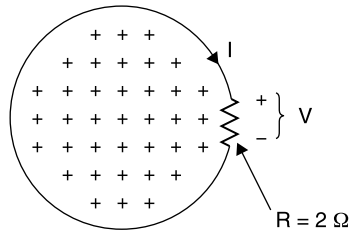

E7.14-1 From Ampere's law, the H field surrounding a wire carrying a DC current I is given by (7.10-2). Find the curl of H as a function of r for $r > a$, the radial distance from the center of the conductor. Assume the conductor is a straight vertically oriented cylinder of radius a.

E7.14-2 Solve for the curl of H inside the conductor of E7.14-1 as a function of r for $0 < r \leq a$.

E7.15-1 Find the Laplacian for a potential function that has cylindrical symmetry and is proportional to ln r, by first evaluating the gradient and then taking its divergence. Interpret the result and describe what geometry could produce this potential.

E7.16-1 It is said that Maxwell's four equations can be reduced to two, since the first two can be derived from the last two. Show that this is so. *Hint:* Start by taking the divergence of the last two equations.

E7.16-2 Using rectangular coordinates show that the defining equation for the vector Laplacian is, in fact, an identity. This identity is key to numerous field derivations, including the proof that plane waves can propagate in free space:

$$\nabla^2\vec{A} = \nabla(\nabla \cdot \vec{A}) - \nabla \times \nabla \times \vec{A} \quad \text{where } \vec{A} = A_x\vec{x} + A_y\vec{y} + A_z\vec{z}$$

E7.17-1 The graphite form of carbon has about the lowest conductivity of the materials used as conductors, with $\sigma \approx 7 \times 10^4$ $\mho$/m. Applying the criterion of (7.17-9), up to what frequency would graphite be considered a "good conductor."

E7.18-1 Create a table showing skin depth in decade frequency increments from 1 to 100,000 MHz for copper, aluminum, brass, and stainless steel (0.1 C, 18 Cr, 8 Ni, balance Fe). Use as respective resistivity values 1.72, 2.62, 3.9, and 90×10^{-6} Ω-cm. Then graph your results on log-log paper. Note that all of these metals are nonmagnetic.

E7.19-1 The manufacturer of a measuring system requires a precise time delay for 0.5-μs-long pulses and uses a temperature controlled, 150-m long air dielectric copper coaxial line of 50 Ω impedance as the delay path for the pulses. Small dielectric beads support the center conductor at various intervals, but the effective relative dielectric constant is approximately unity. The inner conductor diameter is 0.43 cm and the outer conductor has an inside diameter of 1 cm (same as the example in Section 7.19). The pulse generator and load are matched to the coaxial line at both respective ends.

The manufacturer has hired you as a consultant to advise on the electrical effects, if any, of replacing the copper coaxial cable with one made of aluminum because it is less expensive. In this replacement it is proposed that the dielectric and cross-sectional dimensions as well as the length of the line would be unchanged.

a. Estimate the ohmic insertion loss of the copper and aluminum cables at 1 GHz.

b. Estimate the electrical length of each cable relative to a path having the same dielectric constant and physical length at 1 GHz.

c. What assumptions and approximations did you make in arriving at your recommendations?

E7.23-1 Suppose that we radiate a sinusoidal signal into free space having fairly constant $\vec{\mathrm{E}}$ and $\vec{\mathrm{H}}$ fields over a 1 m^2 area with a power density of 1 $\mathrm{W/m}^2$ at some distance from the antenna. What is the $\vec{\mathrm{E}}$ field strength of this wave? *Hint:* Assume we can use an analogy with circuit theory by which $P = V_A^2/Z_0$.

E7.23-2 A sinusoidally varying E_θ *and* H_φ set of fields (using spherical coordinates) is radiated uniformly in all directions (isotropically). Show what the expressions for E_θ *and* H_φ must be as functions of time t and distance r from the transmitter. Assume that the transmitter is an ideal point source of radiation and that the ratio of E_θ *and* H_φ fields is the same as that for plane wave propagation.

E7.24-1 Show that a vertically polarized field can be represented as the sum of judiciously chosen RHCP and LHCP fields.

E7.24-2 Find the equations of a LHCP field and a RHCP field that combine to produce a linearly polarized field oriented at an angle α from the x axis (the vertical direction).

E7.24-3 For the left-hand polarized wave described in Figure 7.24-5:

a. Verify that E is in the negative y direction at $z = 3\lambda/4$ when $t = 0$.

b. What is the direction of E at $z = 3\lambda/4$ when t = T/4?

c. Sketch the wave in the xy plane for $z = 3\lambda/4$ and t increasing from 0 to T/4.

E7.25-1 Solve for the characteristic impedance of coaxial line, deriving the result in (7.25-15) using (7.25-7) for the distributed C of the line and deriving the distributed L of the line based on the stored magnetic energy of the line related to L by $U_M = \frac{1}{2}LI_0^2 = \frac{1}{2}\mu \int_V H^2\, dV$ where I_0 is the peak line current and H is the magnetic field.

E7.25-2 Use Poynting's vector to calculate the average power flow along a coaxial transmission line having the form shown in Figure 7.25-2. Assume sinusoidal excitation and use the phasor forms of $\vec{E}$ and $\vec{H}$.

E7.25-3 Verify that the ratio of E_r to H_φ for the TEM mode in coaxial line is $\eta = \sqrt{\mu/\varepsilon}$. (Use the phasor form of Maxwell's third equation (Faraday's law). Note that for the TEM mode, $k = \omega\sqrt{\mu\varepsilon}$.

E7.25-4 Prove that the propagation constant for a sinusoidal wave on a coaxial transmission line is $k = \omega\sqrt{\mu\varepsilon}$. *Hint:* Begin with the wave equation (7.21-1), assume that k has the value sought and verify that the equation produces an identity.

E7.26-1 Find the approximate characteristic impedance of the parallel-plate transmission line shown in Figure 7.26-1*a*, assuming that the line is lossless and that $w \gg d$ (hence, all fields are uniform and confined to the space between the plates).

E7.26-2 Use Poynting's theorem to derive an expression for the average power flow in an air-filled rectangular waveguide operating in the TE_{10} mode.

E7.26-3 An air-filled rectangular waveguide is operated in the TE_{10} mode. Its dimensions are $a = 2.25$ cm and $b = 1$ cm.

a. Calculate the cutoff frequency of the TE_{10} mode.

b. Which mode has the next lowest cutoff frequency?

c. Repeat part (a) for a dielectric filled rectangular waveguide filled with a nonmagnetic dielectric having $\varepsilon_r = 2.0$.

E7.26-4 In general, the propagation constant for waveguide is $\gamma = \alpha + j\beta$. If γ is real, then $\gamma = \alpha =$ an attenuation constant (in nepers/unit length). The dimensions of an air-filled rectangular waveguide are

$a = 4.0$ cm and $b = 2.0$ cm. Calculate the attenuation constant in decibels/centimeter at 2.5 GHz, assuming TE_{10} mode operation.

E7.26-5 For most transmission line circuits, the usable bandwidth is related to the frequency sensitivity of the line's electrical length, $\theta = 2\pi l/\lambda$ for TEM lines, and $\theta = 2\pi l/\lambda_g$ for waveguides. The average time required for a group of frequencies to transverse a network is called the *group delay* and is equal to $d\theta/d\omega$. To avoid distortion of signals comprising a band of frequencies, all frequencies should traverse the network in the same time (i.e., the same delay for all frequencies, or $d\theta/d\omega = a\ constant$, independent of f).

- **a.** Derive expressions for $d\theta/d\omega$ in both the TEM and TE_{10} cases.
- **b.** Calculate $d\theta/d\omega$ at 7.5 GHz and at 12.0 GHz for air-filled coaxial line.
- **c.** Repeat (b) for air-filled rectangular waveguide with $a = 2.25$ cm and $b = 1.0$ cm, assuming operation in the TE_{10} mode.
- **d.** Compare the results of parts (b) and (c) at the two frequencies.

E7.27-1 A slender cylindrical 20-Ω resistor is mounted across a very narrow height, air-filled, rectangular waveguide on its centerline. The waveguide width is $a = 5$ cm and its height is $b = 0.5$ cm.

- **a.** Calculate the insertion loss caused by the resistor at 4 GHz when the generator and load are matched to the impedance Z_g of the waveguide.
- **b.** Calculate the insertion loss when the centerline of the resistor is 0.5 cm from the narrow wall of the waveguide.

E7.27-2 Use transmission line theory (Chapter 4) to verify (7.27-20).

E7.28-1 A manufacturer has designed an intrusion alarm circuit to operate at 10.525 GHz. The network is realized as an integrated circuit chip that measures only 0.25×0.25 in. The manufacturer wishes to install it in a standard metal "can" measuring $0.625 \times 0.625 \times 0.125$ in. (internal dimensions). The circuit contains transistors having gain up to 18 GHz. Is higher order moding in the circuit enclosure possible?

E7.29-1 A steady DC current exists in a short, straight, thin conductor located at the origin of the right-hand coordinate system (x, y, z). The conductor is in the z direction. Ignore the fact that this short DC current with no return path cannot exist in practice.

- **a.** Sketch the geometry, identifying the rectangular and spherical coordinates.
- **b.** Find the vector potential $\vec{A}$ resulting from this current and express it in spherical coordinates (r, θ, φ).
- **c.** Find the $\vec{H}$ field components and express them in spherical coordinates.

E7.32-1 In the development of (7.32-16) only the terms varying as (1/r) in E_θ and H_φ were used to form Poynting's vector. However, there were other terms in both E_θ and H_φ. Show that including them would not change the result.

E7.32-2 Three short wire antennas of height h are spaced a quarter wavelength apart on the z axis and oriented in the +z direction. The center antenna's midpoint is at $z = 0$. The sinusoidal excitation current in the center antenna is twice as large as the current in each of the other two antennas (currents are 1:2:1).

- **a.** Sketch the antenna array. Then derive an expression for $|E_\theta|$ in the far field for the three-element array. Assume the radii from each antenna element to the far-field point are approximately parallel and hence that the angles (θ) of these radii measured from the z axis are approximately equal to each other. However, do take into account the phase differences due to the differences in path length from the elements to the far-field point (this is necessary to describe the antenna pattern).
- **b.** With power density P proportional to $|E_\theta|^2$, calculate P/P_M at $\theta = 0, \pi/6, \pi/4, \pi/3$, and $\pi/2$ where θ is the cylindrical coordinate angle and P_M is the relative power at $\theta = \pi/2$ (on the horizon). Express your answers both numerically and in decibels.
- **c.** Estimate from your calculations the 3-dB beam width of this array antenna.

E7.33-1 A 10-GHz point-to-point digital communication link is to be established between downtown Boston and the suburb of Lexington. The Boston antenna will be on the top of a 60-story building and the Lexington antenna will be about 100 ft high, resulting in a "line-of-sight path" of 25 miles. Dish antennas 2 ft in diameter will be employed at both sites. A system power margin of 40 dB is judged necessary to accommodate added path loss due to rain and snow and to provide a low bit error rate (BER). How much power must be radiated if the minimum detectable signal strength for the modulation to be used is –90 dBm? Assume the dish antennas are 50% efficient.

E7.34-1 Use a network simulator to plot the insertion loss/isolation of the single open-circuited stub used as the example in Section 7.34.

- **a.** What is the insertion loss of this filter at 1920 MHz?
- **b.** Use a pair of identical stubs spaced appropriately to reduce the insertion loss to less than 1.0 dB from 1900 to 1940 MHz.
- **c.** Use an EM simulator to design the actual layout of this two-stub filter and plot the results over frequency from 1000 to 5000 MHz.

CHAPTER 8

Directional Couplers

8.1 WAVELENGTH COMPARABLE DIMENSIONS

The fact that circuit dimensions are comparable to the operating wavelength is used to advantage in the design of circuits that couple energy according to its direction of propagation. These are called *directional couplers*.

An example is the waveguide multihole coupler shown in Figure 8.1-1. Its operation can be appreciated by noting that a wave incident at port 1 exits at port 4 with a portion of the incident power exiting at port 3. However, no power exits at port 2 because the separate waves that pass through the coupling holes have a differential path length of $\lambda_g/2$ and arrive with equal amplitudes but 180° out of phase at port 2. This is an example of *forward coupling* because the coupled wave travels in the same direction as the incident wave at port 1.

The directivity just described varies with frequency because the physical separation of the coupling holes must be related to the wavelength. This coupler type can be made broadband by using not two but many coupling holes, varying their coupling (hole size) according to an optimal distribution, say a binomial or Chebyshev distribution. More about mathematical distributions in Chapter 9 on filters. Using similar reasoning, it can be seen that a wave entering at port 4 will exit at port 1 with a coupled portion exiting at port 2.

This coupler example shows how a simple measurement system can be arranged. A detector placed at port 3 samples the *incident wave* while a detector placed at port 2 samples the *wave reflected* of a load connected to port 4. The ratio of these two waves is the reflection coefficient of the load at port 4. This is the basis of the *network analyzer*. More about network analyzers later in this chapter.

8.2 THE BACKWARD WAVE COUPLER

Placing two transmission lines in parallel and close together so that energy propagating on one is coupled to the other can form a transmission line cou-

High Frequency Techniques: An Introduction to RF and Microwave Engineering, By Joseph F. White.
ISBN 0-471-45591-1

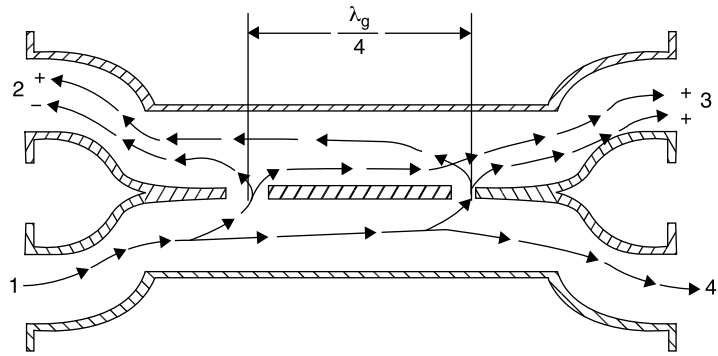

Figure 8.1-1 Cross-sectional view of a two-hole waveguide directional coupler.

pler. Intuitively, one would think that the coupled energy should travel in the same direction as does that on the coupled line, but this is not so. The *coupled power travels backward*, and therefore this coupler is called a *backward wave coupler* (Fig. 8.2-1).

This TEM mode backward wave coupler provides maximum coupling when the electrical length θ of the coupled lines is 90°. When the cross-sectional dimensions of the coupler are properly chosen, power entering port 1 exits at ports 2 and 4, with no energy exiting at port 3. Furthermore, the device presents a matched load at input port 1 and a 90° phase difference between the signals emerging from ports 2 and 4 *at all frequencies*! This coupler is inherently broadband yielding up to an octave bandwidth (the highest frequency twice that of the lowest), as will be seen. Further increases in bandwidth can be

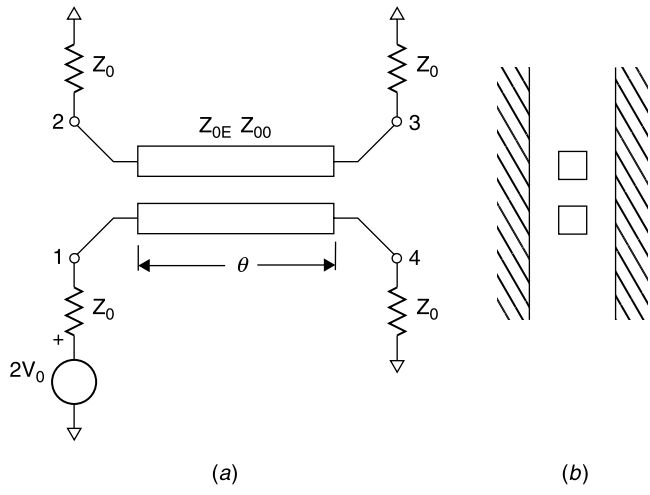

Figure 8.2-1 The TEM backward wave coupler: (*a*) top view and (*b*) cross section.

achieved by using cascaded 90° coupling sections and choosing their coupling characteristics appropriately [1, Sec. 8.3 and 2].

8.3 EVEN- AND ODD-MODE ANALYSIS

Remarkably, all of the progress that we have made so far in analyzing transmission lines, including analysis aided by the Smith chart, has not provided any

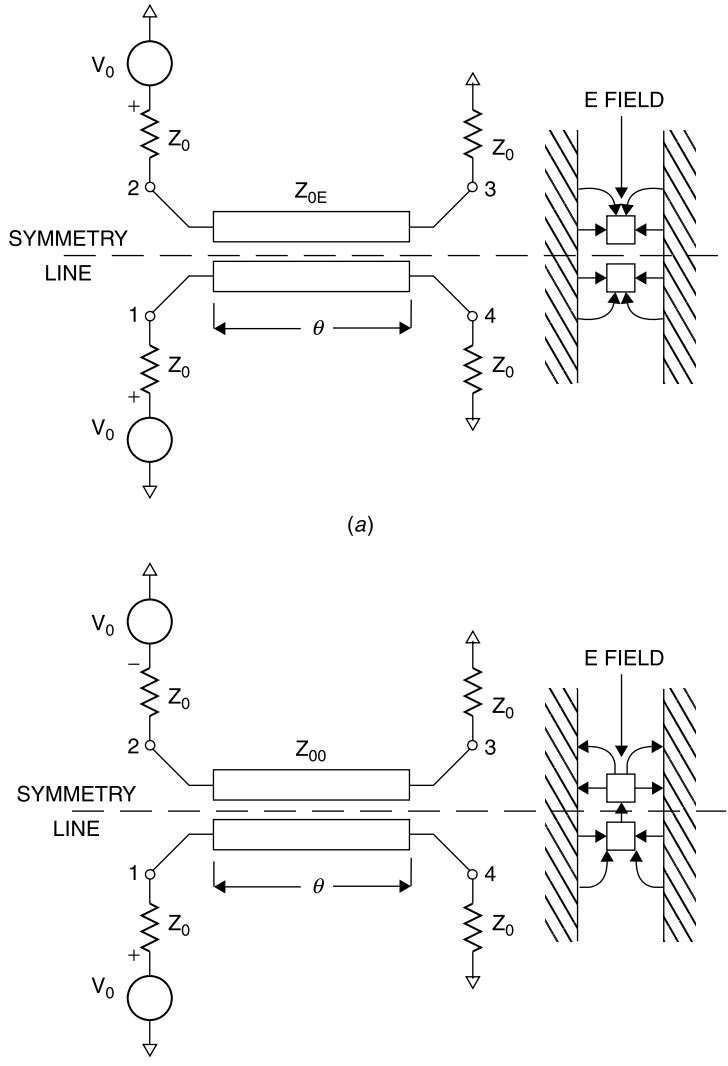

Figure 8.3-1 Even- (*a*) and odd-mode (*b*) excitations of the TEM coupled lines.

means to analyze the four-port network consisting of the two coupled transmissions lines shown in Figure 8.2-1. Our methods only permit the determination of the input impedance to an isolated transmission line given any load. To analyze coupled transmission lines requires a new method. The *even- and odd-mode analysis is* such an approach, a clever insight to accomplish coupled line analysis using single transmission line analysis methods. It consists of representing any voltage excitation of the coupled lines as the sum of an *even mode* and an *odd mode* (Fig. 8.3-1).

Studying Figure 8.3-1, it can be seen that the superposition of the four generator voltages, $\pm V_0$, applied at ports 1 and 2 is equivalent to the application of the single voltage $2V_0$ at port 1 in Figure 8.2-1. The clever part of the even- and odd-mode analysis is that now each transmission line in Figure 8.3-1 can be split away from its companion coupled line and analyzed as a single line with load. In doing so, however, it is necessary to use the *even-mode characteristic impedance* for the circuit in Figure 8.3-1*a* and the *odd-mode characteristic impedance* for Figure 8.3-1*b*.

The even-mode impedance Z_{OE} is defined when the adjacent line has the same voltage excitation. This corresponds to placing a "magnetic wall" (on which the tangential H field is zero) midway between the conductors. The odd-mode impedance Z_{OO} is defined when the adjacent line has the opposite voltage and corresponds to the condition of an electric wall (on which the tangential E field is zero) midway between the conductors. The geometries used for calculating these impedances are shown in Figure 8.3-2.

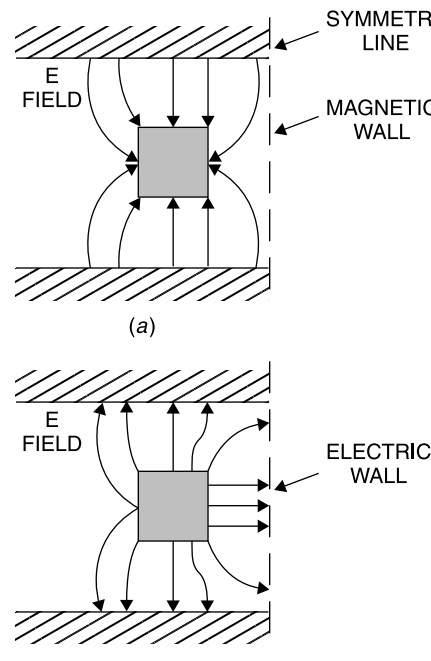

Figure 8.3-2 Geometries for determining Z_{OE} (*a*) and Z_{OO} (*b*).

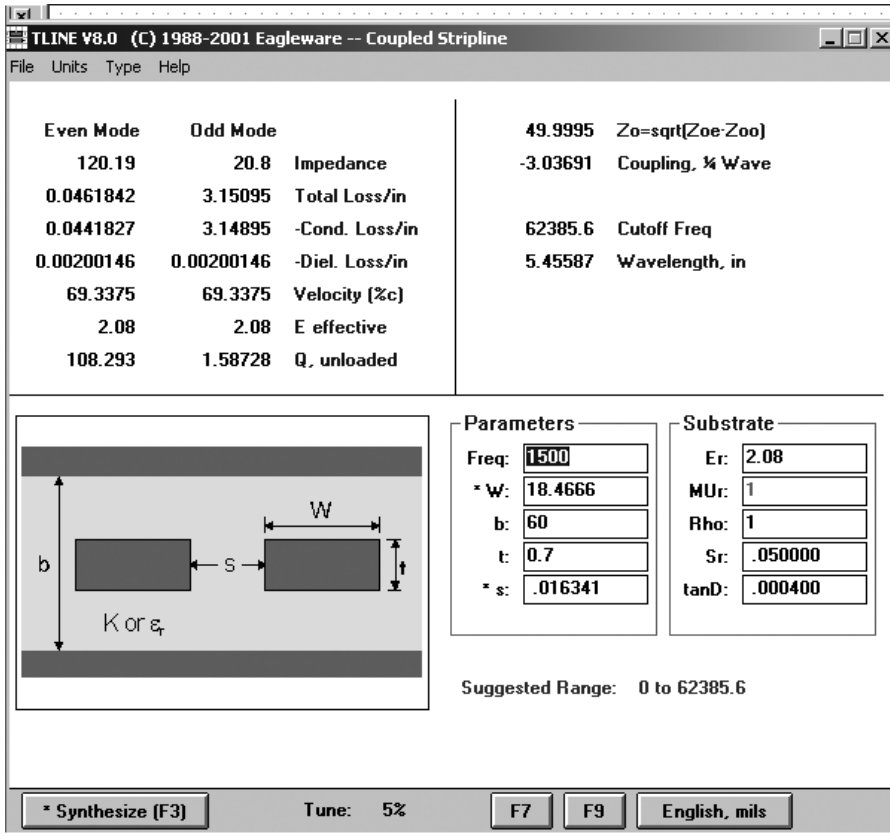

Figure 8.3-3 Software outputs showing the Z_{OE} and Z_{OO} and other parameters required for a 3-dB backward wave coupler. Obtained using Eagleware *TLine*.

These impedances are found in the same manner as was used to determine the characteristic impedance of coaxial line in Section 7.25, albeit with somewhat more mathematical complexity because the geometry is not as simple as that of coaxial line. The even- and odd-mode method dates to the 1950s when the Z_{OE} and Z_{OO} impedances were tabulated for various coupler cross-sectional geometries, but the current method for determining them is to use software. A sample software is shown in Figure 8.3-3 for the geometry to be used for a 3-dB coupler for which $Z_{OE} = 120\ \Omega$ and $Z_{OO} = 20.8\ \Omega$.

Why this choice of even- and odd-mode impedances yields a 3-dB coupler will be evident once the analysis of the coupler is completed. The analysis method [3, Chapter 6] will be demonstrated by solving for the voltages at the coupler's ports 1, 2, 3, and 4 given a generator voltage of $+2V_0$ with Z_0 loads as shown in Figure 8.2-1. We begin by determining the reflection coefficients at ports 1 and 2 for the even and odd mode excitations of Figure 8.3-1. The equivalent circuit used for the individual excitation analysis is shown in Figure 8.3-4.

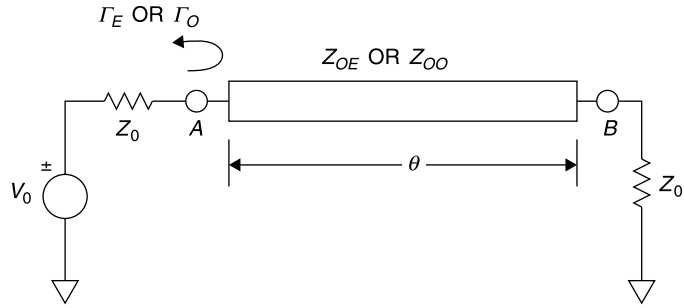

Figure 8.3-4 Circuit used to compute the input reflection coefficients to even- and odd-mode excitations.

The single-mode equivalent circuit in Figure 8.3-4 has input port A and output port B to distinguish these terminals from those of the coupler in Figure 8.2-1. The characteristic impedance of the line is Z_{OE} for the even-mode calculation and $-V_0$ and Z_{OO} for the odd mode. Notice that Z_0 is not a match termination for either the Z_{OE} or the Z_{OO} transmission line.

Given these procedures, the input impedance seen at A for the even mode is found from the input impedance formula (4.14-2):

$$Z_{AE} = Z_{OE}\frac{Z_0 + jZ_{OE}\tan\theta}{Z_{OE} + jZ_0\tan\theta} \tag{8.3-1}$$

and the reflection coefficient at A is

$$\Gamma_E = \frac{Z_{AE} - Z_0}{Z_{AE} + Z_0} \tag{8.3-2}$$

Substituting (8.3-1) into (8.3-2) and simplifying gives

$$\Gamma_E = \frac{j[Z_{OE}^2 - Z_0^2]\tan\theta}{2Z_0Z_{OE} + j[Z_{OE}^2 + Z_0^2]\tan\theta} \tag{8.3-3}$$

Similarly, for the odd excitation,

$$\Gamma_O = \frac{j[Z_{OO}^2 - Z_0^2]\tan\theta}{2Z_0Z_{OO} + j[Z_{OO}^2 + Z_0^2]\tan\theta} \tag{8.3-4}$$

The total reflected voltage at port 1 for the circuit of Figure 8.2-1 is the sum of the even and odd reflection voltages given by

$$V_{1R} = \frac{V_0}{2}\Gamma_E + \frac{V_0}{2}\Gamma_O \tag{8.3-5}$$

At port 2, the even- and odd-mode voltages are of opposite polarity. Therefore,

$$V_2 = \frac{V_0}{2}\Gamma_E - \frac{V_0}{2}\Gamma_O \tag{8.3-6}$$

Substituting (8.3-3) and (8.3-4) into (8.3-5) and (8.3-6) gives a result for V_{1R} (using the plus sign option in (8.3-7) and V_2 by using the minus sign option:

$$V_{1R,2} = \frac{V_0}{2}\Gamma_E \pm \frac{V_0}{2}\Gamma_O$$

$$V_{1R,2} = \frac{N_A^{\pm}}{D_A}$$

$$= \frac{\dfrac{V_0}{2}\left\{\begin{matrix}(j\tan\theta)(Z_{OE}^2 - Z_0^2)[2Z_0Z_{OO} + (j\tan\theta)(Z_{OO}^2 + Z_0^2)] \\ \pm(j\tan\theta)(Z_{OO}^2 - Z_0^2)[2Z_0Z_{OE} + (j\tan\theta)(Z_{OE}^2 + Z_0^2)]\end{matrix}\right\}}{[2Z_0Z_{OE} + (j\tan\theta)(Z_{OE}^2 + Z_0^2)][2Z_0Z_{OO} + (j\tan\theta)(Z_{OO}^2 + Z_0^2)]} \tag{8.3-7}$$

The denominator, D_A, is nonzero for all θ and for all finite Z_0, Z_{OE}, and Z_{OO}. Furthermore, when Z_{OE} and Z_{OO} are selected to satisfy

$$Z_0 = \sqrt{Z_{OE}Z_{OO}} \tag{8.3-8}$$

the even-mode numerator, N_A^+, is identically equal to zero for all θ. This means that the coupler will be *matched to Z_0 at input port 1 at all frequencies* when (8.3-8) is satisfied. This is a remarkable result, doubly so in view of the algebraic complexity with which the early researchers [4] of this coupler had to cope.

After algebraic manipulation, the value of $V_2 = N_A^-/D_A$ can be written

$$V_2 = V_0 \frac{(j\sin\theta)\left(\dfrac{Z_{OE} - Z_{OO}}{Z_{OE} + Z_{OO}}\right)}{\dfrac{2Z_0\cos\theta}{Z_{OE} + Z_{OO}} + j\sin\theta} \tag{8.3-9}$$

and when the coupling length is 90°, (8.3-9) reduces to

$$V_2 = V_0\frac{Z_{OE} - Z_{OO}}{Z_{OE} + Z_{OO}} \tag{8.3-10}$$

This suggests the definition of a *voltage coupling coefficient k* defined as

$$k = \frac{Z_{OE} - Z_{OO}}{Z_{OE} + Z_{OO}} \tag{8.3-11}$$

and the coupling in decibels is

$$\text{Coupling (dB)} = -20 \log k \tag{8.3-12}$$

where the negative sign is used so that the coupling is positive when expressed in decibels.

When (8.3-8) and (8.3-11) are substituted into (8.3-9), the expression for V_2 becomes

$$V_2 = V_0 \frac{jk \sin \theta}{\sqrt{1-k^2}\cos \theta + j \sin \theta} \tag{8.3-13}$$

If a 50-Ω, 3-dB coupler (at $\theta = 90°$) is required, $k = 1/\sqrt{2}$, (since $V_2^2/Z_0 = k^2 V_0^2/Z_0 = \frac{1}{2} V_0^2/Z_0$, where V_0^2/Z_0 is the available power from port 1. Substituting this value of k into (8.3-11) and applying the match criterion of (8.3-8) gives the values $Z_{OE} = 120.19\ \Omega$ and $Z_{OO} = 20.8\ \Omega$ for a 3-dB, 50-Ω coupler that were stated without proof earlier.

Now it remains to calculate the V_3 and V_4 for the coupler in Figure 8.3-1 to complete the analysis. We use the *ABCD* matrix method and include both the source and load impedances (Fig. 8.3-5).

For the even mode the *ABCD* matrix cascade is

$$\begin{pmatrix} A & B \\ C & D \end{pmatrix}_E = \begin{pmatrix} 1 & Z_0 \\ 0 & 1 \end{pmatrix} \begin{pmatrix} \cos\theta & jZ_{OE}\sin\theta \\ jY_{OE}\sin\theta & \cos\theta \end{pmatrix} \begin{pmatrix} 1 & 0 \\ Y_0 & 1 \end{pmatrix}$$

Performing the indicated matrix multiplications and simplifying, this becomes

$$\begin{pmatrix} A & B \\ C & D \end{pmatrix}_E = \begin{pmatrix} \gamma\cos\theta + j\sin\theta(Y_0 Z_{OE} + Z_0 Y_{OE}) & jZ_{OE}\sin\theta + Z_0\cos\theta \\ jY_{OE}\sin\theta + \cos\theta & \cos\theta \end{pmatrix} \tag{8.3-14}$$

If this network is excited by a voltage V_0 (Fig. 8.3-2*a*) and the output current is

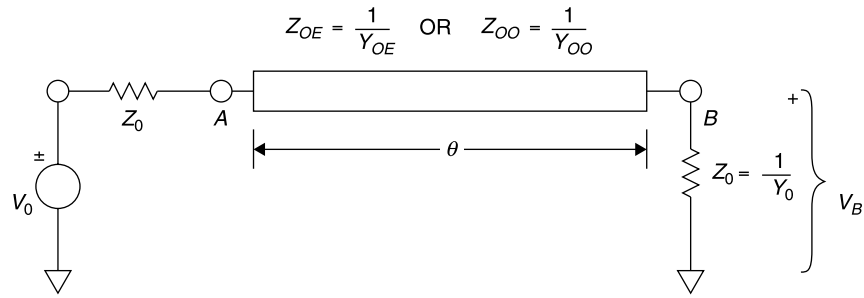

Figure 8.3-5 Circuit used to calculate the output voltages V_3 and V_4 at ports 3 and 4 of the coupler in Figure 8.2-1.

zero (since we included the load in the $ABCD$ network) the output voltage is

$$V_{BE} = \frac{V_0}{A_E} = \frac{V_0}{2\cos\theta + (j\sin\theta)(Y_0 Z_{OE} + Z_0 Y_{OE})} \tag{8.3-15}$$

Similarly, since the odd excitation corresponds to the application of V_0, at port 1 of the coupler and the use of odd-mode impedances,

$$V_{BO} = \frac{V_0}{A_O} = \frac{V_0}{2\cos\theta + (j\sin\theta)(Y_0 Z_{OO} + Z_0 Y_{OO})} \tag{8.3-16}$$

The output voltages at ports 3 and 4 that we seek are given by

$$V_3 = V_{BE} - V_{BO} \tag{8.3-17a}$$

$$V_4 = V_{BE} + V_{BO} \tag{8.3-17b}$$

Combining (8.3-15) and (8.3-16), the optional plus sign gives V_3 and the minus sign gives V_4. Thus,

$$V_{BE} \pm V_{BO} = \frac{N_B^{\pm}}{D_B}$$

$$= V_0 \frac{2\cos\theta + (j\sin\theta)(Y_0 Z_{OO} + Z_0 Y_{OO}) \pm 2\cos\theta + (j\sin\theta)(Y_0 Z_{OE} + Z_0 Y_{OE})}{[2\cos\theta + (j\sin\theta)(Y_0 Z_{OE} + Z_0 Y_{OE})][2\cos\theta + (j\sin\theta)(Y_0 Z_{OO} + Z_0 Y_{OO})]} \tag{8.3-18}$$

where (8.3-17a) is the minus option and (8.3-17b) is the plus option. For finite Z_0, Z_{OE}, and Z_{OO}, the denominator D_B is nonzero for all θ; and, when the matching condition (8.3-8) is substituted into the N_B^- expression of (8.3-18), the result is identically zero for all θ. Thus the voltage V_3 *is identically zero for all frequencies!* For this backward wave coupler, port 2 is the intended coupled port and port 3 is the *isolated port*. No power exits port 3 when power is applied to port 1 for any frequency and for any coupling coefficient k!

To complete the analysis of the backward wave coupler, we determine the direct voltage V_4 output. This is obtained by using the plus sign option in (8.3-18). When this is taken and a common factor taken from numerator and denominator, the result is

$$V_4 = \frac{2V_0}{2\cos\theta + (j\sin\theta)[\sqrt{Z_{OE}/Z_{OO}} + \sqrt{Z_{OO}/Z_{OE}}]} \tag{8.3-19}$$

Then imposition of the matching condition (8.3-8) and the coupling coefficient definition (8.3-11) allows this expression to be written as

$$V_4 = V_0 \frac{\sqrt{1-k^2}}{\sqrt{1-k^2}\cos\theta + j\sin\theta} \tag{8.3-20}$$

Notice that when the coupling length is 90°, from (8.3-13) and (8.3-20), $V_2 = V_4 = V_0/\sqrt{2}$ and exactly one half of the incident power, V_0^2/Z_0 exits the two ports 1 and 4. This makes sense because the coupling is 3 dB and no power is reflected and none exits the decoupled port 3. Of course, practical couplers have mismatches at the ports that degrade this ideal performance. Nevertheless, the backward wave TEM coupler of this analysis is a frequently used component for its broadband performance. The coupling varies with frequency, having maximum coupling (Fig. 8.3-6) when the coupled line length is an odd multiple of 90°. Thus, the performance is repeated in the frequency domain at

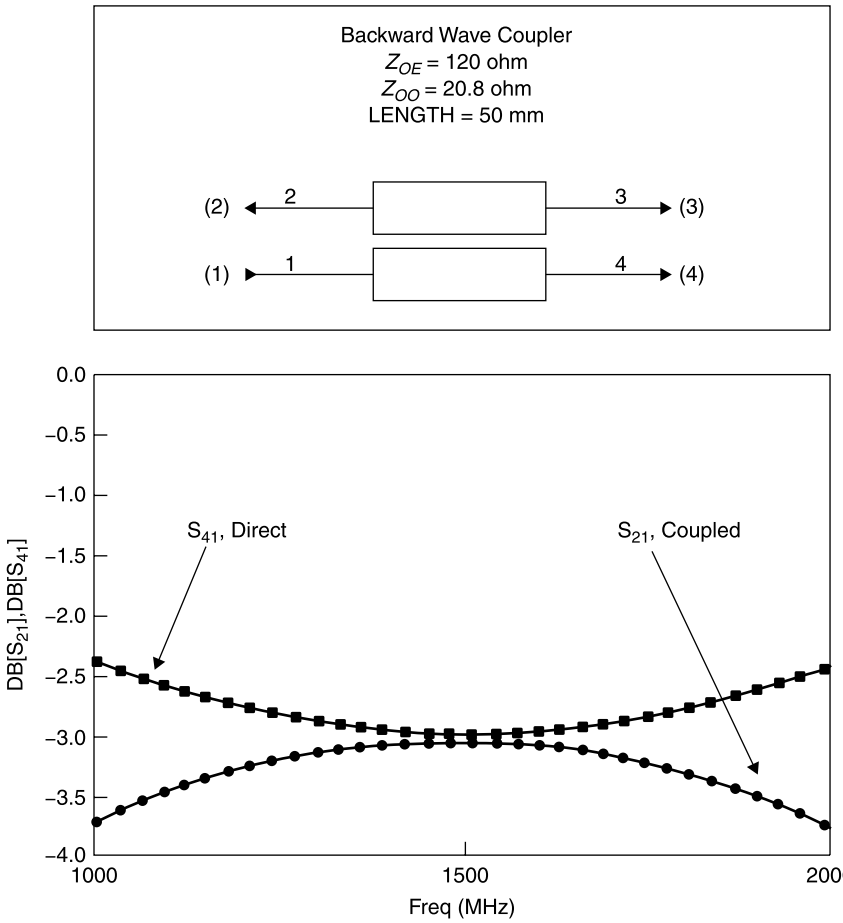

Figure 8.3-6 Direct power and coupled power of the backward wave coupler calculated using *Genesys* simulator.

the third, fifth, seventh, and so forth harmonics. The simulated performance of a 3-dB coupler with air dielectric ($\lambda/4 = 50$ mm) is shown in Figure 8.3-6.

In designing a coupler for a given amount of coupling, it is convenient to express the even- and odd-mode impedances in terms of the desired coupling coefficient. This is done by solving (8.3-8) and (8.3-9) for Z_{OE} and Z_{OO}:

$$Z_{OE} = Z_0\sqrt{\frac{1+k}{1-k}} \tag{8.3-21}$$

$$Z_{OO} = Z_0\sqrt{\frac{1-k}{1+k}} \tag{8.3-22}$$

For a given coupling tolerance, a broader bandwidth can be obtained by *overcoupling* at the center frequency. For example, if a center frequency coupling of 2.7 dB is chosen, $k = 0.724$ and (8.3-21) and (8.3-22) yield $Z_{OE} = 125\ \Omega$ and $Z_{OO} = 20\ \Omega$. For this design the variation of coupling is within 0.3 dB of 3.0 dB from 1000 to 2000 MHz, an octave bandwidth, as shown in Figure 8.3-7.

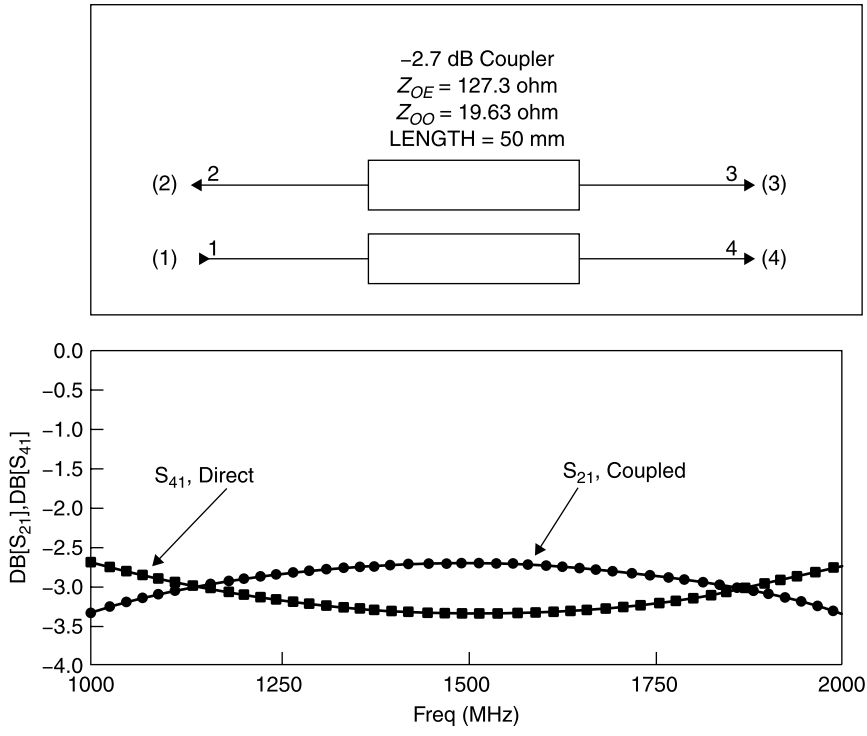

Figure 8.3-7 A −2.7 dB, over coupled, backward wave coupler.

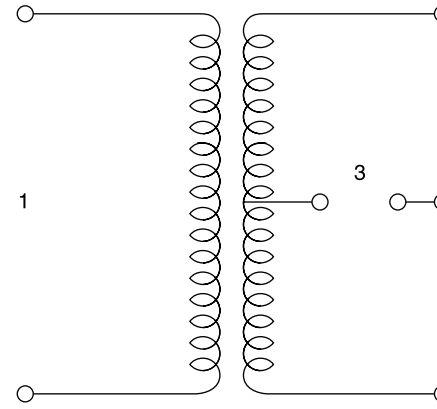

Figure 8.3-8 Hybrid coil with ports defined for comparison with the backward wave coupler.

The remarkable performance of the homogeneous (same dielectric constant for even and odd modes) TEM backward wave coupler can be summarized as follows:

1. The coupler is matched ($V_1 = V_0$) *at all frequencies!*
2. The directivity is infinite ($V_3 = 0$) *at all frequencies!*
3. The direct (V_4) and coupled (V_2) voltages are exactly 90° out of phase *at all frequencies!*
4. The magnitude of the coupled output voltage relative to the input voltage is $k = (Z_{OE} - Z_{OO})/(Z_{OE} + Z_{OO})$.

When designed such that the coupled and direct waves are equal, or nearly so, it is also called a *hybrid coupler* [5, p. 280]. This nomenclature may have been derived from the *hybrid coil* (Fig. 8.3-8) used widely in lower frequency telephone systems [6, p. 282]. When properly terminated, the hybrid coil has the property that a signal at 1 divides evenly between ports 2 and 4, and there is no output at 3. A signal at 2 also divides between 1 and 3 with no output at 4, and so forth. The 3 dB backward coupler has performance similar to the hybrid coil, but it also has a 90° phase shift between the two equal outputs whereas the hybrid coil does not.

The single quarter-wave coupler provides up to an octave (2/1) bandwidth for about 3 dB $\pm$ 0.4 dB of coupling. Considerably broader bandwidth can be obtained by cascading odd numbers of coupling sections. A 5/1 bandwidth with 3 dB $\pm$ 0.4 dB can be obtained by cascading three sections having 12.64, 1.28, and 12.64 dB coupling, respectively. This three-section coupler is described in a classic paper by Seymour Cohn [2]. The simulated performance of an air dielectric version of the model that he built is shown in Figure 8.3-9.

To achieve the very tight coupling in the center coupler Cohn invented a transmission line format called a *reentrant section*. It consists of a pair of con-

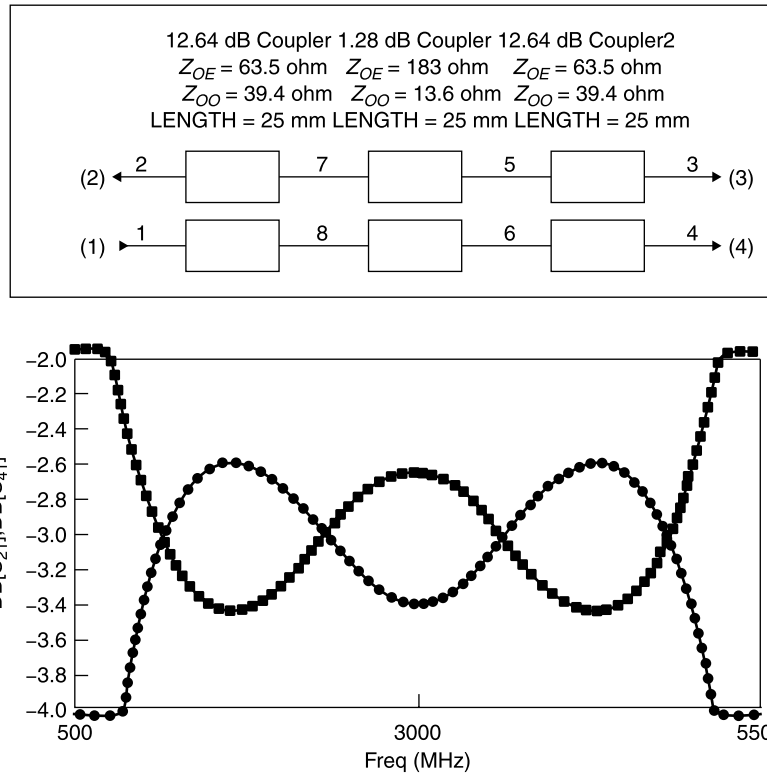

Figure 8.3-9 Performance of a three-section coupler cascade [2].

ductors, A and B, embedded as separate coaxial lines within an ungrounded (electrically "floating") intermediate conductor C that is suspended within an outer conductor D, as shown in Figure 8.3-10. The intermediate conductor C might seem to shield A and B from each other. However, C is not grounded, and its presence increases the distributed capacitance between A and B and, with it, their coupling to each other.

For the reentrant section

$$Z_{OE} = Z_{02} + 2Z_{01} \tag{8.3-23}$$

$$Z_{OO} = Z_{02} \tag{8.3-24}$$

where Z_{01} is the characteristic impedance of a solid conductor having the same outer dimensions as the intermediate conductor C, within the outer conductor D; and Z_{02} is the characteristic impedance of A (or B) within the coaxial region inside C.

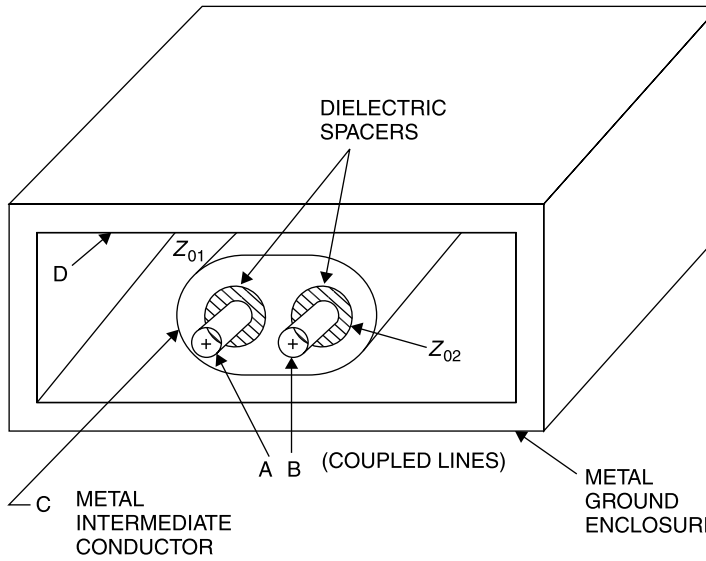

Figure 8.3-10 Cohn's reentrant coupling section [2].

8.4 REFLECTIVELY TERMINATED 3-dB COUPLER

As was derived in Section 8.3, when terminated in matched Z_0 loads defined by (8.3-8) and fed by a Z_0 generator at port 1, the backward wave coupler has no reflection at port 1 and no power output at port 3. The output voltages at ports 2 and 4 are given by (8.3-13) and (8.3-20), respectively. With this information the scattering matrix for this four-port network can be written directly by alternately assuming an input at each port with the remaining ports terminated in matched loads. The result is

$$S = \begin{pmatrix} 0 & f_1 & 0 & f_2 \\ f_1 & 0 & f_2 & 0 \\ 0 & f_2 & 0 & f_1 \\ f_2 & 0 & f_1 & 0 \end{pmatrix} \tag{8.4-1a}$$

where

$$f_1 = \frac{jk \sin \theta}{\sqrt{1-k^2}\cos \theta + j \sin \theta} \quad \text{and} \quad f_2 = \frac{\sqrt{1-k^2}}{\sqrt{1-k^2}\cos \theta + j \sin \theta} \tag{8.4-1b,c}$$

The scattering matrix is useful for determining the performance of the coupler when it has multiple inputs as, for example, when reflective circuits terminate ports 2 and 4.

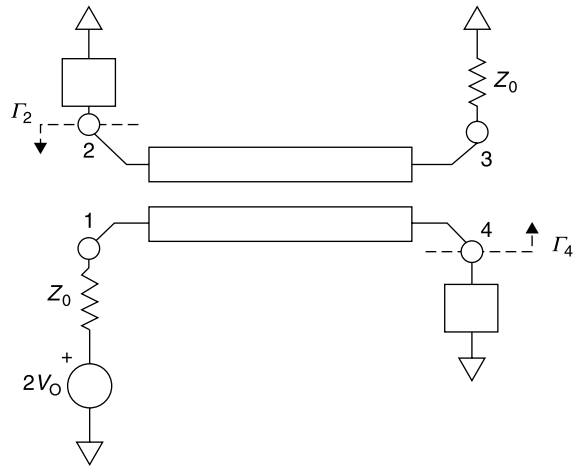

Figure 8.4-1 The 3-dB backward wave coupler with symmetric reflecting terminations on ports 2 and 4.

A frequent application consists of employing a 3-dB coupler to convert a symmetric pair of reflective circuits into a transmission network. This need may arise, for example, when it is necessary to design a diode phase shifter. The symmetric reflective terminations are connected to the direct arm (port 4) and coupled arm (port 2) of the coupler. Because of their equal amplitude and 90° phase difference for each pass through the coupler, when the energy is reflected back into the coupler (Fig. 8.4-1), it emerges from the normally decoupled port 3.

This process requires that the complex reflection coefficients at ports 2 and 4 are identical, or

$$\Gamma_2 = \Gamma_4 = \Gamma \tag{8.4-3}$$

With an input at port 1, symmetric reflections at ports 2 and 4, and a matched Z_0 load at port 3, the scattering matrix equations for the network are

$$\begin{pmatrix} b_1 \\ b_2 \\ b_3 \\ b_4 \end{pmatrix} = \begin{pmatrix} 0 & f_1 & 0 & f_2 \\ f_1 & 0 & f_2 & 0 \\ 0 & f_2 & 0 & f_1 \\ f_2 & 0 & f_1 & 0 \end{pmatrix} \begin{pmatrix} a_1 \\ a_2 \\ a_3 \\ a_4 \end{pmatrix} = \begin{pmatrix} 0 & f_1 & 0 & f_2 \\ f_1 & 0 & f_2 & 0 \\ 0 & f_2 & 0 & f_1 \\ f_2 & 0 & f_1 & 0 \end{pmatrix} \begin{pmatrix} a_1 \\ \Gamma f_1 a_1 \\ 0 \\ \Gamma f_2 a_1 \end{pmatrix} \tag{8.4-2a,b,c,d}$$

The reflection coefficient at input port 1 is found from (8.4-2a), specifically

$$b_1 = f_1 \Gamma f_1 a_1 + f_2 \Gamma f_2 a_1 \tag{8.4-5}$$

and the input reflection coefficient is

$$\Gamma_1 = \frac{b_1}{a_1} = \Gamma(f_1^2 + f_2^2) = \Gamma \frac{1 - k^2(1 + \sin^2 \theta)}{[\sqrt{1 - k^2} \cos \theta + j \sin \theta]^2} \tag{8.4-6}$$

From (8.4-4) it can be seen that when $\theta = 90^\circ$ and $k = 1/\sqrt{2}$ (for 3-dB coupling), then $\Gamma_1 = 0$, and the input port is matched. From (8.4-2c)

$$b_3 = f_2 \Gamma f_1 a_1 + f_1 \Gamma f_2 a_1 \tag{8.4-7}$$

This can be written as

$$b_3 = a_1 \Gamma \frac{j(2k \sin \theta)\sqrt{1 - k^2}}{\sqrt{1 - k^2} \cos \theta + j \sin \theta} \tag{8.4-8}$$

We note from (8.4-8) that when $\theta = 90^\circ$ and $k = 1/\sqrt{2}$, and $|\Gamma| = 1$, the output wave $b_3 = \Gamma a_1$. That is, when symmetric, totally reflecting circuits are connected to ports 2 and 4 of a 3-dB coupler, the output wave equals the input in amplitude but is changed by the angle of the reflection coefficient of the reflective terminations at ports 2 and 4. This is what is desired in a phase shifter circuit.

As frequency is varied, the value of θ varies, and the power split of the coupler is no longer exactly 3 dB, as is required for a perfect match at the input with symmetric reflections at ports 2 and 4. As a result, some power is reflected at port 1 and a corresponding insertion loss is experienced in the transmission from port 1 to port 3. Despite this fact, the reflection coefficient at port 1 remains fairly low due to the fact that the waves reflected back into the coupler at ports 2 and 4 remain 90° out of phase with one another at all frequencies and hence combine 180° out of phase at port 1.

The input VSWR at port 1 and the transmission loss from port 1 to port 3 is shown in Figure 8.4-2 for a coupler with center frequency at 1500 MHz and symmetric, totally reflecting circuits at ports 2 and 4. The VSWR is 1.1 or less from 1100 to 1900 MHz, a bandwidth of 800 MHz. Notice that *for TEM devices whose bandwidth depends upon line lengths, the center frequency f_0 is the arithmetic mean of the band edge frequencies.*

The matched performance at port 1 with symmetric reflections at the 3-dB ports can be obtained with other types of 3-dB, 90° couplers such as the *branch line coupler* and the *hybrid ring coupler* (or *rat race coupler*) fitted with an extra 90° line length. The principles of these couplers will be covered shortly. However, these devices do not maintain the 90° phase difference at all frequencies for the signals emerging from their coupled and direct ports and do not achieve as broad a bandwidth in the reflection mode as that of the backward wave hybrid.

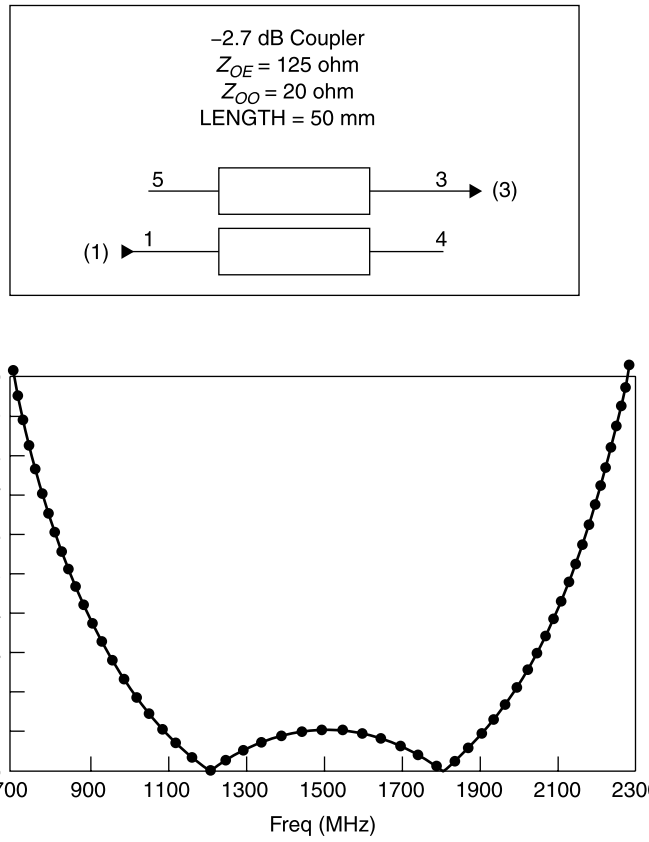

Figure 8.4-2 Input VSWR for a reflectively terminated −2.7-dB backward wave, hybrid coupler.

8.5 COUPLER SPECIFICATIONS

In the practical construction of a hybrid coupler, the region of the coupled lines can be constructed in a nearly ideal realization; however, it is necessary to make transitions from the ends of the coupled lines in order to attach connectors at the ports. It is at these transitions that significant reflections occur in a practical coupler, causing the operation of the coupler to depart from the ideal performance previously described.

Consider the coupler in Figure 8.5-1. Power P_I enters the coupler at port 1. Ideally, the desired coupled power P_C exits at port 2, and the remaining power P_L exits at port 4. However, due to coupler imperfections some power, P_D, exits at port 3 (the "decoupled" port). Furthermore, some power, P_R, is reflected at the input port.

The parameters of couplers are defined as numbers greater than unity so that the values are positive when expressed in decibels [1, p. 369].

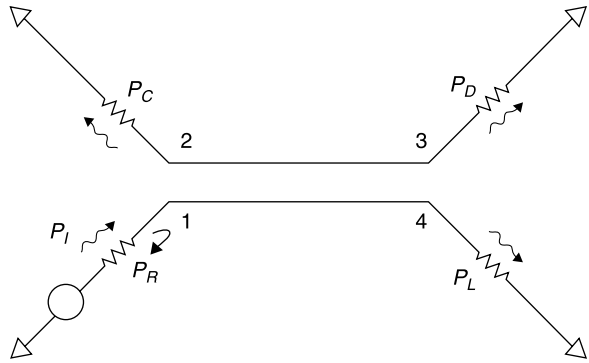

Figure 8.5-1 Practical directional coupler has return loss and finite directivity.

The *coupling* (in decibels) is defined as

$$\text{Coupling} = 10 \log\left(\frac{P_I}{P_C}\right) \quad ($$

The *directivity* (in decibels) is defined as

$$\text{Directivity} = 10 \log\left(\frac{P_C}{P_D}\right) \quad ($$

The *isolation* (in decibels) is defined as

$$\text{Isolation} = 10 \log\left(\frac{P_I}{P_D}\right) \quad ($$

Note that when expressed in decibels the isolation is equal to the coupling plus the directivity.

The *return loss* (in decibels) is defined as

$$\text{Return loss} = 10 \log\left(\frac{P_I}{P_R}\right) \quad ($$

The *insertion loss** (in decibels), which includes the diversion of coupled power, is

$$\text{Insertion loss} = 10 \log\left(\frac{P_I}{P_L}\right) \quad ($$

*Some manufacturers may subtract the coupled power from insertion loss ratings, defining the insertion loss as the amount of power loss to reflection and absorption in the coupler.

Note that in a symmetrically constructed coupler the same imperfections that give rise to reflections at the input also produce the undesired leakage at the directive port.

In a symmetric coupler the return loss equals the directivity. For example, a symmetric coupler having 20-dB directivity has a return loss of 20 dB as well. This corresponds to a VSWR of 1.22.

8.6 MEASUREMENTS USING DIRECTIONAL COUPLERS

Suppose we wish to use a directional coupler to determine the VSWR of a device under test (DUT) (Fig. 8.6-1). Consider the signals emanating from the coupler's measurement port. First, there is a voltage wave proportional to the desired measurement ρ_L. But then there is also an error voltage wave D due to the directivity. *It is to be emphasized that D is a voltage wave (not power); we can only use superposition for linear quantities (voltage, current, a and b waves, etc.)* Accordingly, there is a wave resulting from the interaction of the source and load reflections. This wave is the result of an infinite number of re-reflections. But this infinite series converges, as we've seen previously:

$$\rho_S\rho_L + (\rho_S\rho_L)^2 + (\rho_S\rho_L)^3 + \cdots = \frac{\rho_S\rho_L}{1 - \rho_S\rho_L} \tag{8.6-1}$$

We ignore the phases of the measured and error waves since we want to know the worst-case limits when the error waves either add or subtract from the measured ρ_L wave.

The total (combined) error wave can have magnitudes between

$$E_T = \text{total error wave magnitude} = \pm D\left[1 + \frac{\rho_S\rho_L}{1 - \rho_S\rho_L}\right]\left(\tag{8.6-2}$$

Say that the coupler has 20-dB directivity, that the VSWR of the source is 1.3, that the VSWR of the coupler input is 1.22, and that the load we wish to measure actually has a VSWR of 1.25. Then $D = 0.1$, $\rho_S = 0.13$, and $\rho_L = 0.11$.

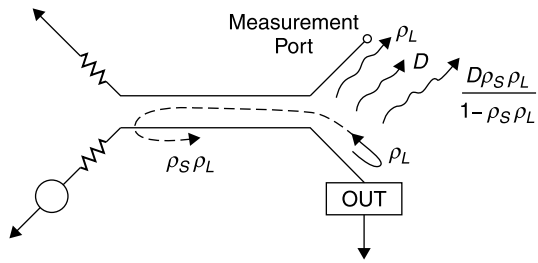

Figure 8.6-1 Measurement of the reflection coefficient of a device under test (DUT) using a backward wave coupler. Two error waves are also shown.

Then the error wave can be

$$E_T = \pm(0.1)\left[1 + \frac{(0.13)(0.11)}{1-(0.13)(0.11)}\right] = \pm(0.1)[1.015] = \pm 0.10 \quad (8.6\text{-}3)$$

This wave can combine in any phase with that of Γ_L, whose magnitude is 0.11. The resulting measured magnitude of Γ_L will be within

$$0.01 \leq \text{measured } \rho_L \leq 0.21 \quad (8.6\text{-}4)$$

The corresponding values for measured VSWR are

$$1.02 \leq \text{VSWR}_{\text{MEAS}} \leq 1.53 \quad (8.6\text{-}5)$$

This is insufficient accuracy for practical measurements. To circumvent this inaccuracy, the same coupler can be used in a *network analyzer* system, whose computer determines the error waves (phase and magnitude) during the calibration part of the measurement (when precision short circuit, open circuit and matched loads are connected) and then subtracts these error phasors from the actual measurements at each test frequency. This is described in the next section.

8.7 NETWORK ANALYZER IMPEDANCE MEASUREMENTS

Network analyzers (Fig. 8.7-1) measure both impedance (by measuring reflection coefficient at any port) and scattering parameters (insertion loss and inser-

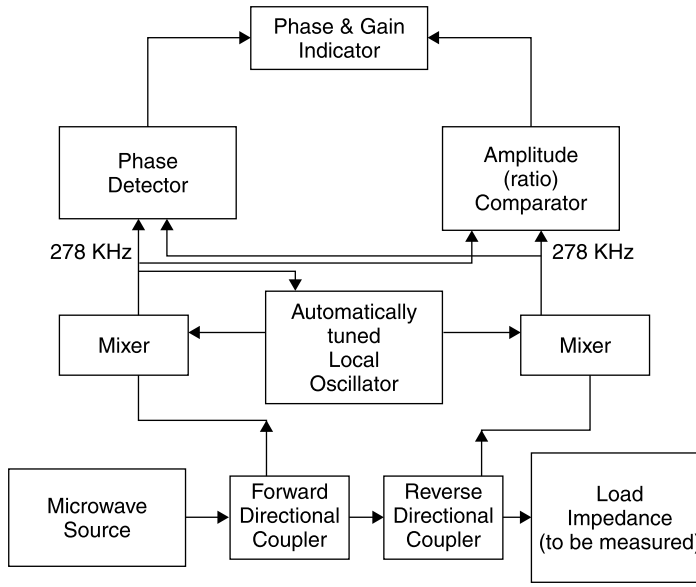

Figure 8.7-1 Network analyzer in the impedance measurement mode (after Gupta [7], reprinted with permission).

tion phase to any port). Impedance measurement is based on the direct measurement of reflection coefficient, the complex ratio of the reflected and incident waves of a terminating impedance. The incident and reflected waves are separated using directional couplers. The outputs of the couplers are fed to a harmonic frequency converter (mixer), which translates the test frequency to a fixed frequency near 300 kHz [7, pp. 114–115]. Usually an autotuning local oscillator and two identical mixers are used for this purpose. The mixing process preserves amplitude and phase information that are readily measurable at low frequency. The reflected wave vector, normalized to the incident wave (and corrected for coupler errors), can be displayed on a CRT (cathode ray tube) screen with a Smith chart overlay for direct determination of normalized impedance.

8.8 TWO-PORT SCATTERING MEASUREMENTS

The network analyzer (Fig. 8.8-1) contains microwave switches of high precision (good reproducibility and low VSWR). Using the switches the procedure to measure S_{nm} is [7, p. 115]:

1. Connect a source to port m and a matched load to port n. These two ports are connected to a network analyzer via two directional couplers as shown in Figure 8.8-1.
2. Terminate all other ports in matched loads so that all other a's (incident wave amplitudes) are zero.
3. The network analyzer provides the complex value of S_{nm} in terms of amplitude and phase (for $n \neq m$, i.e., a two-port measurement).

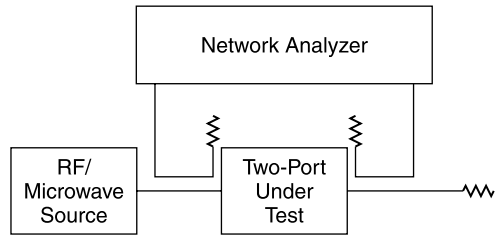

Figure 8.8-1 Network analyzer in the two-port measurement mode used to determine S parameters.

8.9 BRANCH LINE COUPLER

Over a narrow bandwidth, the performance of the 3-dB backward wave hybrid coupler can be obtained with the *branch line coupler*. This consists of four 90° transmission lines connected together in a square. It has the form of a 50-Ω line

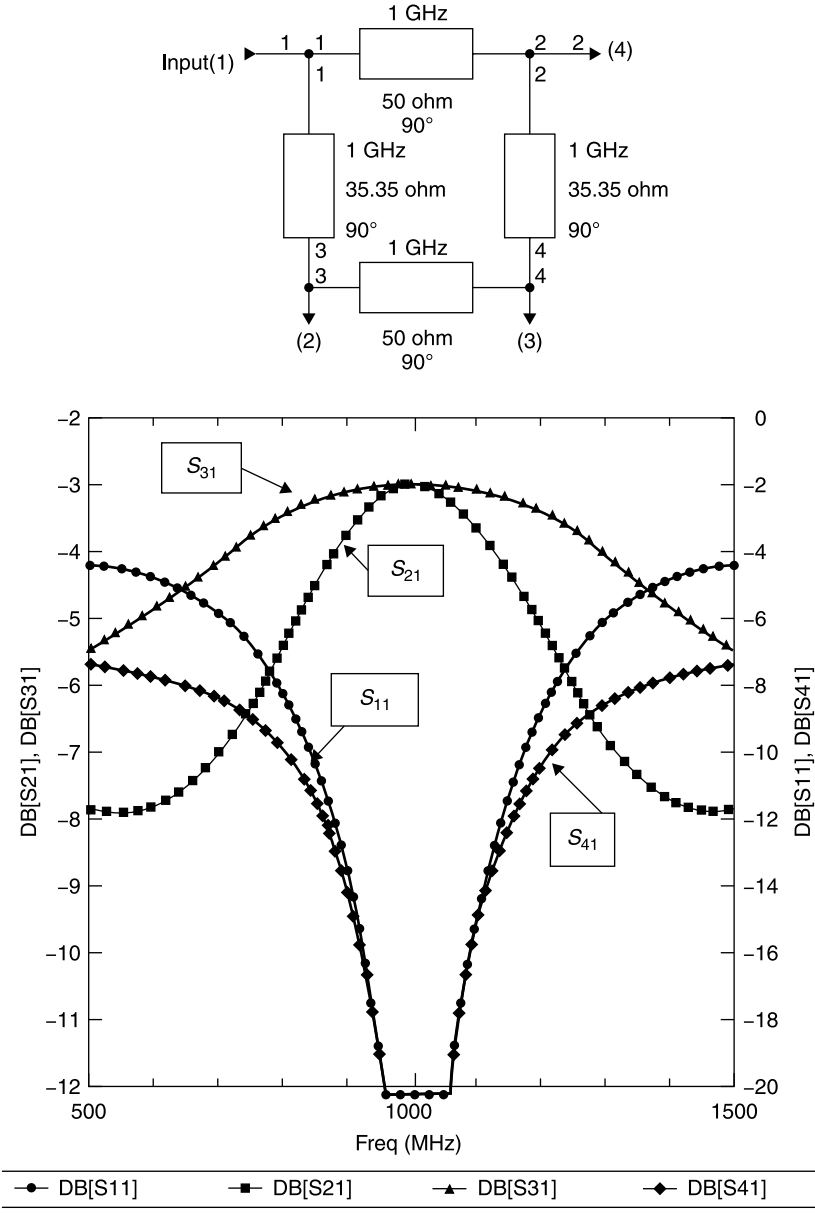

Figure 8.9-1 Equivalent circuit and performance of the 3-dB branch line coupler.

loaded at 90° intervals by 35.35-Ω (more precisely, $50/\sqrt{2}$) stubs that are interconnected at their ends with another 50-Ω line. The "stub ends" form the 3-dB ports. Like the backward wave hybrid, a 90° phase difference occurs between these two equal outputs, but for the branch line coupler this occurs only at the center frequency.

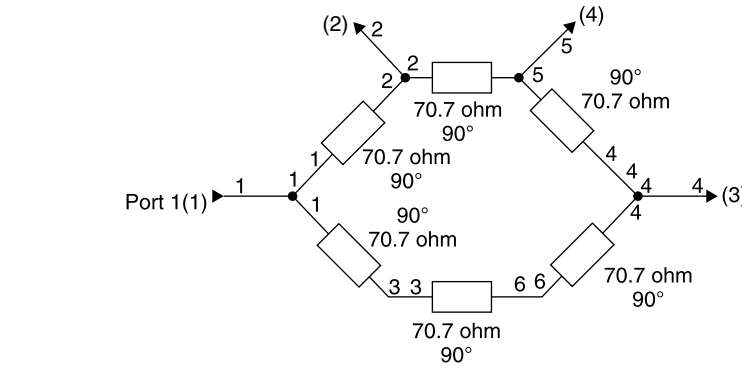

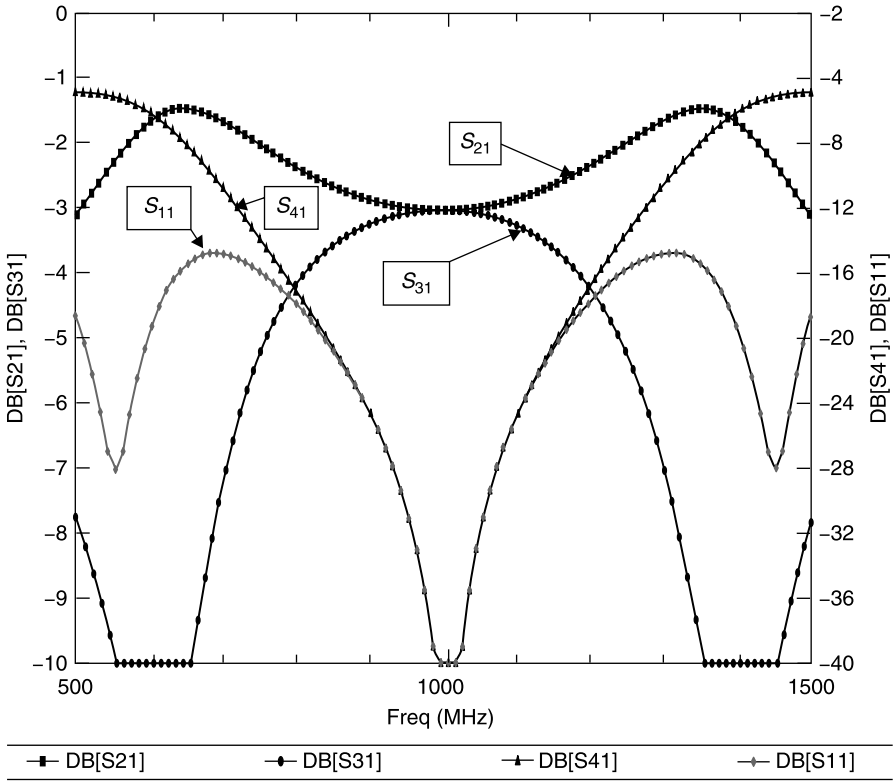

Figure 8.10-1 Circuit and performance of 3-dB hybrid ring coupler when realized in a homogeneous TEM transmission line format.

When power enters at port 1 (Fig. 8.9-1), it divides evenly between ports 2 and 3. At the center frequency, port 4 is isolated when match loads are placed at ports 2 and 3.

This coupler has the constructional advantage that it lies entirely in one center conductor plane, hence it is easy to print or incorporate within an integrated circuit. However, this coupler is fairly narrowband, usually having only about a 10% bandwidth. Furthermore, the 35.35-Ω lines are wide relative to their 90° length at microwave frequencies, making it hard to distinguish where those lines end and the 50-Ω lines begin, the problem encountered with the stub filter in Section 7.34. Accordingly, the branch line coupler is a candidate for EM simulation.

8.10 HYBRID RING COUPLER

The disadvantage of the branch line coupler is the need to make 35-Ω lines. Their low impedance line sections make the junctions so large it is difficult to estimate where one 90° line section ends and the next begins, necessitating considerable trial and error or EM simulation to realize a satisfactorily performing design.

The hybrid ring coupler, also called the *rat race coupler*, actually requires 1.5 wavelengths of transmission line (one section is 270° long), but it is easier to realize because the lines are 70.7 Ω (more precisely $Z_0\sqrt{2}$), quite narrow, and consequently their electrical lengths are more easily predicted. While this coupler is called the *hybrid ring*, the name is misleading, since its 3-dB ports are 180° out of phase rather than 90° (Fig. 8.10-1). The hybrid ring coupler can be realized in a TEM transmission line format or in a waveguide. In a waveguide, its circular chamber is likely the basis for the "rat race" name.

Remarkably, for a given VSWR specification the rat race usually is broader band than the branch line coupler. Although its 3-dB outputs are 180° out of phase rather than 90°, a 90° phase difference in its −3-dB outputs can be obtained simply by adding a 90° length of 50-Ω line to one of the 3-dB outputs. The 90° phase difference between 3-dB outputs is necessary if the coupler is to be used in a reflection transmission circuit, as for a phase shifter.

8.11 WILKINSON POWER DIVIDER

An equal-phase output, 3-dB divider can be obtained by transforming two 50-Ω loads to 100 Ω and connecting them in parallel to an input 50-Ω line (Fig. 8.11-1). When the output ports are bridged with a 100-Ω resistor, the result is a power divider whose output ports are matched and perfectly isolated at the design frequency [1, Sec. 8.2]. The resulting circuit is called a *Wilkinson power divider* (Fig. 8.11-2). To the extent that the output loads at 2 and 3 are

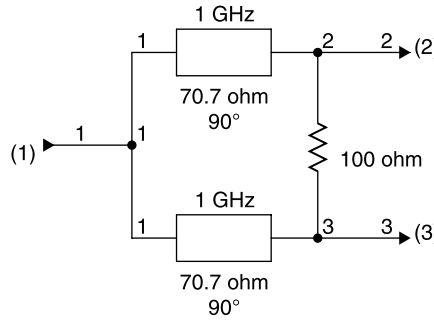

Figure 8.11-1 Wilkinson power divider provides two in-phase, 3-dB outputs and some isolation of the input from asymmetrical.

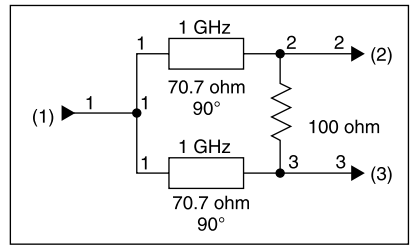

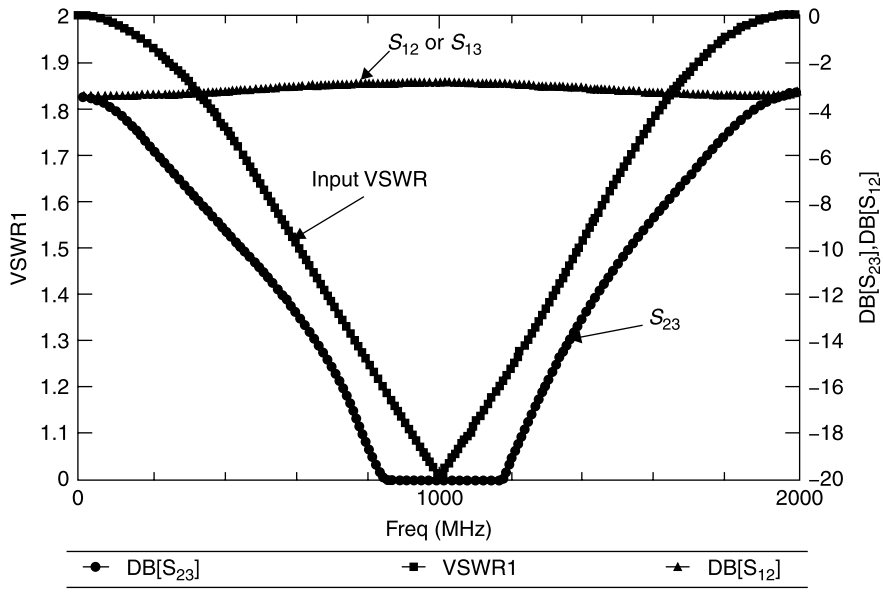

Figure 8.11-2 Performance of the Wilkinson power divider.

asymmetric, their reflections are absorbed by the 100-Ω resistor. When the loads are symmetric, no power will be absorbed in this resistor.

Another advantage of the Wilkinson divider is that very broad bandwidth can be obtained by using multiple section transformers (quarter-wave line sections) to transform the 50-Ω loads to 100-Ω inputs that, when paralleled, give an input impedance of 50 Ω. [4]

REFERENCES

1. Peter A. Rizzi, *Microwave Engineering, Passive Circuits*, Prentice-Hall, Englewood Cliffs, NJ, 1988. *Fundamental microwave engineering textbook covering theory and design of transmission lines, couplers, filters, and numerous other passive devices.*
2. Seymour Cohn, "The Re-Entrant Cross Section and Wide-Band 3-dB Hybrid Couplers," *IEEE Transactions on Microwave Theory and Techniques, MTT-11*, July, 1963, pp. 254–258.
3. Joseph F. White, *Microwave Semiconductor Engineering*, Noble Publishing, Norcross GA. *Extensive treatment of PIN diodes and their switching and phase shifting applications. Also includes fundamentals of microwave circuits.*
4. Matthei, Young, and Jones, *Microwave Filters, Impedance Matching Networks, and Coupling Structures*, McGraw-Hill, New York, 1964 (now also available from Artech House, Norwood, MA). *This is considered the Bible of the filter world.*
5. Fred E. Gardiol, *Introduction to Microwaves*, Artech House, Norwood, MA, 1984. *This is a good text on microwaves, containing many practical experimental setups.*
6. Robert E. Collin, *Foundations of Microwave Engineering*, McGraw-Hill, New York, 1966. *Collin is a superb theoretician.*
7. K. C. Gupta, *Microwaves*, Halsted Press, Wiley, New York, 1978. *Easily readable introduction to microwave engineering. Originally published in India.*

EXERCISES

E8.3-1 Derive the expressions (8.3-23) and (8.3-24) for Z_{OE} and Z_{OO} of the backward wave coupler in terms of the characteristic impedance Z_0 and the voltage coupling coefficient k, beginning with (8.3-8) and (8.3-11).

E8.3-2 **a.** What even and odd impedances are needed to form a 50-Ω, 15-dB coupler? *Hint:* The result from E8.3-1 is helpful.

b. What is the physical length of the coupling region if the relative dielectric constant throughout the insulating region surrounding the coupled lines is 2.1?

E8.3-3 Verify that the numerator N_A^+ in (8.3-7) is zero given the matching condition of (8.3-8).

E8.3-4 Derive the expression for the straight-through voltage V_4 of the backward coupler (8.3-20) beginning with (8.3-18) and using the conditions of (8.3-8) and (8.3-11).

E8.4-1

a. Determine the coupling coefficient k for a 50-Ω, backward wave coupler that when used with perfectly reflecting short circuits on its coupled and direct arms will have a perfect input match at $f_0 - 0.3f_0$ and at $f_0 + 0.3f_0$ where $f_0 = 1000$ MHz is its center frequency (at which the coupling region is 90° long).

b. What is the center frequency coupling value (in decibels) of the coupler?

c. What are Z_{OE} and Z_{OO} for this coupler?

d. What is the VSWR at the input at 1000 MHz?

e. Model the circuit on a network simulator and verify your predicted values.

E8.4-2

a. Use a network simulator to model a 3-dB backward wave coupler with open circuits on its direct and coupled arms (ports 2 and 4) and center frequency of 1 GHz (at which the coupled line length is 90°). Plot the input VSWR (at port 1) from 500 to 1500 MHz.

b. Repeat (a) with short-circuit terminations on ports 2 and 4 instead of open circuits.

c. Using a network simulator, plot the transmission phase (ang[S_{31}]) over the 500- to 1500-MHz band of the circuits in (a) and (b) and show that the difference (phase shift obtained by switching from an open to a short circuit on ports 2 and 4) is equal to 180° over a frequency band of 10% or more. This is an example of a transmission phase shifter obtained by converting variable reflection angle terminations into a two-port network using a 3-dB coupler.

d. Plot the insertion loss of the circuits in (a) and (d) over the 500- to 1500-MHz bandwidth. With what minimum efficiency, in percent of incident power, do the circuits in (a) and (b) convert reflecting terminations into a transmission circuit over the 700- to 1300-MHz bandwidth?

e. Show the VSWR of the cascade connection of the circuits in (a) and (b) over the 500- to 1500-MHz bandwidth.

E8.5-1 A symmetrically designed backward wave coupler has 30 dB of directivity at its center frequency. What is its input VSWR at this frequency.

E8.6-1 An engineering team at your microwave components company proposes to design a dedicated test setup to measure products having a VSWR of 1.25 at a single frequency. They propose to build a coupler and tune it for low VSWR and high directivity at a single test frequency. The source available has a VSWR of 1.3. It is necessary to

measure an actual VSWR value of 1.25 as being between 1.23 and 1.27.

a. What coupler directivity is required?

b. What is the corresponding input VSWR of the coupler?

c. Is this measurement setup practically achievable?

E8.9-1 **a.** Use a circuit simulator to model the branch line 3-dB coupler with open circuits at its 3 dB ports. What is its bandwidth for a maximum input VSWR = 1.2 (20 dB return loss)?

b. Repeat (a) but place short circuits on the two 3-dB ports. What is the bandwidth for VSWR = 1.2 or less?

c. Next, cascade two of the circuits used in (a) and interconnect them with a 50-Ω line that is 600 long at 1 GHz. What is the 1.2 maximum VSWR bandwidth of the cascade? How does this compare with the similar experiment of exercise E8.4-2e?

E8.10-1 Repeat Exercise 8.9-1 this time using the TEM mode hybrid ring (rat race) coupler.

a. How does the VSWR bandwidth compare to that of the branch line?

b. When you cascade two circuits, how does the performance compare with the cascaded branch line couplers?

E8.11-1 The Wilkinson power divider shown in Figure 8.11-1 uses single quarter-wave inverters to transform the 50-Ω loads to 100 Ω at its tee junction.

a. Design new inverters with a center frequency of 1000 MHz having three cascaded 90° line sections to obtain broader bandwidth. What are the characteristic impedance values for the three line sections? *Hint:* Use the constant ratio step method used in the multisection Q matching.

b. Use a network simulator to plot the VSWR of your divider and compare it to that of the single inverter mode over the 0- to 2000-MHz frequency interval. Model your design using a network simulator. How broad a −20 dB return loss bandwidth can you get?

c. Based on the single inverter design shown in Figure 8.11-1, select the values of the three bridging resistors to be used in your design and use the network simulator to plot the isolation obtained over the 0- to 2000-MHz band with your choices. *Hint:* Guess starting values for the three resistors and then use the optimizer of the network simulator with a goal of 30-dB minimum isolation between the output ports from 500 to 1500 MHz.

CHAPTER 9

Filter Design

9.1 VOLTAGE TRANSFER FUNCTION

In the specification and design of filters we are interested in the ratio of the sinusoidal voltage at the load, V_L, relative to that of the generator, V_G, as a function of frequency. Classical filter theory begins with LLFPB (lumped, linear, finite, passive, and bilateral) elements. These designs can be extended to high frequencies at which distributed elements are employed having resonances, such as reactively terminated transmission lines with zero and infinite input impedance values.

In Section 2.9 we proved that maximum power is transferred between a generator and load when the impedance of the generator, Z_G, is related to the impedance of the load, Z_L, by $Z_G = Z_L^*$. In our treatment of filters we consider only cases in which the source and load impedances are both real. Then $Z_G = R_G$ and $Z_L = R_L$ as shown in Figure 9.1-1. Under these conditions [1, pp. 11–13], *the available voltage V_{avail} is defined as the voltage across the load when all of the available power from the generator is transferred to the load.*

When source and load have different resistances

$$V_{\text{avail}} = \sqrt{\frac{R_L}{R_G}}\left(\frac{V_G}{2}\right) \tag{9.1-1}$$

Dividing both sides by V_L,

$$\frac{V_{\text{avail}}}{V_L} = \frac{1}{2}\sqrt{\frac{R_L}{R_G}}\left(\frac{V_G}{V_L}\right) \tag{9.1-2}$$

The *voltage transmission coefficient t* is defined as

$$t = \frac{V_L}{V_{\text{avail}}} = 2\sqrt{\frac{R_G}{R_L}}\left(\frac{V_G}{V_L}\right) \tag{9.1-3}$$

High Frequency Techniques: An Introduction to RF and Microwave Engineering, By Joseph F. White.
ISBN 0-471-45591-1

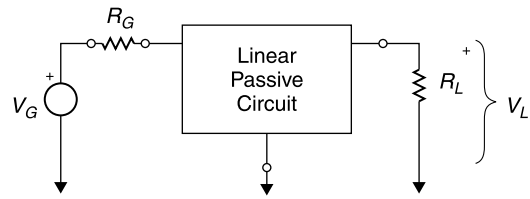

Figure 9.1-1 Two-port network driven by a voltage source and terminated at both ports.

For the filters that we shall consider, t will be unity or less. Since we wish to describe the insertion loss ratio as a number equal to unity or greater, we define the *transfer function of a network* as H where

$$H = \frac{1}{t} \tag{9.1-4}$$

Then the *attenuation of the network*, also called the *transducer loss of the network* (previously defined in Section 2.10), in decibels, is

$$\text{TL} = 10 \log \frac{P_{\text{avail}}}{P_L} = 20 \log|H| \tag{9.1-5}$$

where $P_L = V_L^2/R_L$. These definitions are the basis by which the attenuation of filters can be described. For the filter examples to be presented in this chapter $R_G = R_L = Z_0$ in which case *transducer loss* and *insertion loss* are equal, and the attenuation of the network can be written as

$$\text{IL} = -20 \log|S_{21}| \tag{9.1-6}$$

where S_{21} is one of the S parameters of the network defined under the condition that source and load are equal to the real value Z_0. The format of (9.1-6) is used because this is an available output of the network simulator used to evaluate the filter design examples.

9.2 LOW-PASS PROTOTYPE

Many microwave filters are designed based upon a *low-pass filter prototype*, consisting of alternating shunt admittances and series impedances, or vice versa, series impedances and shunt admittances (Fig. 9.2-1). For nearly all designs lossless elements are employed, thus the alternating elements are actually reactances and susceptances. As lumped circuits these are L and C elements.

When the input impedance Z_{IN} of a three-element ladder network with a 1-Ω load and maximally flat low-pass response with 3-dB cutoff frequency of 1

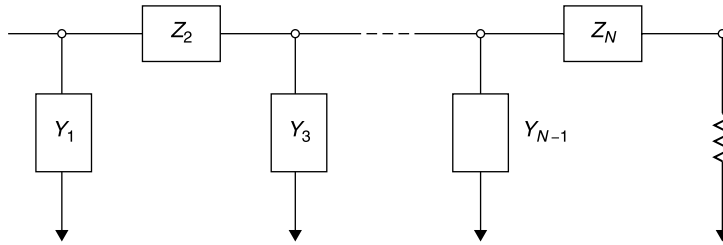

Figure 9.2-1 Filter prototype ladder network, synthesized by continued fraction expansion. Shunt elements are susceptances and series elements are reactances. A resistive termination loads the network.

rad/s is written as a fractional expansion, it takes the form [1, p. 26]

$$Z_{\text{IN}} = \cfrac{1}{s + \cfrac{1}{2s + \cfrac{1}{s+1}}} \tag{9.2-1}$$

where $s = \sigma + j\omega$ is used to express the transfer function of the filter. The corresponding values for the elements of the three-element ladder network are

$$Y_3 = 1s \qquad C_3 = 1 \text{ F} \tag{9.2-1a}$$

$$Z_2 = 2s \qquad L_2 = 2 \text{ H} \tag{9.2-1b}$$

$$Y_1 = 1s \qquad C_1 = 1 \text{ F} \tag{9.2-1c}$$

This example defines an $N = 3$, low-pass filter.

In a similar fashion the element values for filters having 2 to N elements can be determined. The element values are called *g values* because the filter can be initiated with either a series L or a shunt C to which alternating elements are added. Thus the same set of g values for an N element filter can be used for either of two designs, depending upon whether one begins with a series or a shunt element. Thus, starting with a series inductor, the g_1 value is its inductance in henrys, while starting with a shunt capacitor requires interpreting the g_1 value as the capacitance in farads. Thereafter the elements of the filter alternate both in kind (inductance or capacitance) *and* in topology (series or shunt).

9.3 BUTTERWORTH OR MAXIMALLY FLAT FILTER

The maximally flat low-pass prototype filter is called a *Butterworth* response. It has the attributes that *the transducer loss and all of its derivatives are zero at zero frequency*; hence it provides maximum flatness.

TABLE 9.3-1 g Values for Butterworth Low-Pass Prototype Filter

N	g_1	g_2	g_3	g_4	g_5	g_6	g_7	g_8	g_9	g_{10}	g_{11}
2	1.4142	1.4142	1								
3	1.0000	2.0000	1.0000	1							
4	0.7654	1.8478	1.8478	0.7654	1						
5	0.6180	1.6180	2.0000	1.6180	0.6180	1					
6	0.5176	1.4142	1.9318	1.9318	1.4142	0.5176	1				
7	0.4450	1.2470	1.8019	2.0000	1.8019	1.2470	0.4450	1			
8	0.3902	1.1111	1.6629	1.9616	1.9616	1.6629	1.1111	0.3902	1		
9	0.3473	1.0000	1.5321	1.8794	2.0000	1.8794	1.5321	1.0000	0.3473	1	
10	0.3129	0.9080	1.4142	1.7820	1.9754	1.9754	1.7820	1.4142	0.9080	0.3129	1

Source: After Rhea [1, p. 47]. Used with permission.

This is because it is a mathematical fact that *if two polynomials of order N have N points in common they are identical*. Consequently, if by alternate means we find a filter function having a zero value and zero derivatives at zero frequency, we can be confident that it is the one and only such solution, the Butterworth.

The order N of a filter is equal to the number of poles and zeros in its transmission response. In the stopband of a filter N determines how rapidly the isolation increases after the cutoff frequency (it increases at $6N$ dB/octave). In the passband N equals the number of derivatives of the response characteristic. This affects the flatness of the passband response or, in the case of the Chebyshev response to be described, the number of ripples in the passband.

For a lumped-element filter, N is equal to the number of nontrivial elements in the filter network. Nontrivial elements are those which alternate in type between L and C elements. In a filter, nontrivial L and C elements each produce a pole at zero frequency and a zero at infinite frequency or vice versa.

Trivial elements are those that can be combined without changing the response. For example, two capacitors in series or in parallel count as only one *nontrivial element* because they could be replaced by a single capacitor having an appropriately defined value. Similarly, two inductors in series or parallel also would count as only one nontrivial element.

In a filter network a resonator consisting of one L in series or in parallel with one C element counts as two nontrivial elements. Such a resonator produces a pole or zero in the filter response at a finite frequency.

The low-pass prototype Butterworth filter response is obtained by having alternating L and C elements with the values listed in Table 9.3-1, normalized to 1 Ω and having a cutoff frequency (3 dB loss) of 1 rad/s. Notice that there is an additional g value listed for each filter type. For example, for $N = 2$ there is a g_3 value listed. This is the value of the load with which the filter delivers its response. The generator impedance in these tables is always assumed to be a unity resistance. Note that *the g_i values in the prototype filter tables correspond to the value of series reactance or shunt susceptance of the respective lumped elements at the cutoff frequency f_C*. For the prototype filter circuit f_C is 1 rad/s.

All Butterworth filters have a unity load, but we shall see that for certain filters a nonunity load would be required to obtain the specified response (Fig. 9.3-1). Since there is no practical way to build an ideal transformer to transform a Z_0 load to another real value at all frequencies simultaneously, we will avoid filter design examples requiring unequal source and load resistances, except in the special case of diplexer filters.

9.4 DENORMALIZING THE PROTOTYPE RESPONSE

Of course, we do not want a 1-Ω filter with cutoff at 1 rad/s (0.16 Hz). Therefore, we scale both the impedance and frequency of the filter by adjusting the L

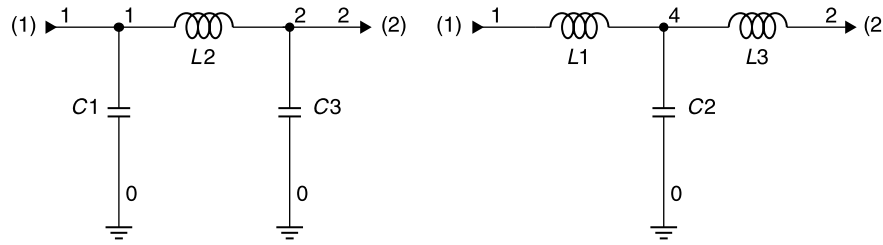

Figure 9.3-1 Either of these networks yields the same Butterworth low-pass response into a unity load.

and C values. Since the reactance of an inductor is

$$X_i = \omega L_i \tag{9.4-1}$$

it follows that to obtain a series impedance at our desired characteristic impedance Z_0 and cutoff frequency f_C, we must multiply the prototype g_i value so that

$$L_i = \frac{g_i Z_0}{2\pi f_C} \tag{9.4-2}$$

Similarly, since the reactance of a capacitor is

$$X_i = \frac{1}{\omega C_i} \tag{9.4-3}$$

then the corresponding value of C_i for our Z_0, f_C and g_i is

$$C_i = \frac{g_i}{Z_0 2\pi f_C} \tag{9.4-4}$$

In these filter design examples Z_0 is the impedance of the system. Later, if a lumped-element filter is used in a high frequency network, the Z_0 impedance of source and load will be presented to the filter when the filter is connected to them using transmission lines of Z_0 characteristic impedance.

As a filter design example, suppose that we wish to design a low-pass Butterworth filter with 3-dB cutoff at 1 GHz and $Z_0 = 50\ \Omega$. The g values are

$$g_1 = 1.000 \tag{9.4-5a}$$

$$g_2 = 2.000 \tag{9.4-5b}$$

$$g_3 = 1.000 \tag{9.4-5c}$$

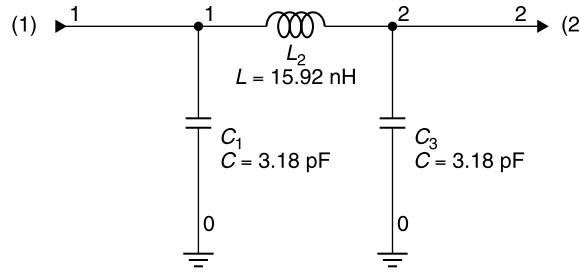

Figure 9.4-1 Three-element Butterworth low-pass filter with 3-dB cutoff at 1 GHz and $Z_0 = 50\ \Omega$.

Furthermore, let's say that we want the filter to be in the π configuration, having a C as the first (shunt) element. Then

$$C_1 = C_3 = \frac{1.000}{(50)(2\pi)(1 \times 10^9)} = 3.18 \text{ pF} \qquad (9.4\text{-}6a,b)$$

$$L_2 = \frac{(2.000)(50)}{(2\pi)(1 \times 10^9)} = 15.92 \text{ nH} \qquad (9.4\text{-}6c)$$

The filter, scaled to our frequency and impedance, is shown in Figure 9.4-1.

In the network simulation of the circuit in Figure 9.4-1 the implicit source and load impedances are 50 Ω in the specifications of input port (1) and output port (2). The response of the filter in Figure 9.4-1 is shown in Figure 9.4-2.

In Figure 9.4-2 the lower curve uses the left y axis coordinates (expanded insertion loss), and the upper curve uses the right y axis (to show isolation), where the terms *insertion loss* (commonly used to describe transducer loss) and *isolation* are selected to describe the intended *passband* and *stopband* of the filter, respectively. Note that the insertion loss is 3 dB at 1 GHz as predicted.

Next, note that the isolation at 2 GHz is 18 dB and that the isolation at 4 GHz is 36 dB, an increase of 18 dB/octave. This also is expected for a three-element filter for which the isolation increases by $6N$ dB/octave, or 18 dB/octave. Had we used a five-element filter, the isolation would have increased by 30 dB/octave.

Filters made with lossless L and C elements achieve their frequency selective attenuation by reflecting power. For the low-pass Butterworth example the insertion loss at 1 GHz is 3 dB. This means that the reflected power is 50% of that which is incident. The corresponding reflection coefficient magnitude is 0.707 and the VSWR is 5.82. Figure 9.4-3 shows the VSWR of this low-pass filter example.

It should be emphasized that because reactive filters have high reflection coefficients their performance can be changed if they are interconnected with

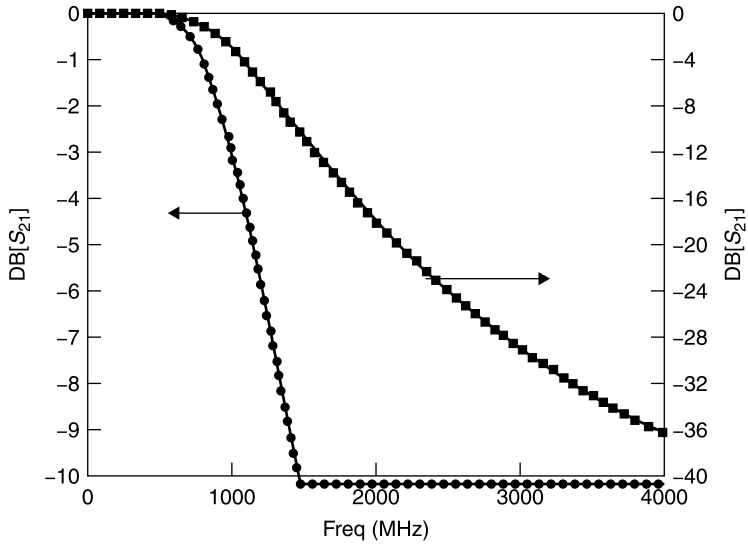

Figure 9.4-2 Insertion loss/isolation of the three-element low-pass filter with 1 GHz, 3-dB cutoff, and 50 Ω impedance.

other networks that also have appreciable reflections. The reflection interaction or *mismatch error*, as described in Section 4.7, can dramatically change the insertion loss performance from that expected using filter design theory. For example, suppose two of the three-element Butterworth low-pass filters as described in the preceding example are cascaded with a 60° long interconnecting

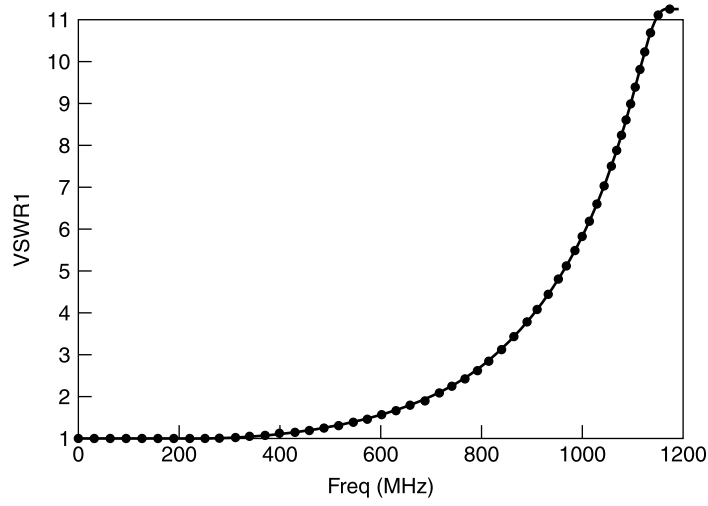

Figure 9.4-3 VSWR of the three-element Butterworth low-pass filter.

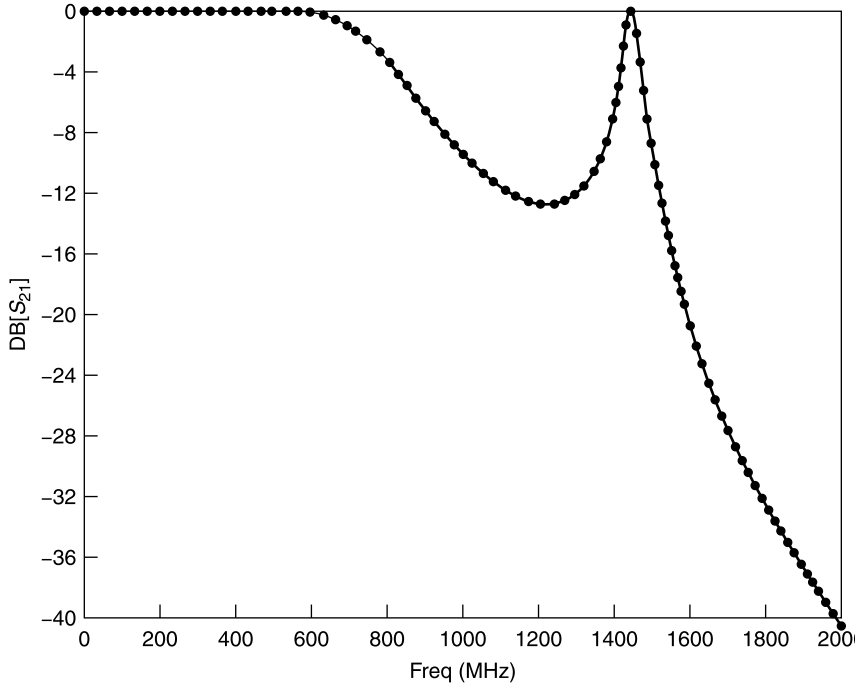

Figure 9.4-4 Two of the three-element Butterworth low-pass filters cascaded with a 60° long 50-Ω transmission line between them.

length of 50-Ω transmission line between them. The resulting insertion loss with frequency is shown in Figure 9.4-4.

From Figure 9.4-2 we might have expected about 8 dB of isolation from each filter at 1.4 GHz. However, with this spacing the reflective interactions of the two filters cause a canceling of their separate reflective attenuations, resulting in no net attenuation for the cascade at 1.4 GHz. For this reason, *it is not sufficient to design a reactive filter without also considering the environment in which it will be used.*

9.5 HIGH-PASS FILTERS

To design a highpass filter:

1. Begin with the low-pass prototype, replacing all C's with L's and all L's with C's, respectively.
2. Invert all g_i values.
3. Denormalize the resulting high-pass prototype C's and L's using

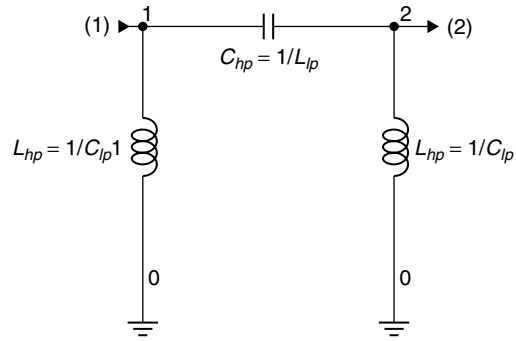

Figure 9.5-1 Conversion of the low-pass prototype filter to the high-pass prototype filter.

$$L_i = \frac{g_i Z_0}{2\pi f_C} \tag{9.5-1}$$

$$C_i = \frac{g_i}{Z_0 2\pi f_C} \tag{9.5-2}$$

For example, if we wish to convert our three-element low-pass filter to a high-pass filter, the prototype circuit is as shown in Figure 9.5-1 and the highpass prototype element values are

$$C_{\text{hp}} = \frac{1}{L_{\text{lp}}} = \frac{1}{2.000} = 0.500 \tag{9.5-3}$$

$$L_{\text{hp}} = \frac{1}{C_{\text{lp}}} = \frac{1}{1.000} = 1.000 \tag{9.5-4}$$

Denormalizing these to our 50 Ω impedance and 1 GHz cutoff frequency gives

$$L_i = \frac{g_i Z_0}{2\pi f_C} \tag{9.5-5}$$

$$C_i = \frac{g_i}{Z_0 2\pi f_C} \tag{9.5-6}$$

$$L_1 = L_3 = \frac{(1.000)(50)}{(2\pi)(1 \times 10^9)} = 7.96 \text{ nH} \tag{9.5-7}$$

$$C_2 = \frac{0.500}{(50)(2\pi)(1 \times 10^9)} = 1.59 \text{ pF} \tag{9.5-8}$$

The resulting circuit and performance is shown in Figure 9.5-2. Notice that the isolation at 250 MHz is about 18 dB greater than at 500 MHz, consistent with the 18-dB/octave isolation slope for a third-order filter.

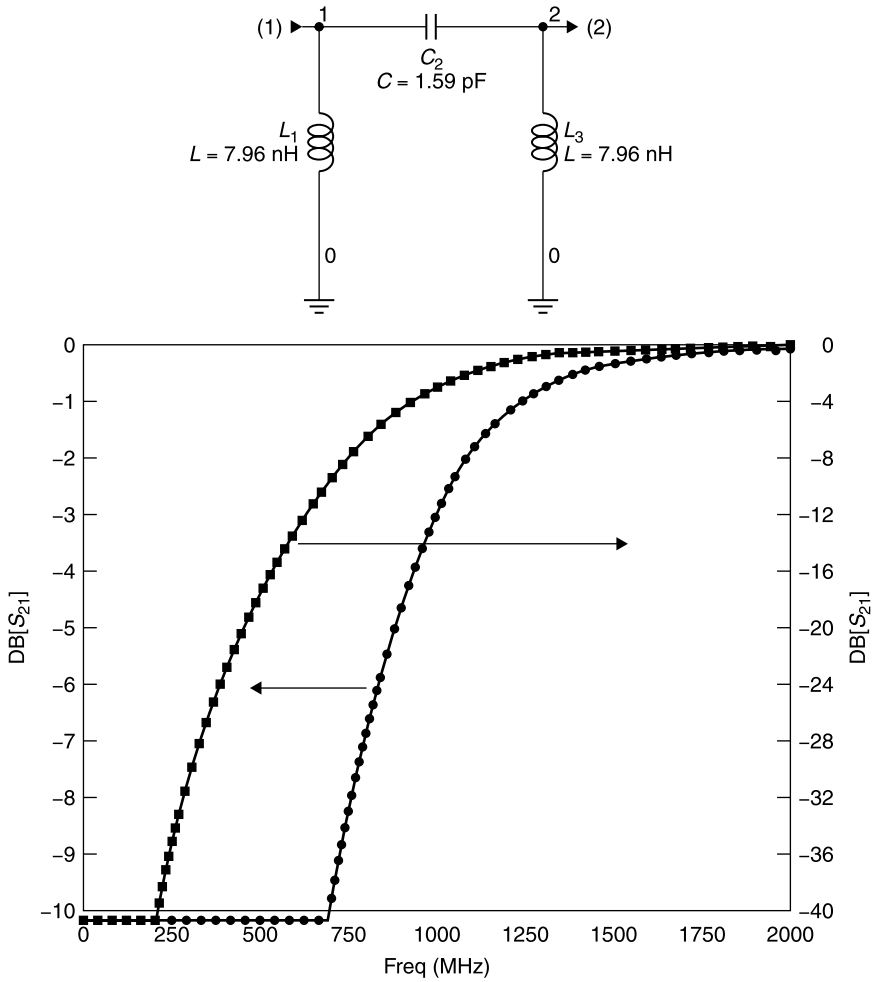

Figure 9.5-2 Loss/isolation of the high-pass filter.

9.6 BANDPASS FILTERS

Lumped-element bandpass and bandstop filters can be designed by starting with the low-pass and high-pass prototypes presented in the preceding sections. It is also possible to design transmission equivalents to these filters using Richard's transformation and Kuroda's identities [2, Sec. 9.5]. We will cover these topics shortly. For these reasons the low-pass and high-pass prototypes are important beyond their immediate importance as lumped-element filters. This and the following sections will concentrate on the lumped-element filters, which are common in high frequency applications. Their use extends well into

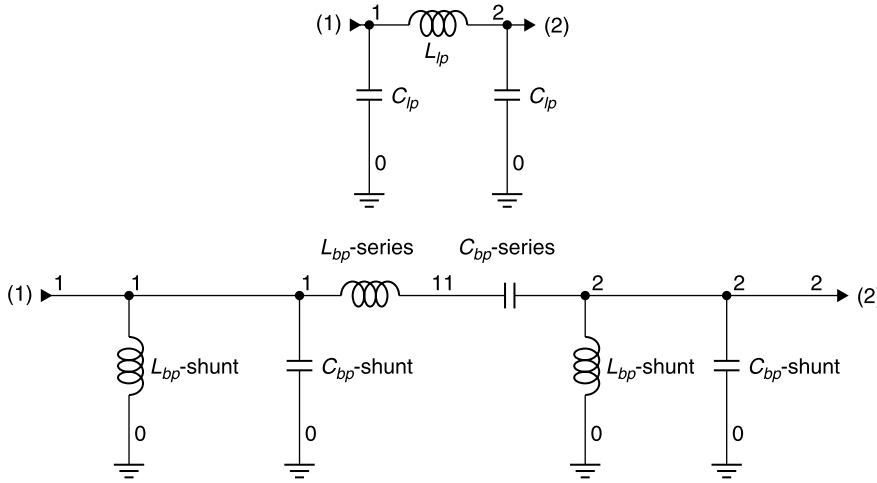

Figure 9.6-1 Transformation relations to convert the low-pass prototype filter to a bandpass prototype filter.

the microwave frequency bands as integrated circuit techniques allow realization of the small values of L and C that they require.

To design a bandpass filter starting with a low-pass prototype [1, p. 146] (Fig. 9.6-1):

1. Define the following:

$$f_l = \text{lower 3-dB cutoff frequency} \tag{9.6-1}$$

$$f_u = \text{upper 3-dB cutoff frequency} \tag{9.6-2}$$

$$f_0 = \text{geometric center frequency}$$

$$f_0 = \sqrt{f_l f_u} \tag{9.6-3}$$

$$\text{BW} = f_u - f_l = \text{absolute bandwidth} \tag{9.6-4}$$

$$\text{bw} = \frac{\text{BW}}{f_0} = \text{fractional bandwidth} \tag{9.6-5}$$

$$\text{Percentage bandwidth} = 100\%(\text{bw}) \tag{9.6-6}$$

2. Replace each series inductor with a series capacitor and series inductor resonator.
3. Replace each shunt capacitor with a shunt capacitor and parallel shunt inductor resonator.
4. Create the prototype (normalized) bandpass filter, assigning its elements the values shown below.

Transformed shunt elements:

$$C_{\text{bp-shunt}} = \frac{C_{\text{lp}}}{\text{bw}} \tag{9.6-7}$$

$$L_{\text{bp-shunt}} = \frac{1}{C_{\text{bp-shunt}}} \tag{9.6-8}$$

Transformed series elements:

$$L_{\text{bp-series}} = \frac{L_{\text{lp}}}{\text{bw}} \tag{9.6-9}$$

$$C_{\text{bp-series}} = \frac{1}{L_{\text{bp-series}}} \tag{9.6-10}$$

5. Denormalize all elements to obtain the final filter design. Note: Use f_0 in place of f_c. Thus,

$$L_i = \frac{g_i Z_0}{2\pi f_0} \tag{9.6-11}$$

$$C_i = \frac{g_i}{Z_0 2\pi f_0} \tag{9.6-12}$$

We now design a bandpass example based on our previous three-element low-pass prototype (Fig. 9.6-2). Suppose we wish a 3-dB passband from 800 to 1200 MHz. Then, BW = 400 MHz and

$$f_0 = \sqrt{(800)(1200)} = 979.8 \text{ MHz}$$
$$\text{bw} = 400/979.8 = 0.4082$$

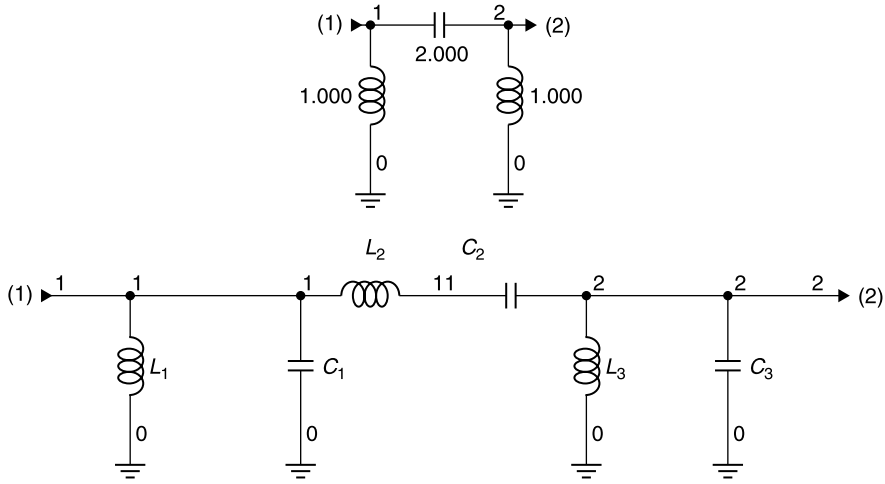

Figure 9.6-2 Schematic for the transition from low-pass to band-pass filter prototype.

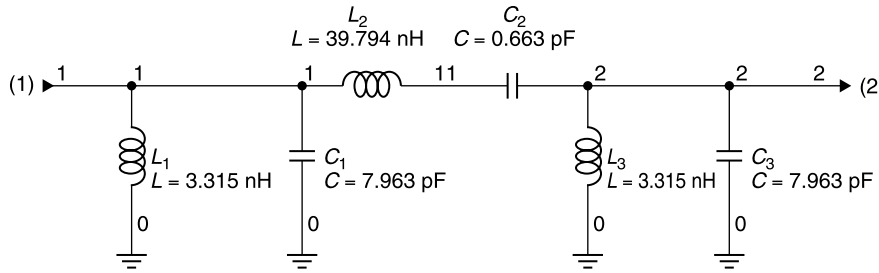

Figure 9.6-3 Denormalized bandpass filter schematic.

First, performing the prototype (normalized circuit) conversion:

$$c_1 = c_3 = \frac{c_{\text{lp}}}{\text{bw}} = \frac{1.000}{0.4082} = 2.4498$$

$$l_1 = l_3 = \frac{1}{c_1} = \frac{1}{2.4498} = 0.4082$$

$$l_2 = \frac{l_{\text{lp}}}{\text{bw}} = \frac{2.000}{0.4082} = 4.8996$$

$$c_2 = \frac{1}{l_2} = \frac{1}{4.8996} = 0.2041$$

where the lowercase letters designate the impedance and frequency normalized prototype filter. Next, denormalize the circuit (Fig. 9.6-3).

$$C_1 = C_3 = \frac{c_1}{Z_0 2\pi f_0} = \frac{2.4498}{(50)(2\pi)(979.8 \times 10^6)} = 7.9628 \text{ pF}$$

$$L_1 = L_3 = \frac{l_1 Z_0}{2\pi f_0} = \frac{(0.4082)(50)}{(2\pi)(979.8 \times 10^6)} = 3.315 \text{ nH}$$

$$L_2 = \frac{l_2 Z_0}{2\pi f_0} = \frac{(4.8996)(50)}{(2\pi)(979.8 \times 10^6)} = 39.7936 \text{ nH}$$

$$C_2 = \frac{c_2}{Z_0 2\pi f_0} = \frac{0.2041}{(50)(2\pi)(979.8 \times 10^6)} = 0.66306 \text{ pF}$$

The performance of this design can be seen in Figure 9.6-4, which shows the expanded insertion loss on the left y axis and the isolation on the right y axis. The 3-dB bandwidth extends from 800 to 1200 MHz, as was intended by design. Also note the steep isolation "skirts" of the performance plot. At 500 and 2000 MHz, for frequencies that are an octave removed from the center frequency of about 1000 MHz, the isolation is nearly 36 dB. This is appropriate for a $N = 6$ filter, the number of nontrivial elements in the circuit of Figure

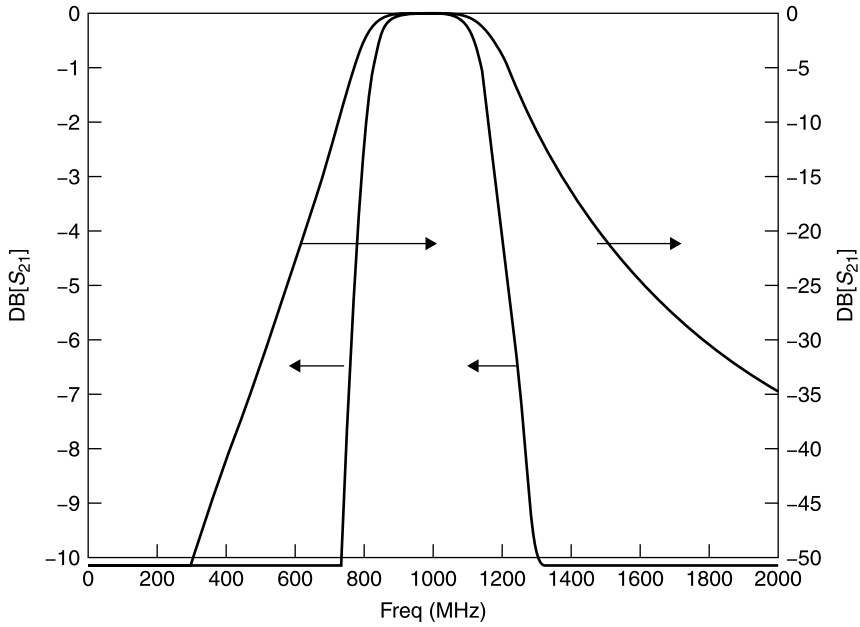

Figure 9.6-4 Calculated loss/isolation of the denormalized bandpass filter.

9.6-3. A consequence of scaling a bandpass filter from a low-pass prototype is that the order, N, of the filter is doubled.

9.7 BANDSTOP FILTERS

The design procedure for bandstop filters is similar to that of bandpass filters. However, for the bandstop filters the series resonant circuits are in shunt with the transmission line and the parallel resonant circuits are in series (Fig. 9.7-1).

The shunt resonator elements are found from [1, p. 151]

$$L_{\text{bs-shunt}} = \frac{1}{C_{\text{lp}}\text{bw}} \tag{9.7-1}$$

$$C_{\text{bs-shunt}} = \frac{1}{L_{\text{bs-shunt}}} \tag{9.7-2}$$

and the series resonator elements are found as

$$C_{\text{bs-series}} = \frac{1}{L_{\text{lp}}\text{bw}} \tag{9.7-3}$$

$$L_{\text{bs-series}} = \frac{1}{C_{\text{bs-series}}} \tag{9.7-4}$$

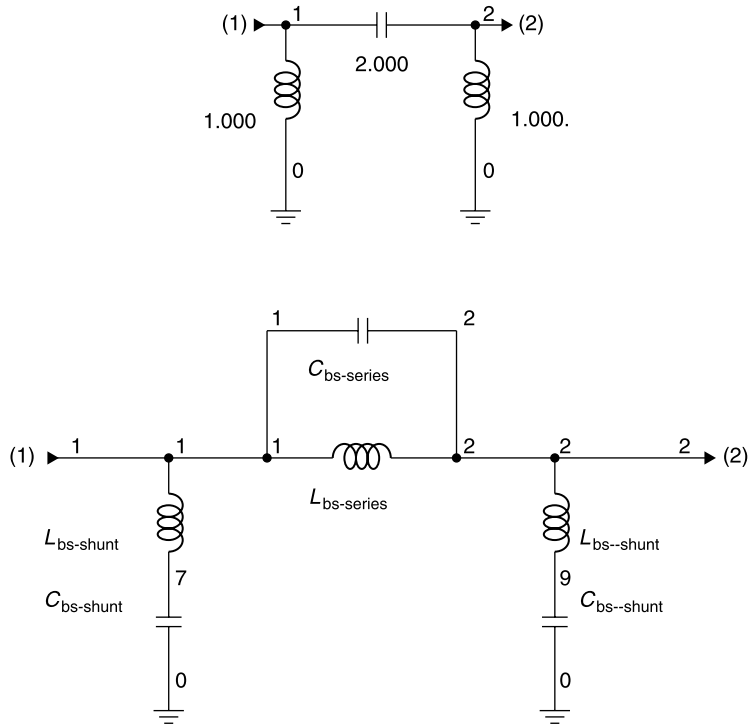

Figure 9.7-1 Developing a bandstop filter from the low-pass prototype.

Following our three-element filter examples, suppose we wish to design a bandstop filter with stopband from 800 to 1200 MHz. The steps are as follows. Using (9.7-1) to (9.7-4),

$$l_1 = l_3 = \frac{1}{c_{\text{lp}}\text{bw}} = \frac{1}{(1.000)(0.4082)} = 2.4498$$

$$c_1 = c_3 = \frac{1}{l_1} = \frac{1}{2.4498} = 0.4082$$

$$c_2 = \frac{1}{l_{\text{lp}}\text{bw}} = \frac{1}{(2.000)(0.4082)} = 1.2249$$

$$l_2 = \frac{1}{c_2} = \frac{1}{1.2249} = 0.8164$$

After computing the values of the normalized bandstop prototype from (9.7-1) to (9.7-4), the elements are denormalized, in the manner used for the bandpass filter. Denormalizing,

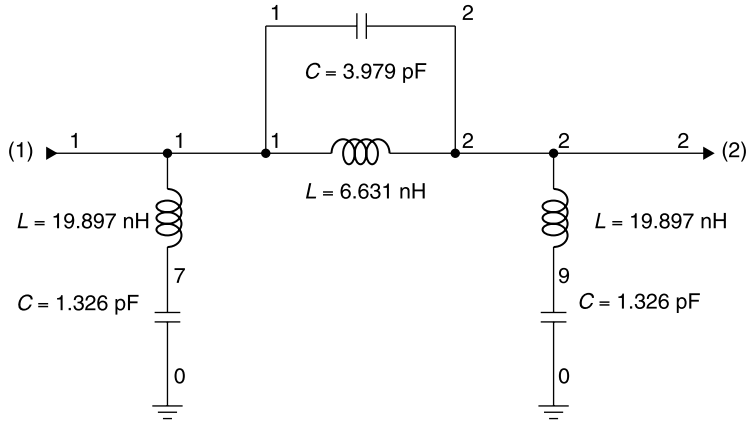

Figure 9.7-2 The 800- to 1200-MHz bandstop filter.

$$L_1 = L_3 = \frac{l_1 Z_0}{2\pi f_0} = \frac{(2.4498)(50)}{(2\pi)(979.8 \times 10^6)} = 19.8968 \text{ nH}$$

$$C_1 = C_3 = \frac{c_1}{Z_0 2\pi f_0} = \frac{0.4082}{(50)(2\pi)(979.8 \times 10^6)} = 1.3261 \text{ pF}$$

$$L_2 = \frac{l_2 Z_0}{2\pi f_0} = \frac{(0.8164)(50)}{(2\pi)(979.8 \times 10^6)} = 6.6306 \text{ nH}$$

$$C_2 = \frac{c_2}{Z_0 2\pi f_0} = \frac{1.2249}{(50)(2\pi)(979.8 \times 10^6)} = 3.9794 \text{ pF}$$

The resulting circuit is shown in Figure 9.7-2 and its performance in Figure 9.7-3. The 3-dB loss values border the stopband at 800 and 1200 MHz as planned. The isolation for this lossless filter is infinite at the band center near 1000 MHz.

9.8 CHEBYSHEV FILTERS

Chebyshev (his name is anglicized and sometimes written as Tchebyscheff, also anglicized) was a Russian mathematician credited with the Chebyshev polynomials. The polynomials have the interesting property that they have equal ripples (values at zero slope) the number of which is equal to half the order N of the polynomial. Since the order of a filter is equal to its number of nontrivial elements, an N element filter can have N changes of slope, or $N/2$ ripples, in its passband. Matching the filter's response to a Chebyshev polynomial provides an *equal ripple* response in the passband.

The reasoning behind matching a filter's transmission characteristic to a Chebyshev polynomial is that, if one can accept a certain amount of insertion

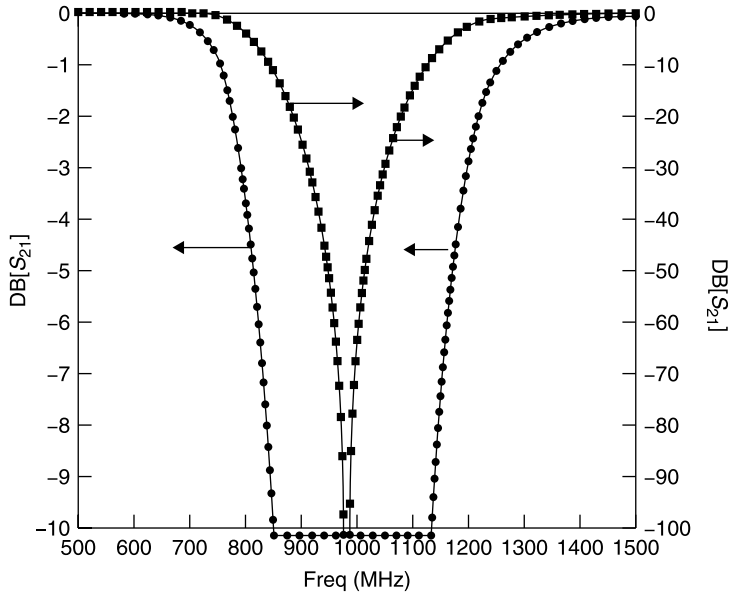

Figure 9.7-3 Calculated loss/isolation of the 800- to 1200-MHz bandstop filter.

loss at the band edges of a filter, perhaps that same loss allowance could be tolerated anywhere within the passband. If this is acceptable, then, for a given width passband, the Chebyshev filter response yields a lower peak value of passband loss or a wider bandwidth for the same peak passband loss.

However, to design Chebyshev filters, we require a *separate table of prototype values for each value of maximum ripple*. Another consequence of the loss ripple is that *even-order Chebyshev filters cannot have equal source and load resistances*. This is because the even-order filters must have a mismatch at zero frequency, and this can only occur if source and load resistances are correspondingly different. Designing filters that are only odd-order circumvents this problem; source and load can have equal impedances.

For the filter tables, it is assumed that the source impedance, $g(0)$, is unity, and the last value in the table for a given order filter is the magnitude of the required load resistance. We confine our examples to those having unity load resistance.

Given these distinctions, the design of Chebyshev filters proceeds exactly as presented for the Butterworth designs. Tables 9.8-1 to 9.8-5 give the normalized low-pass prototype values. Transformations to high-pass, bandpass, and bandstop filters proceed as previously described. There are other sources for Chebyshev filter tables; however, these tables by Rhea are especially convenient to use because the g values yield filters having a cutoff frequency at the maximum ripple value rather than at the 3-dB loss frequency.

TABLE 9.8-1 Chebyshev 0.01-dB Equal Ripple (RL = 26.4 dB)

N	g_1	g_2	g_3	g_4	g_5	g_6	g_7	g_8	g_9	g_{10}	g_{11}
2	0.4489	0.4078	0.9085								
3	0.6292	0.9703	0.6292	1							
4	0.7129	1.2004	1.3213	0.6476	0.9085						
5	0.7563	1.3049	1.5773	1.3049	0.7563	1					
6	0.7814	1.3600	1.6897	1.5350	1.4970	0.7098	0.9085				
7	0.7970	1.3924	1.7481	1.6331	1.7481	1.3924	0.7970	1			
8	0.8073	1.4131	1.7824	1.6833	1.8529	1.6193	1.5555	0.7334	0.9085		
9	0.8145	1.4271	1.8044	1.7125	1.9058	1.7125	1.8044	1.4271	0.8145	1	
10	0.8197	1.4370	1.8193	1.7311	1.9362	1.7590	1.9055	1.6528	1.5817	0.7446	1

Source: After Rhea [1, pp. 48–49]. Used with permission.

TABLE 9.8-2 Chebyshev 0.0432-dB Equal Ripple (RL = 20 dB)

N	g_1	g_2	g_3	g_4	g_5	g_6	g_7	g_8	g_9	g_{10}	g_{11}
2	0.6648	0.5445	0.8190								
3	0.8516	1.1032	0.8516	1							
4	0.9314	1.2920	1.5775	0.7628	0.8190						
5	0.9714	1.3721	1.8014	1.3721	0.9714	1					
6	0.9940	1.4131	1.8933	1.5506	1.7253	0.8141	0.8190				
7	1.0080	1.4368	1.9398	1.6220	1.9398	1.4368	1.0080	1			
8	1.0171	1.4518	1.9667	1.6574	2.0237	1.6107	1.7726	0.8330	0.8190		
9	1.0235	1.4619	1.9837	1.6778	2.0649	1.6778	1.9837	1.4619	1.0235	1	
10	1.0281	1.4690	1.9952	1.6906	2.0882	1.7102	2.0642	1.6341	1.7936	0.8420	0.8190

Source: After Rhea [1, pp. 48–49]. Used with permission.

TABLE 9.8-3 Chebyshev 0.10-dB Equal Ripple (RL = 16.4 dB)

N	g_1	g_2	g_3	g_4	g_5	g_6	g_7	g_8	g_9	g_{10}	g_{11}
2	0.8431	0.6220	0.7378								
3	1.0316	1.1474	1.0316	1							
4	1.1088	1.3062	1.7704	0.8181	0.7378						
5	1.1468	1.3712	1.9750	1.3712	1.1468	1					
6	1.1681	1.4040	2.0562	1.5171	1.9029	0.8618	0.7378				
7	1.1812	1.4228	2.0967	1.5734	2.0967	1.4228	1.1812	1			
8	1.1898	1.4346	2.1199	1.6010	2.1700	1.5641	1.9445	0.8778	0.7378		
9	1.1957	1.4426	2.1346	1.6187	2.2054	1.6167	2.1346	1.4426	1.1957	1	
10	1.2000	1.4482	2.1445	1.6266	2.2254	1.6419	2.2046	1.5822	1.9629	0.8853	0.7378

Source: After Rhea [1, pp. 48–49]. Used with permission.

TABLE 9.8-4 Chebyshev 0.20-dB Equal Ripple (RL = 13.5 dB)

N	g_1	g_2	g_3	g_4	g_5	g_6	g_7	g_8	g_9	g_{10}	g_{11}
2	1.0379	0.6746	0.6499								
3	1.2276	1.1525	1.2276	1							
4	1.3029	1.2844	1.9762	0.8468	0.6499						
5	1.3395	1.3370	2.1661	1.3370	1.3395	1					
6	1.3598	1.3632	2.2395	1.4556	2.0974	0.8838	0.6499				
7	1.3723	1.3782	2.2757	1.5002	2.2757	1.3782	1.3723	1			
8	1.3804	1.3876	2.2964	1.5218	2.3414	1.4925	2.1349	0.8972	0.6499		
9	1.3861	1.3939	2.3094	1.5340	2.3728	1.5340	2.3094	1.3939	1.3861	1	
10	1.3901	1.3983	2.3181	1.5417	2.3905	1.5537	2.3720	1.5066	2.1514	0.9035	0.6499

Source: After Rhea [1, pp. 48–49]. Used with permission.

TABLE 9.8-5 Chebyshev 0.50-dB Equal Ripple (RL = 9.6 dB)

N	g_1	g_2	g_3	g_4	g_5	g_6	g_7	g_8	g_9	g_{10}	g_{11}
2	1.4029	0.7071	0.5040								
3	1.5963	1.0967	1.5963	1							
4	1.6704	1.1926	2.3662	0.8419	0.5040						
5	1.7058	1.2296	2.5409	1.2296	1.7058	1					
6	1.7254	1.2478	2.6064	1.3136	2.4759	0.8696	0.5040				
7	1.7373	1.2582	2.6383	1.3443	2.6383	1.2582	1.7373	1			
8	1.7451	1.2647	2.6565	1.3590	2.6965	1.3389	2.5093	0.8795	0.5040		
9	1.7505	1.2690	2.6678	1.3673	2.7240	1.3673	2.6678	1.2690	1.7505	1	
10	1.7543	1.2722	2.6755	1.3725	2.7393	1.3806	2.7232	1.3484	2.5239	0.8842	0.5040

Source: After Rhea [1, pp. 48–49]. Used with permission.

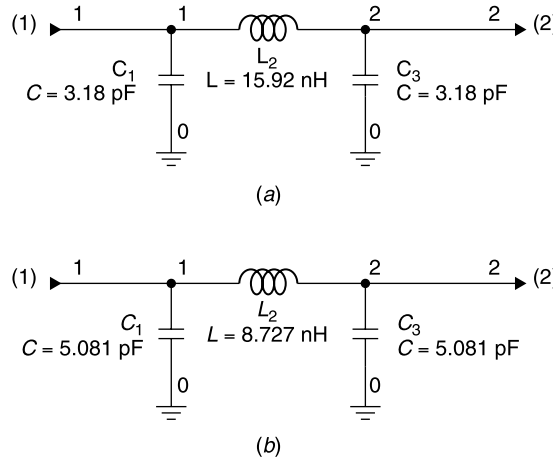

Figure 9.8-1 Comparison of element values for Butterworth and Chebyshev filters. (*a*) Three-section 50-Ω Butterworth low-pass filter with $f_C = 1$ GHz. (*b*) Three-section, 50-Ω, 0.5-dB ripple, Chebyshev low-pass filter with $f_C = 1$ GHz.

As an example, a 50-Ω, three-section, 0.2-dB ripple Chebyshev low-pass filter is designed using the procedure described for the low-pass Butterworth filter. The circuit is shown in Figure 9.8-1 and its performance compared to the three-element Butterworth low-pass filter in Figure 9.8-2.

Notice that the Chebyshev filter has a maximum loss up to 1 GHz of only 0.5 dB, while the Butterworth filter has 3.0-dB loss at 1 GHz. Also, the Chebyshev filter has a steeper slope outside the passband, yielding slightly greater isolation at frequencies above the passband.

9.9 PHASE AND GROUP DELAY

Previously, we described the transfer function H of the network. In the filter performance described up to now, we have been concerned only with the amplitude of the transfer function versus frequency. Usually, this is the predominant characteristic that comes to mind when considering filters.

However, in communication systems the variation of phase shift with frequency through a network becomes of importance when the signal bandwidth is large, as when rapid rise time pulses or video information is transmitted. Then the phase variation with frequency through the network also must be controlled.

The *phase delay* φ (or *phase shift*) through a network is just the argument (angle) of the complex transfer function H. Any network having reactive elements produces a delay in the signal propagation with time [1, pp. 34–36].

If a network passes all frequencies with equal amplitude attenuation and a transmission phase φ *that increases linearly with frequency, the signal will be*

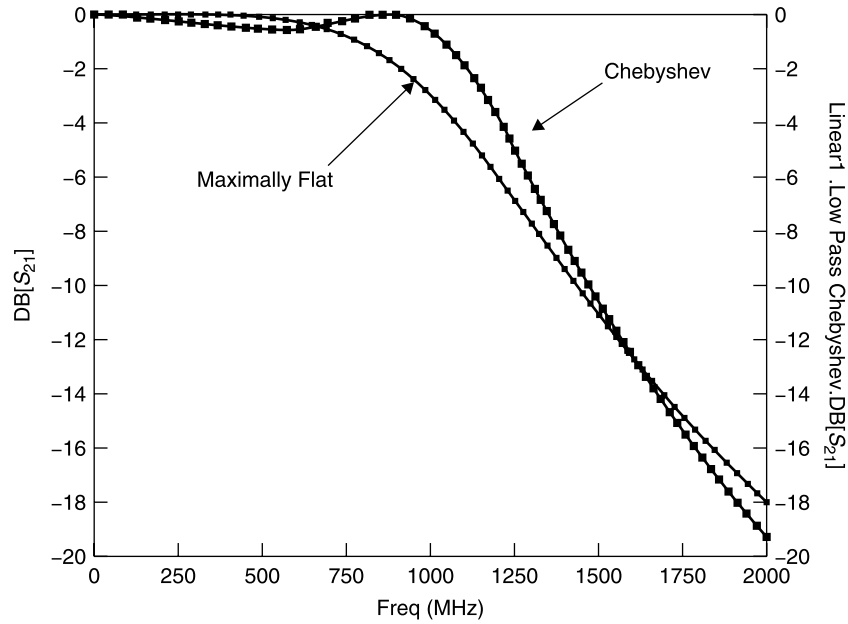

Figure 9.8-2 Calculated loss comparison of Butterworth and 0.5-dB-ripple Chebyshev low-pass filters.

delayed and level shifted but not distorted. The *phase delay* of a network is

$$t_p = \frac{\varphi}{\omega} \tag{9.9-1}$$

and the *group delay* is

$$t_d = -\frac{\partial\varphi}{\partial\omega} \tag{9.9-2}$$

The group delay (also called *envelope delay*) is related to the time required for the envelope of a signal to transverse the network. These characteristics were introduced in Section 4.12 through phase and group velocities.

Unfortunately, good frequency selectivity and constant group delay are mutually exclusive in the passive ladder networks we have been considering. Signal distortion occurs when different frequency components of the composite signal are unequally delayed. This difference is called *differential delay*. Differential group delay is the absolute difference in the group delay at two specified frequencies. It will be seen that the more frequency selective the filter network, the greater the differential delay within the passband. A class of filters that minimizes this distortion is the *Bessel filter*. Table 9.9-1 lists the Bessel g values for this response.

TABLE 9.9-1 Bessel Prototype Filter g Values[a]

N	g_1	g_2	g_3	g_4	g_5	g_6	g_7	g_8	g_9	g_{10}	g_{11}
2	0.5755	2.1478	1								
3	0.3374	0.9705	2.2034	1							
4	0.2334	0.6725	1.0815	2.2404	1						
5	0.1743	0.5072	0.8040	1.1110	2.2582	1					
6	0.1365	0.4002	0.6392	0.8538	1.1126	2.2645	1				
7	0.1106	0.3259	0.5249	0.7020	0.8690	1.1052	2.2659	1			
8	0.0919	0.2719	0.4409	0.5936	0.7303	0.8695	1.0956	2.2656	1		
9	0.0780	0.2313	0.3770	0.5108	0.6306	0.7407	0.8639	1.0863	2.2649	1	
10	0.0672	0.1998	0.3270	0.4454	0.5528	0.6493	0.7420	0.8561	1.0781	2.2641	1

Source: After Rhea [1, p. 49]. Used with permission.

[a]Cutoff frequency loss = 3 dB and source resistance = 1.0.

TABLE 9.9-2 Bessel Equal-Ripple Phase Error 0.05° Filter g Values[a]

N	g_1	g_2	g_3	g_4	g_5	g_6	g_7	g_8	g_9	g_{10}	g_{11}
2	0.6480	2.1085	1								
3	0.4328	0.0427	2.2542	1							
4	0.3363	0.7963	1.1428	2.2459	1						
5	0.2751	0.6541	0.8892	1.1034	2.2873	1					
6	0.2374	0.5662	0.7578	0.8760	1.1163	2.2448	1				
7	0.2085	0.4999	0.6653	0.7521	0.8749	1.0671	2.2845	1			
8	0.1891	0.4543	0.6031	0.6750	0.7590	0.8427	1.0901	2.2415	1		
9	0.1718	0.4146	0.5498	0.6132	0.6774	0.7252	0.8450	1.0447	2.2834	1	
10	0.1601	0.3867	0.5125	0.5702	0.6243	0.6557	0.7319	0.8178	1.0767	2.2387	1

Source: After Rhea [1, p. 50]. Used with permission.

[a]Cutoff frequency loss = 3 dB, source resistance = 1.0.

TABLE 9.9-3 Bessel Equal-Ripple Phase Error 0.5° Filter g Values[a]

N	g_1	g_2	g_3	g_4	g_5	g_6	g_7	g_8	g_9	g_{10}	g_{11}
2	0.8245	1.9800	1								
3	0.5534	1.0218	2.4250	1							
4	0.4526	0.7967	1.2669	2.0504	1						
5	0.3658	0.6768	0.9513	1.0113	2.4446	1					
6	0.3313	0.5984	0.8390	0.7964	1.2734	2.0111	1				
7	0.2876	0.5332	0.7142	0.6988	0.9219	0.9600	2.4404	1			
8	0.2718	0.4999	0.6800	0.6312	0.8498	0.7447	1.3174	1.9626	1		
9	0.2347	0.4493	0.5914	0.5747	0.7027	0.6552	0.8944	0.9255	2.4332	1	
10	0.2359	0.4369	0.5887	0.5428	0.7034	0.5827	0.8720	0.6869	1.4317	1.8431	1

Source: Rhea [1, p. 50]. Used with permission.

[a] $A_a = 3$ dB, $G(0) = 1.0$.

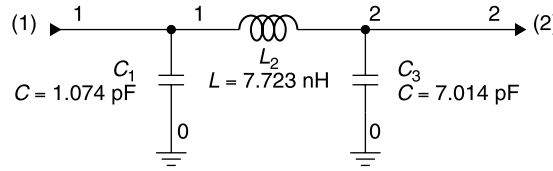

Figure 9.9-1 Bessel 50-Ω, low-pass filter with 3-dB cutoff at 1 GHz.

In addition to the pure Bessel prototype, additional tables provide an "equal phase ripple" in the transmission phase similar to the Chebyshev designs, which provide equal loss ripple in the passband attenuation. Allowing increasing phase ripple in the passband improves the rejection band performance of the Bessel filter. Tables 9.9-2 and 9.9-3 for 0.05° and 0.5° equal-ripple phase error give the g values for these filters.

Constructing our three-element filter using the Bessel response yields the circuit shown in Figure 9.9-1 and the performance shown in Figure 9.9-2. Note that the filter is not symmetric, as were the Butterworth and Chebyshev filters.

Viewing only amplitude response, one might consider the Bessel filter to be so inferior, even to the Butterworth filter, as to warrant no further consider-

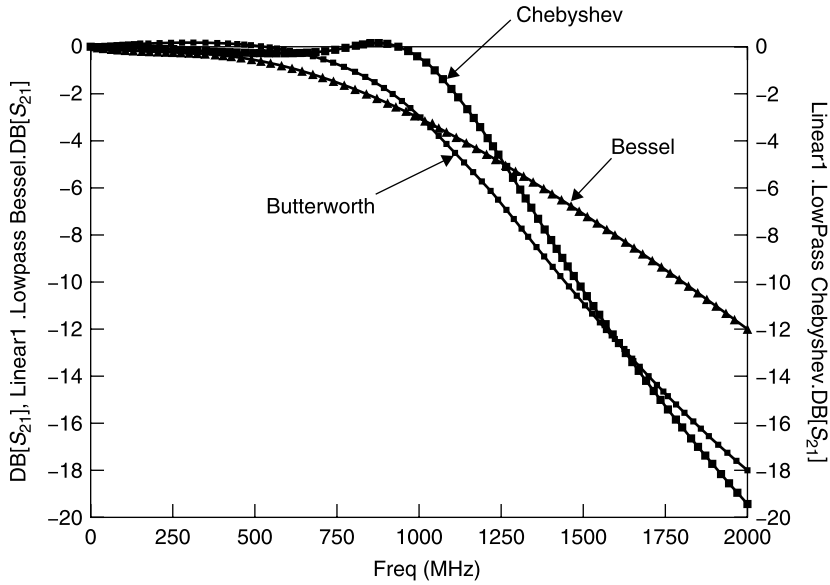

Figure 9.9-2 Bessel low-pass filter compared in amplitude response to Butterworth and Chebyshev filters of the same order.

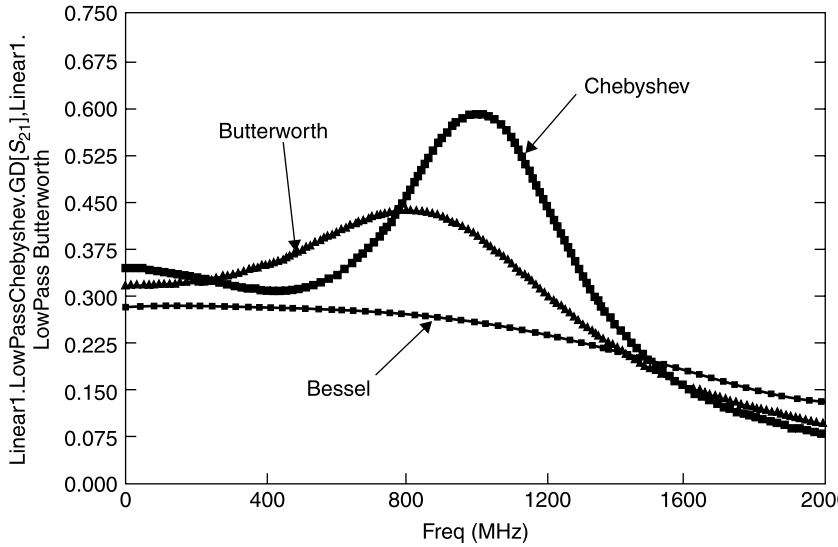

Figure 9.9-3 Group delay (in nanoseconds) comparison of Bessel, Chebyshev, and Butterworth filters, all having three sections and 1 GHz cutoff frequency.

ation. However, considering the group delay performance reveals a considerable advantage of the Bessel design.

The Bessel low-pass filter has nearly constant group delay up to 1000 MHz, its 3-dB cutoff frequency. The Chebyshev has a nearly 2 to 1 variation in group delay to its 0.5-dB cutoff, and the Butterworth has an intermediate value of group delay over the 0 to 1000 MHz band (Fig. 9.9-3). These data confirm that *the greater the selectivity, the greater the delay variation and the greater the potential signal distortion.*

9.10 FILTER *Q*

To illustrate filter types, we have reviewed only lossless representations. Real filters, of course, must be made with components having finite Q. The effect of finite Q components on filter insertion loss in the passband is greatest in those having the most frequency selectivity. The effect of finite Q can be seen in the Chebyshev low-pass filter shown in Figure 9.10-1. Both the L and C components are assumed to have the Q value listed.

In the case of the three-section Chebyshev low-pass filter, the lossless component assumption (actually $Q = 1{,}000{,}000$ is the Genesys default if Q is not specified) yields the expected 0.5-dB insertion loss over the passband of 0 to 1000 MHz. However, setting all circuit elements to have $Q = 50$ increases the

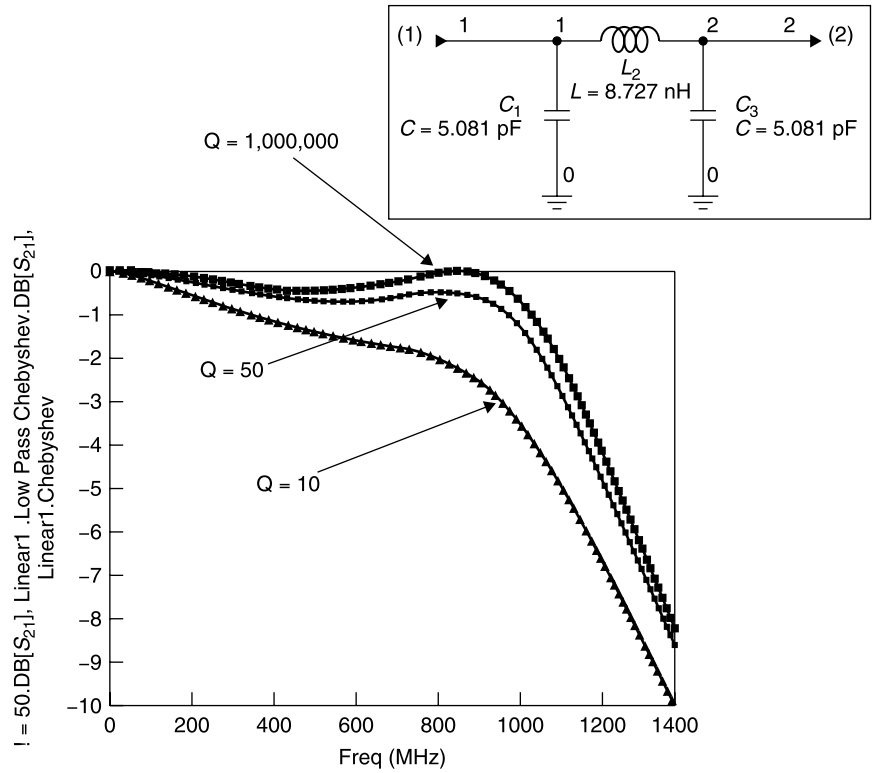

Figure 9.10-1 Effect of finite Q circuit elements on the performance of the Chebyshev 0.5-dB ripple, 1 GHz cutoff frequency filter.

loss at the cutoff frequency of 1000 MHz to about 1 dB. Further reducing element Q to 10 results in about 3.5 dB of insertion loss at 1000 MHz, as seen in Figure 9.10-1.

However, this example should not be considered a reference scale of the passband loss increase when circuit Q is 50 or 10. The change in passband loss depends upon the selectivity of the filter as well.

Figure 9.10-2 shows a five-section Chebyshev filter having 0.1 dB passband ripple for the bandwidth 175 to 225 MHz. Its insertion loss response is simulated using $Q = 1{,}000{,}000$ for all element values. This is shown in Figure 9.10-3.

Next, the filter shown in Figure 9.10-2 has its element Q changed to 50. The resulting performance is shown in Figure 9.10-4. A change of scale was made because the center frequency loss increased by 5 dB. Notice that not only has the center frequency loss increased by 5 dB, but the loss increase near the band

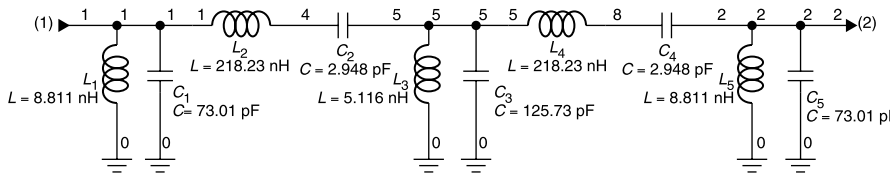

Figure 9.10-2 Five-section 0.1-dB-ripple Chebyshev bandpass filter for 175 to 225 MHz.

edges is much more, about 8 dB, resulting in a severe change in the passband shape. This filter design is not intended as representing a filter whose execution is practical, but rather to show that the effect of Q on passband loss depends on the selectivity of the filter, itself.

This design example has very sharp passband skirts, theoretically. But realizing such a design would require very low loss elements. Also note that the elements used in this simulation did not have parasitic inductance and capacitances, as discussed in Section 2.11. Inclusion of parasitics would make this design even less practical to realize. The point of this example is that it is important to check proposed filter designs using realistic models for their elements.

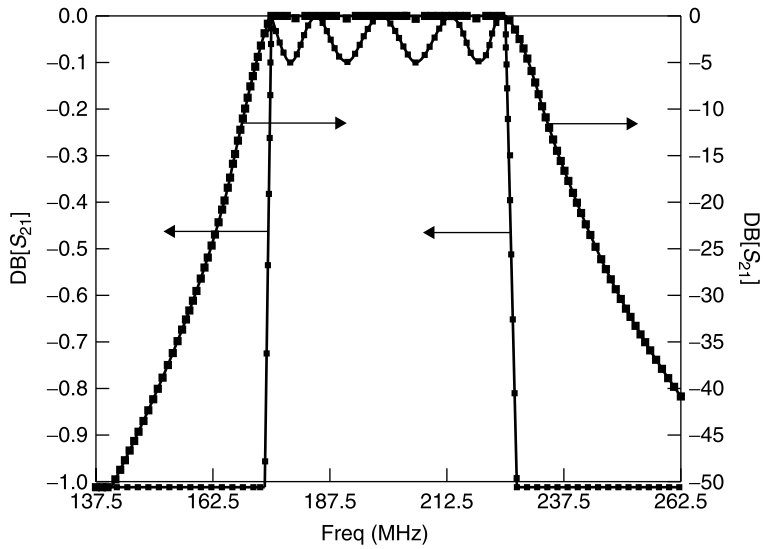

Figure 9.10-3 Calculated loss/isolation of five-section Chebyshev filter when L and C elements have $Q_U = 1{,}000{,}000$.

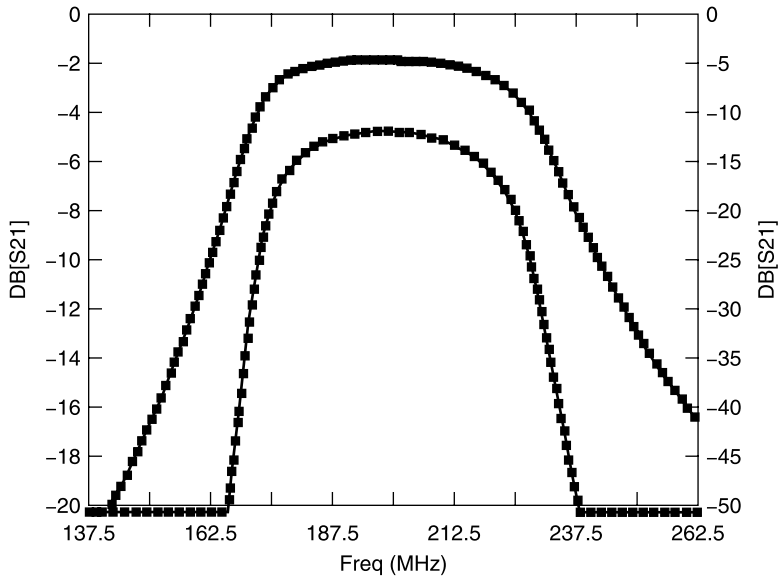

Figure 9.10-4 Calculated loss/isolation of the Chebyshev filter when elements have $Q = 50$.

9.11 DIPLEXER FILTERS

A *frequency diplexer* is a network that connects two networks that operate at different frequencies to a common terminal. For example, two radios operating at different frequency bands could be connected to a common antenna using a frequency diplexer. One commonly used realization of a frequency diplexer consists of two complementary filters connected to a tee junction. One filter is a high pass and the other a low pass. For the diplexer function, both filters have the same 3-dB cutoff frequency. Frequencies above the cutoff are directed along one side of the tee junction; frequencies below the cutoff are directed along the other side of the tee junction.

The two filters are designed using the *singly terminated* method by which the tee end of the filter is designed for an infinite load impedance for the high-pass arm and a zero load impedance for the low-pass arm. Although it is not intuitively apparent, when two such filters are connected together it is found that *a match is seen at all frequencies at the input to the tee*. The input impedance of the two filters, R_{in}, is made equal to the desired system impedance, in this case 50 Ω.

The tables given in Sections 9.3, 9.8 and 9.9 for Butterworth, Chebyshev, and Bessel filter designs are for doubly terminated filters, i.e., those having

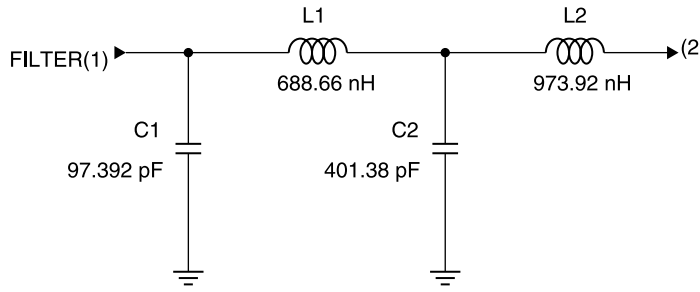

Figure 9.11-1 Singly terminated low-pass Butterworth filter with 3-dB cutoff frequency of 12.5 MHz.

the same characteristic impedance at both ports, therefore cannot be used for this design. Singly terminated designs are available with software, such as the FILTER program within the Genesys software suite.

Suppose we wish to build a diplexer having a 3-dB cutoff (transition frequency) of 12.5 MHz. This might be used to connect two radios to a common antenna, with one radio operating below 10 MHz and the other operating above 16 MHz. The two singly terminated designs realized using the FILTER software are shown in Figures 9.11-1 and 9.11-2. Notice that input port 1 is well matched. The return loss is between 50 and 60 dB and the signal input at port 1 is routed smoothly between ports 2 and 3 according to the frequency. Notice also that this is a means of providing filtering one port of which port 1 is matched at all frequencies.

When the two filters are connected together at their respective zero and infinite impedance ports the resulting diplexer shown in Fig. 9.11-3 is obtained.

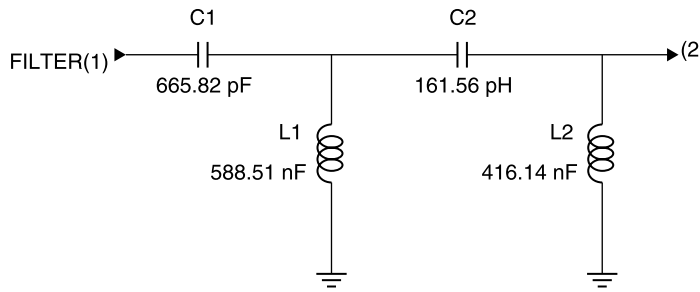

Figure 9.11-2 Singly terminated high-pass Butterworth filter with 3-dB cutoff frequency of 12.5 MHz.

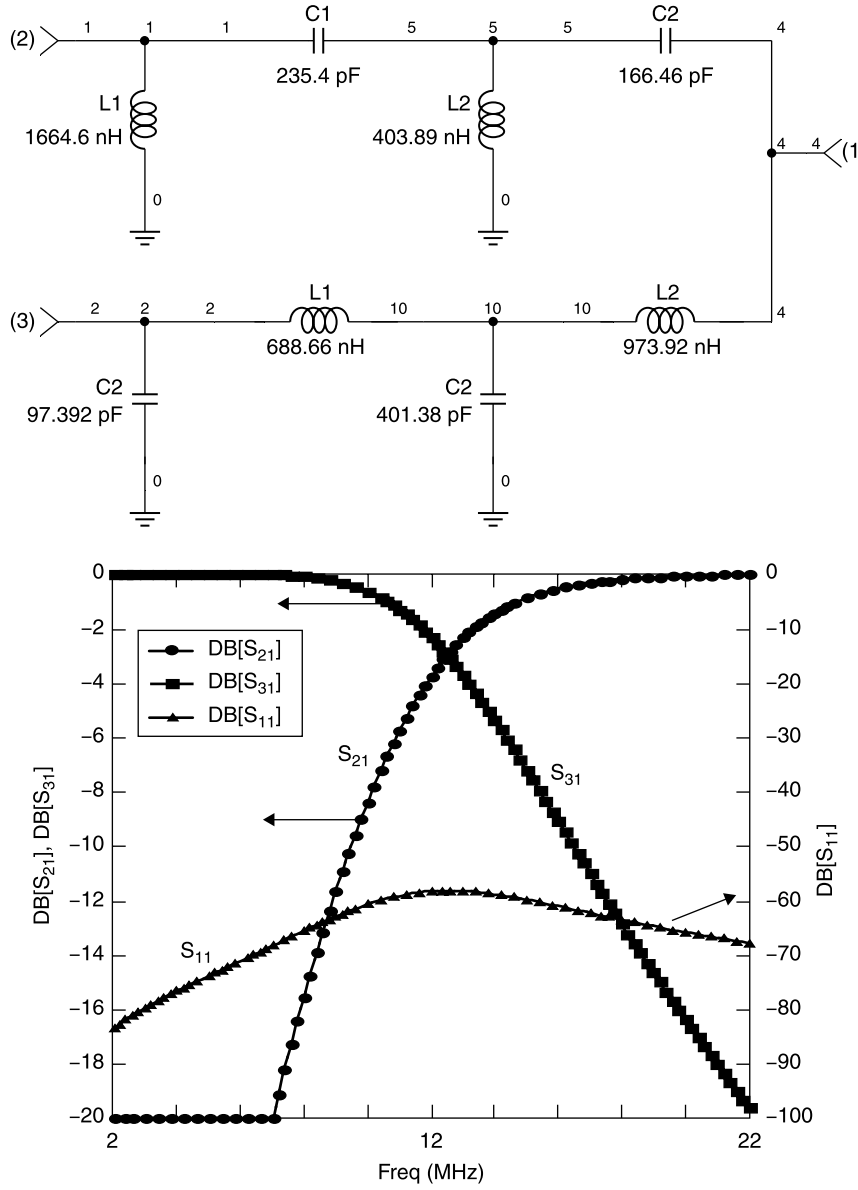

Figure 9.11-3 Frequency diplexer having matched transmission at all frequencies from its common port.

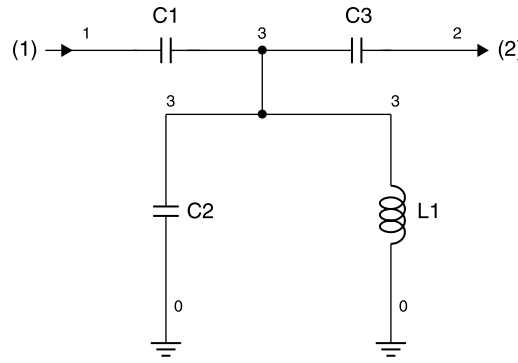

Figure 9.12-1 Top-coupled filter.

9.12 TOP-COUPLED BANDPASS FILTERS

In Section 3.4 we examined top-C, lightly coupled resonators. When used as a filter, this circuit is called a *top-coupled filter*. This simple circuit shown in Figure 9.12-1 often can provide sufficient filtering for many applications. Since

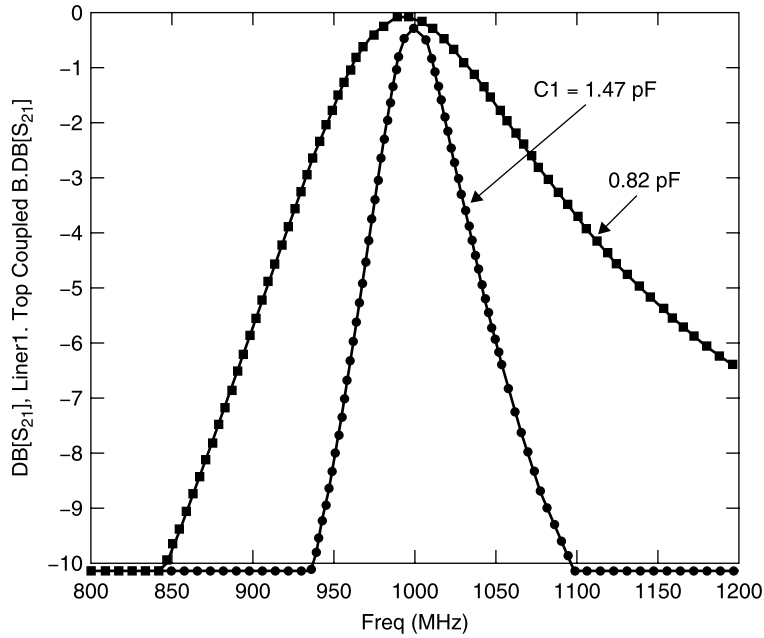

Figure 9.12-2 Varying the coupling of the top-coupled resonator changes the loaded Q.

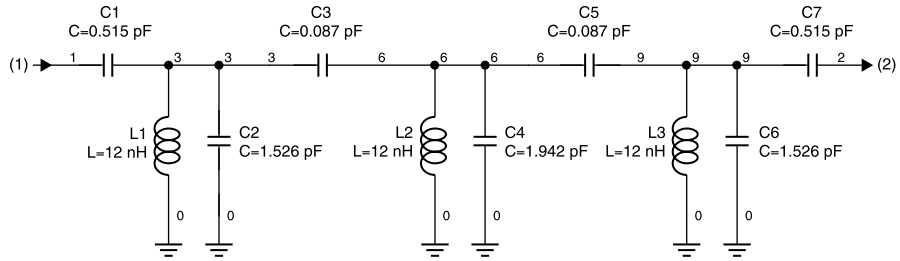

Figure 9.12-3 Three-section, Chebyshev, 0.25-dB ripple, 975 to 1025 MHz, top-coupled filter.

there are so few degrees of engineering freedom for the circuit, the design can be accomplished using the tune feature or the optimizer of a network simulator. The L_1C_2 product determines the center frequency $(f_0 = 1/\sqrt{L_1C_2})$ and $C_1 = C_3$ (for symmetry) controls the loaded Q. However, there is some interaction between resonance and coupling because C_1 affects the total capacitance of the resonator somewhat, therefore retuning of L_1 and/or C_2 is necessary to return to f_0 as C_1 and C_2 are tuned (synchronously) to adjust the coupling. The higher the reactance of C_1, the higher the loaded Q.

As an example, the resonance was set equal to 1 GHz by selecting values of $L_1 = 3.18$ nH and C_2 to resonate at 1 GHz (about 6 pF, as needed according to

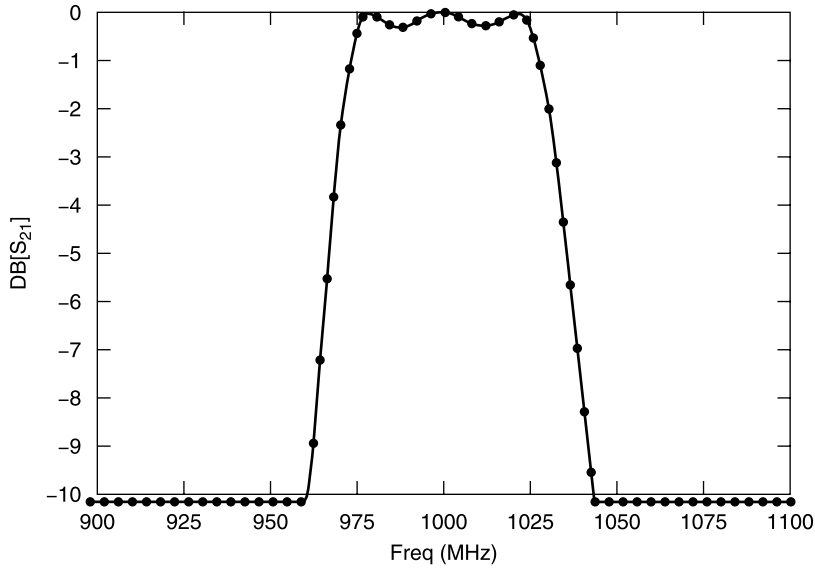

Figure 9.12-4 Calculated loss/isolation of the filter in Figure 9.12-3.

the coupling). If placed directly in parallel with a 50-Ω source and 50-Ω load, the resonator would have a loaded Q of nearly unity and a very broad 3-dB bandwidth. Using a coupling capacitance of $C_1 = C_3 = 0.82$ pF, the 3-dB bandwidth is 50 MHz with f_0 loss of 0.3 dB. This is equivalent to $Q_L = 20$ as shown in Figure 9.12-2. To accomplish the same Q_L with direct coupling would require that the inductance be reduced by a factor of 20, or $L_2 = 0.2$ nH, a very impractically small value. Increasing the coupling capacitors to 1.47 pF gives a 3-dB bandwidth of 150 MHz with f_0 loss of 0.1 dB.

The coupling that results in 0-dB insertion loss at f_0 is called critical coupling. For this simple circuit, critical coupling and the desired 3-dB bandwidth may not be accomplished simultaneously. More selectivity can be obtained using multiple resonators. A three-section, Chebyshev filter with 0.25 dB ripple over the 975 to 1025 MHz bandwidth is shown in Figure 9.12-3 and its loss performance shown in Figure 9.12-4. Notice that the resonators have 12-nH inductors, more practical to realize than those which would be necessary for a direct coupled resonator.

9.13 ELLIPTIC FILTERS

Just as it is desirable to place a ripple response in the passband, there can be advantages to having equal isolation ripple in the stopband. This can make possible a more rapid increase of isolation with frequency at the passband edge. Filters having a ripple in the stopband can be realized using *elliptic filter* designs.

While the sharp increase in isolation just outside the passband can be very advantageous for some applications, *it comes at the price of reduced isolation at frequencies considerably higher than the filter's cutoff frequency*.

We will compare the performance of a Chebyshev 0.5-dB- (passband) ripple, five-section, 1-GHz low-pass filter with a comparably designed elliptic filter designed for the same cutoff. The straight Chebyshev filter is shown in Figure 9.13-1.

The elliptic filter, designed using the Genesys SFILTER software, to similar specifications, is shown in Figure 9.13-2. Notice that the stopband attenuation drops more rapidly just above the 1 GHz cutoff frequency, due to the parallel resonant series elements, but that the maximum isolation is only 48 dB, even at frequencies far from cutoff. This limit on the isolation is the performance tradeoff for the more rapid isolation increase near the cutoff frequency.

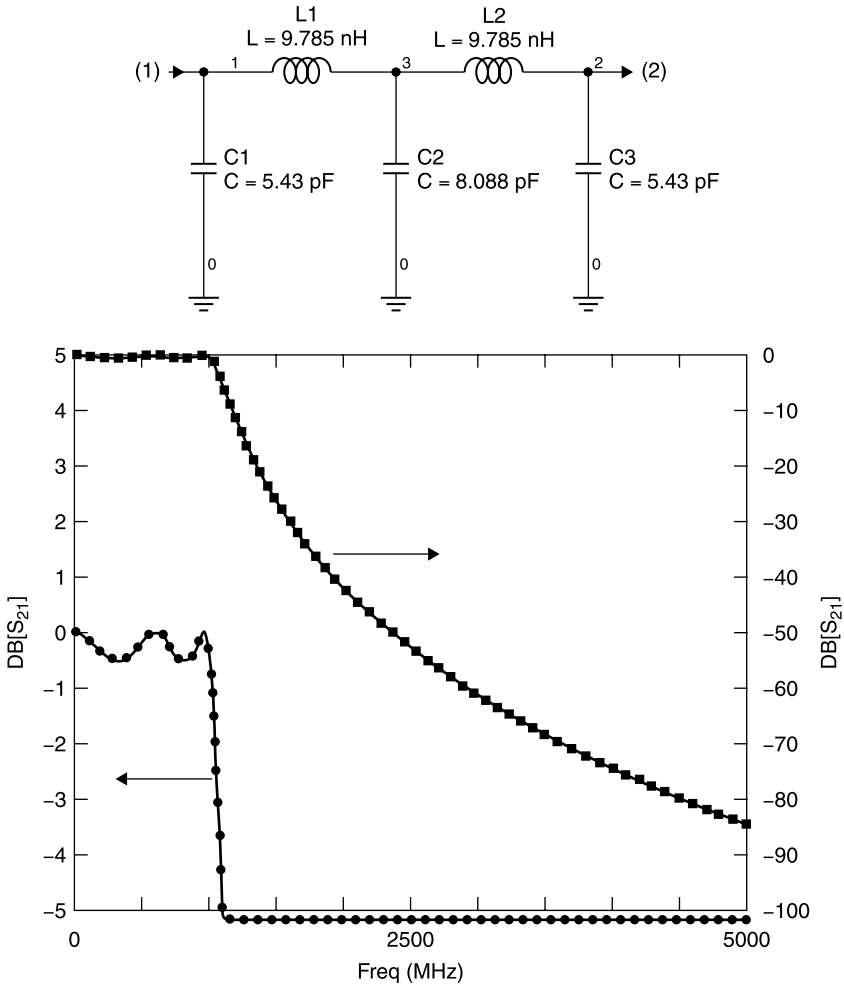

Figure 9.13-1 Five-section, low-pass, 0.5-dB-ripple Chebyshev filter.

9.14 DISTRIBUTED FILTERS

Most lumped-element filter designs are limited to realizations up to only a few hundred megahertz before element values become impractically small. To design filters for use above 500 MHz, it is more practical to design *distributed filters*, that is, *filters using distributed structures, such as lengths of transmission lines, as resonant elements*. The top-coupled filter in Figure 9.12-1 is a resonator capacitively coupled near its high-voltage node. A similar resonant structure can be obtained using a half-wave transmission line capacitively coupled to

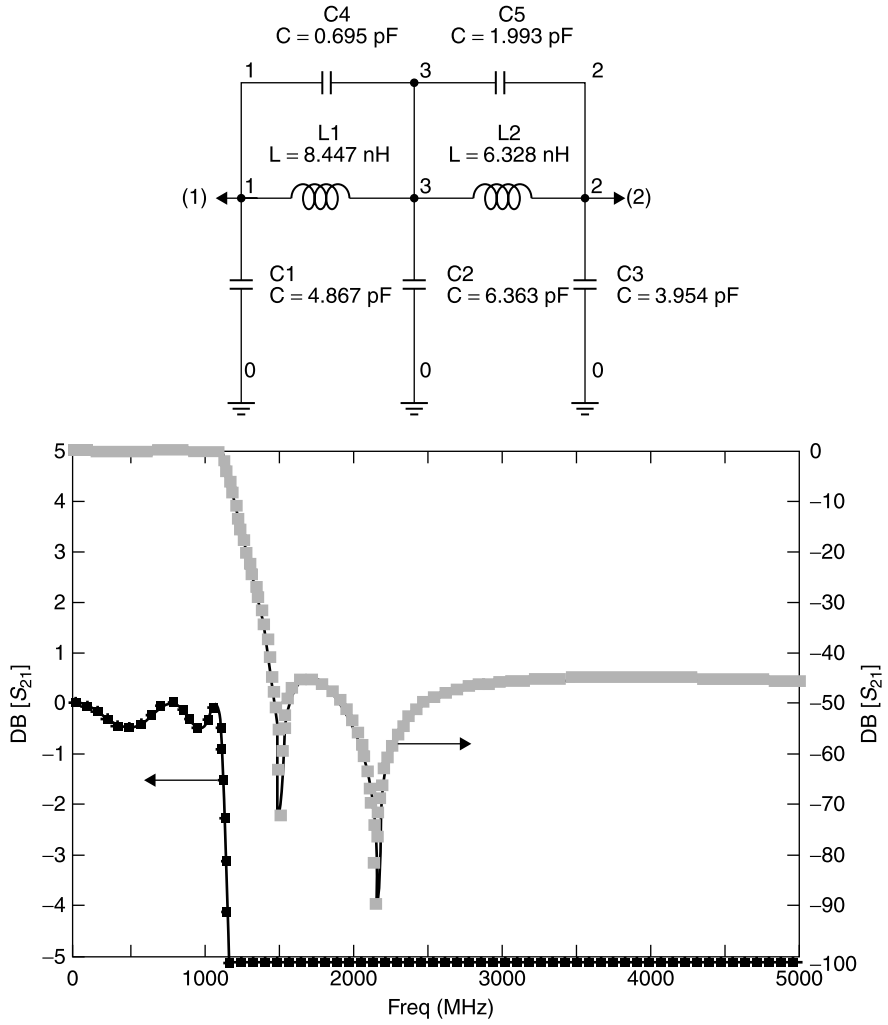

Figure 9.13-2 Five-section, low-pass elliptic filter.

generator and load, as shown in Figure 9.14-1 and its loss performance is shown in Figure 9.14-2.

The half-wave resonator stores energy in the form of standing waves with voltage maxima at its two ends. Thus, the capacitive coupling shown is electrically similar to that of the top-coupled filter previously described. The 3-dB bandwidth of this example filter is only 8 MHz with $f_0 = 1000$ MHz, yielding an effective $Q_L = 125$. Yet the resonator consists of only a length of 50-Ω transmission line, an easily realized structure. The coupling capacitors might be realized as gaps in the transmission line and designed either using an EM sim-

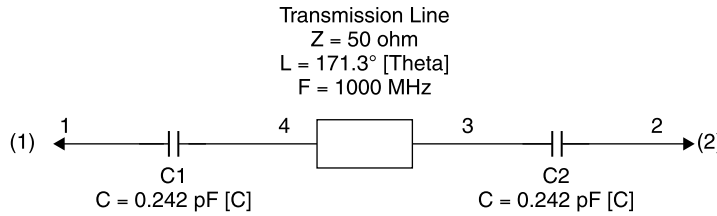

Figure 9.14-1 End-coupled, half-wave resonator filter.

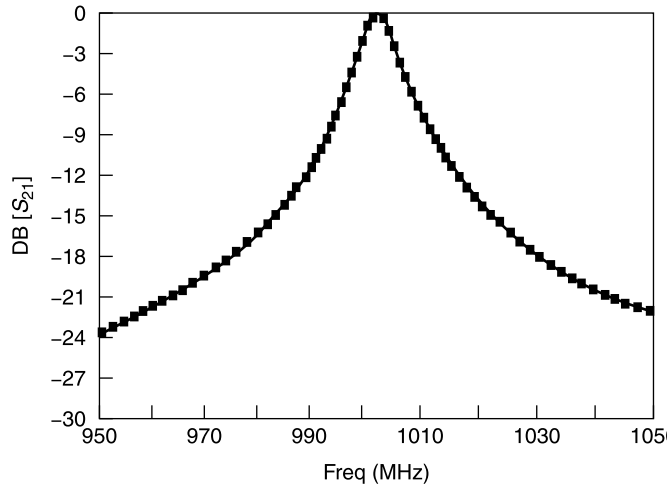

Figure 9.14-2 Calculated loss/isolation of the half-wave filter shown in Figure 9.14-1.

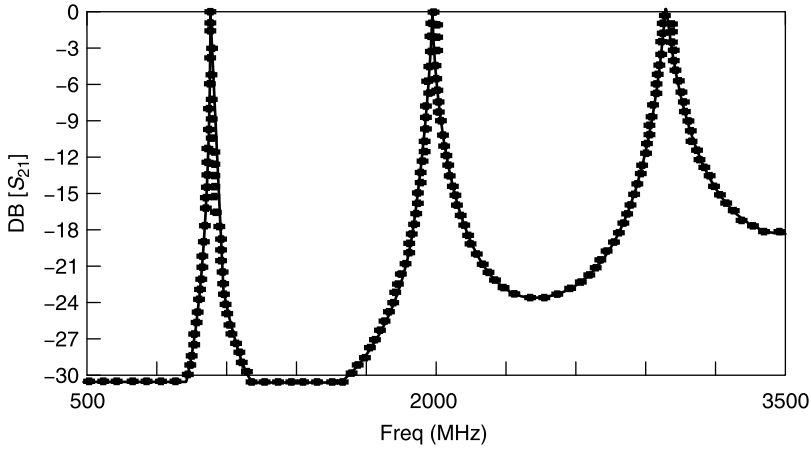

Figure 9.14-3 Recurring passbands of the half-wave resonator filter.

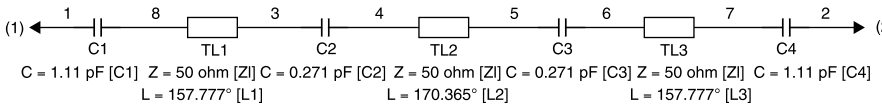

Figure 9.14-4 Three-section, half-wave resonator filter with $f_0 = 1$ GHz designed using the optimizer of the network simulator.

ulator or empirically, but once designed, could be reproduced by means of the printing process used to form the transmission line circuitry.

The circuit was modeled using a network simulator, and the resonator's length was adjusted in conjunction with the adjustment of the coupling capacitors, C_1 and C_2, to return the resonance to 1 GHz. As with the lumped-element, top-coupled filter, the coupling capacitors lower the resonant frequency; so readjustment of the line length was needed to return f_0 to 1 GHz. Notice that the isolation is greater than 20 dB at 960 and 1040 MHz. On the other hand, transmission line filters of which this is an example have recurring passbands, in this case roughly at integer multiples of f_0, as shown in Figure 9.14-3.

As with lumped filters, multiple half-wave resonators can be used. Figure 9.14-4 shows a three-resonator circuit designed using the optimizer of the network simulator. Initial values of 180° at 1 GHz and 50 Ω were selected for the

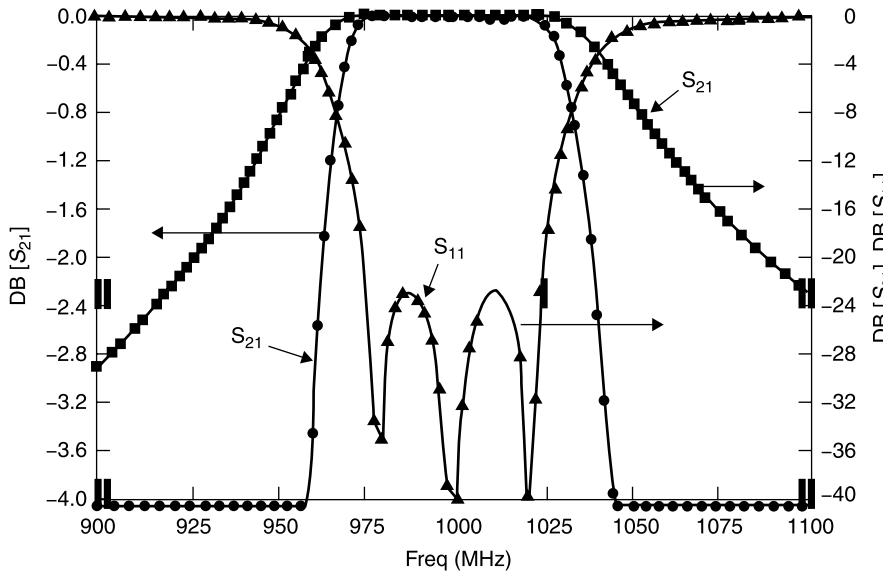

Figure 9.14-5 Calculated loss/isolation of the filter described in Figure 9.14-4.

resonators and 1 pF for the coupling capacitors. The optimization goals were $|S_{11}| < -20$ dB for $975 \leq f \leq 1025$ MHz and $|S_{21}| < -20$ dB at 900 and 1100 MHz. After some cut-and-try techniques with the optimizer, the goals were changed from -20 dB to -24 dB. The circuit shown in Figure 9.14-4 resulted and its performance is shown in Figure 9.14-5.

Unlike the lossless lumped element simulations previously performed, this simulation has an allowance for component losses, and so the insertion loss performance is a reasonable approximation to what might actually be obtained. A value of 0.05 dB/wavelength of loss is assumed in the calculation for all three half-wave resonator lines, and the coupling capacitors are assumed to have $Q = 100$.

There are numerous topologies for distributed filters, some of which use distributed coupling as was demonstrated for the backward wave coupler in Section 8.2. They can be designed using proprietary software such as the FILTER program, which provides electrical schematics and mechanical layout drawings. Many can also be designed using cut-and-try techniques aided by the optimizer of the network simulator. Further descriptions and discussion of distributed filters is provided by Rhea [1].

9.15 THE RICHARDS TRANSFORMATION

The previous sections of this chapter have shown that there is a large body of filter synthesis theory applicable to lumped elements. It would be desirable if this can be applied to distributed filters. An insight into how to do this can be gained by comparing the impedance variation with frequency of a lumped inductor and a short-circuited length of transmission line [2, 3]. In particular a short-circuited length of transmission line can be substituted for a lumped inductor by defining an equivalence between the two elements described by (9.15-1) and (9.15-2), respectively:

$$Z_L = j\omega L \tag{9.15-1}$$

$$Z_{\text{shorted line}} = jZ_0 \tan\theta = jZ_0 \tan\left(\frac{\pi}{2}\frac{f}{f_R}\right) \tag{9.15-2}$$

where f_R is the frequency at which the shorted stub length is 90° long. Note that the shorted line has the same mathematical variation as the inductor if we equate

$$L = Z_0 \tag{9.15-3}$$

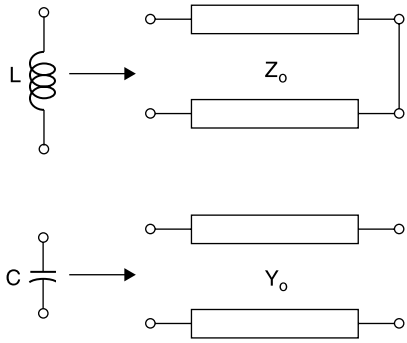

Figure 9.15-1 With the Richards transformation, inductors are replaced by short-circuited transmission lines and capacitors by open-circuited transmission lines.

where L is in henrys and Z_0 in ohms, and define a new frequency variable, Ω, according to

$$j\Omega = j \tan\left(\frac{\pi}{2}\frac{f}{f_R}\right) \qquad (9.15\text{-}4)$$

The expression in (9.15-4) is the *Richards frequency transformation* (Fig. 9.15-1).

Under this same transformation the behavior of an open-circuited transmission line is mathematically equivalent to that of a capacitor:

$$Y_C = j\omega C \qquad (9.15\text{-}5)$$

$$Y_{\text{open-circuited line}} = jY_0 \tan\theta = jY_0 \tan\left(\frac{\pi}{2}\frac{f}{f_R}\right) \qquad (9.15\text{-}6)$$

The mathematical equivalence that we propose does not mean that an inductor's reactance has the same frequency variation as a shorted line, or that a capacitor's reactance variation is the same as that of an open-circuited line, except in the new frequency domain defined by (9.15-4).

As an example of this equivalence, we will design a three-element, low-pass, Chebyshev filter with 0.5-dB ripple, $f_C = 1$ GHz and stub resonant frequency $f_R = 1.4$ GHz. Notice that f_R is an additional degree of freedom in the distributed circuit design. In the low-pass prototype $f_R = \infty$.

Since this is a Chebyshev 0.5-dB ripple design, the loss at 1 GHz will be 0.5 dB and will not exceed this value between 0 and 1 GHz. For this example, we use the tee circuit. The g_i values, from Table 9.8-5 are

$$g_i = 1.5963 \quad 1.0967 \quad 1.5963 \quad 1.000 \text{ (load)}$$

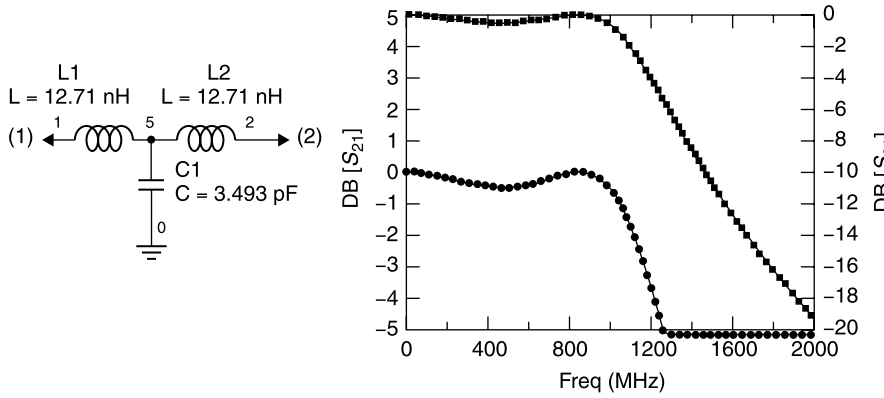

Figure 9.15-2 The 0.5-dB ripple, 50-Ω, Chebyshev low-pass filter.

The corresponding lumped-element tee circuit is obtained by frequency and impedance scaling the g_i values using (9.4-2) and (9.4-4) as shown in Figure 9.15-2 along with its frequency response.

Recall from Section 9.4 that the g_i values are the respective series reactances and shunt susceptances of the filter elements at f_C. This means that the shorted transmission line Z_{01} that replaces a series inductor must have a reactance at f_C of

$$g_1 Z_0 = Z_{01}\Omega_C$$

where

$$\Omega_C = \tan\left(\frac{\pi}{2}\frac{1.0\text{ GHz}}{1.4\text{ GHz}}\right) = 2.08$$

Then

$$Z_{01} = Z_{03} = \frac{g_1 Z_0}{\Omega_C} = \frac{1.5963(50\ \Omega)}{2.08} = 38.4\ \Omega$$

Similarly, the open-circuited stub Y_{02} that replaces a shunt capacitor in the low-pass prototype filter must have a susceptance at f_C given by

$$g_2 Y_0 = \frac{g_2}{Z_0} = Y_{02}\Omega_C$$

from which

$$Y_{02} = \frac{g_2}{Z_0\Omega_C} = \frac{1.0967}{(50\ \Omega)2.08} = 0.01050\ \mho$$

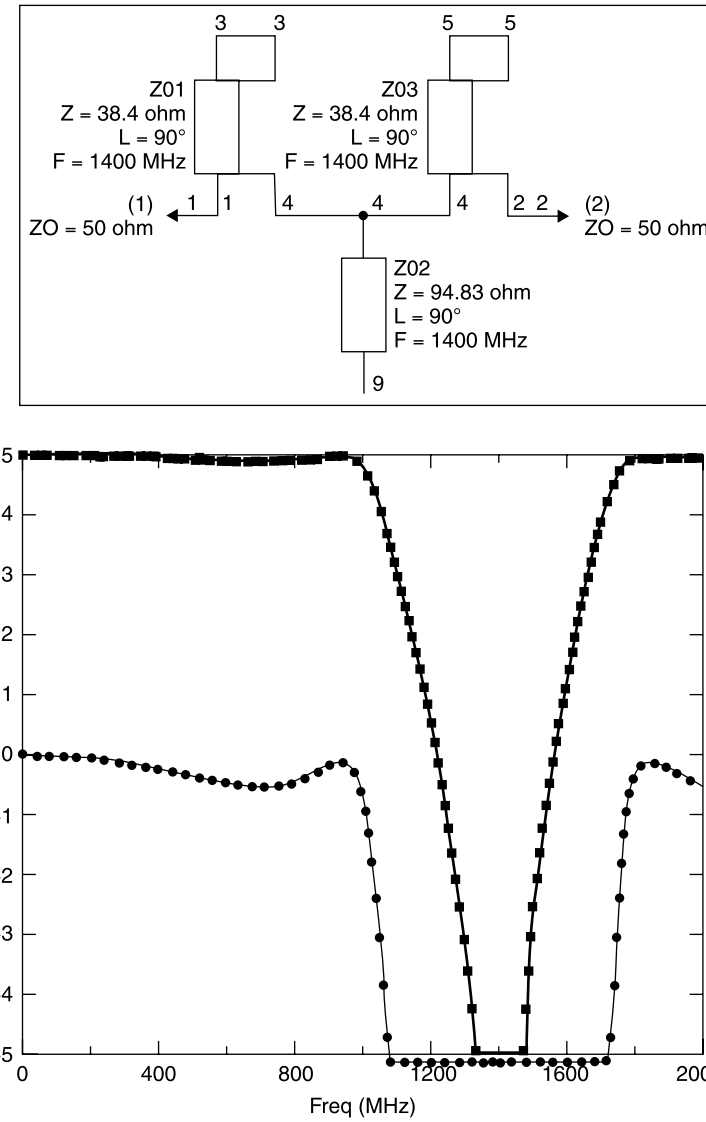

Figure 9.15-3 Circuit and performance of the three-element, 0.5-dB ripple, Chebyshev distributed element filter.

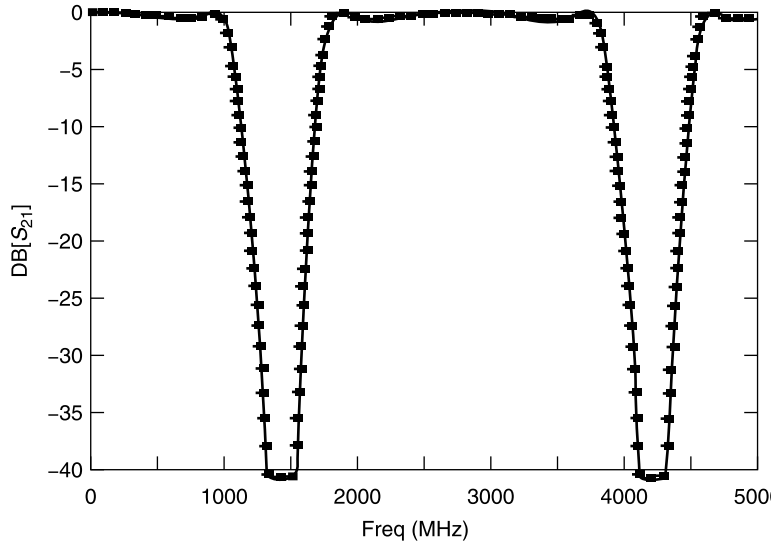

Figure 9.15-4 Extended frequency plot of the distributed filter of Figure 9.15-3.

and

$$Z_{02} = \frac{1}{Y_{02}} = 94.83\ \Omega$$

This circuit and its performance is shown in Figure 9.15-3.

Notice that the frequency translation has shrunk the frequency domain of the low-pass prototype circuit of Figure 9.15-1 from $0 \leq f \leq \infty$ to the new Ω domain for which $0 \leq f \leq f_R$. That is, while the entire frequency response of the low-pass lumped-element circuit extended from zero to infinity in frequency, that loss performance region has been condensed into the range from zero to f_R, the resonant frequency of the stubs in the distributed filter. At the same time the transformation has introduced a new realm of circuit behavior beyond f_R. In this new domain the loss performance is repeated, mirrorlike, about f_R thereby creating a bandstop filter response. In a similar fashion, a bandpass filter could be created based on the design of a high-pass lumped-element filter.

The stopband of the new distributed filter extends equally on either side of f_R out to f_C. Thus the stopband is 1.0 to 1.8 GHz. Since the filter's performance is defined by transmission line lengths, *the center frequency of the stopband is the arithmetic mean, 1.4 GHz, of its f_C band edge frequencies, 1.0 and 1.8 GHz*. Also, since this is a distributed element filter using quarter-wave resonators, its performance recurs at odd integer multiples of f_R $(f_R, 3f_R, 5f_R, \ldots)$, as shown in Figure 9.15-4.

This distributed filter can be realized in coaxial transmission line by embedding the two short-circuit terminated stubs within the center conductor of the main transmission line, as shown in Figure 9.15-5.

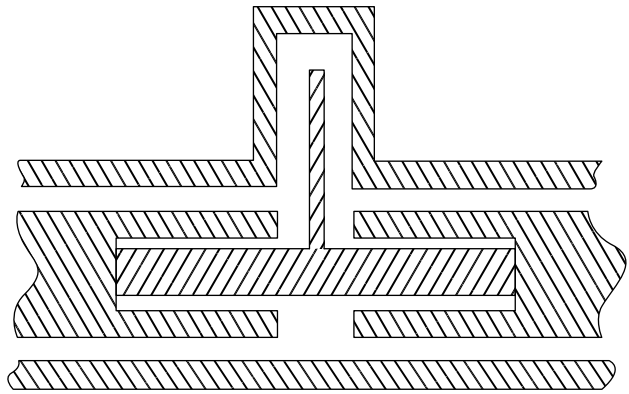

Figure 9.15-5 Cross-sectional sketch of a coaxial line realization of the distributed bandpass filter with series stubs embedded within the center conductor of the main line.

9.16 KURODA'S IDENTITIES

The circuit of Figure 9.15-5 can be realized in coaxial transmission line but not in microstrip or stripline, as would often be desirable, due to the necessity for series short-circuited stubs. *Kuroda's identities of the first kind* (Fig. 9.16-1) al-

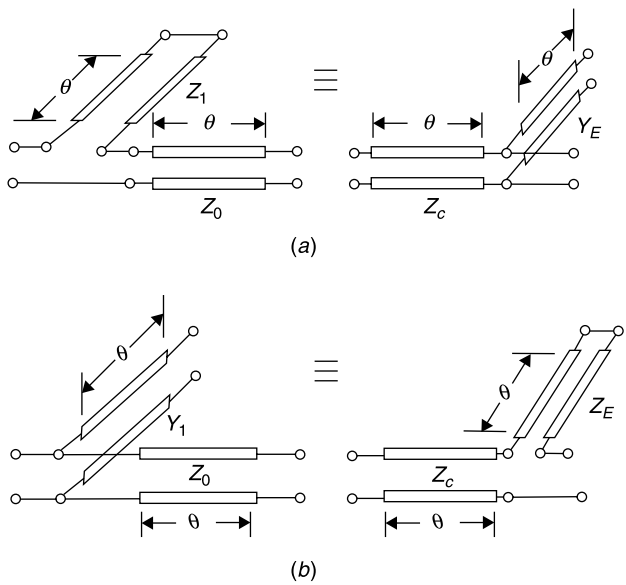

Figure 9.16-1 Kuroda's identities of the first kind applied to transmission lines: (*a*) $Z_C = nZ_0$ and $Y_E = (n-1)/nZ_0$ where $n = 1 + Z_1/Z_0$. (*b*) $Z_C = Z_0/n$ and $Z_E = ((n-1)/n)Z_0$ where $n = 1 + Y_1Z_0$.

low the replacement of a series-shorted stub and a cascade Z_0 line with a shunt open-circuited stub and a different cascade line, and vice versa [2, 4]. Note that all lines have the same electrical length, θ. Given this requirement and the formulas in Figure 9.16-1, *the Kuroda equivalences apply at all frequencies.*

Notice that the series-shorted stub must be combined with a section of Z_0 line before the equivalence with an open-circuited shunt stub can be made. The addition to the input and output of sections of Z_0 transmission line has no effect on the VSWR or insertion loss of the filter, but it does cause the transformed filter to have added electrical length, which may be significant in some applications. The circuits otherwise are equivalent.

We transform the distributed filter of Figure 9.15-3 to one using all shunt stubs using Kuroda's identity in Figure 9.16-1*a* to transform the series short-circuited stubs to shunt open-circuited stubs. In this filter $Z_{01} = Z_{03} = 38.4\ \Omega$.

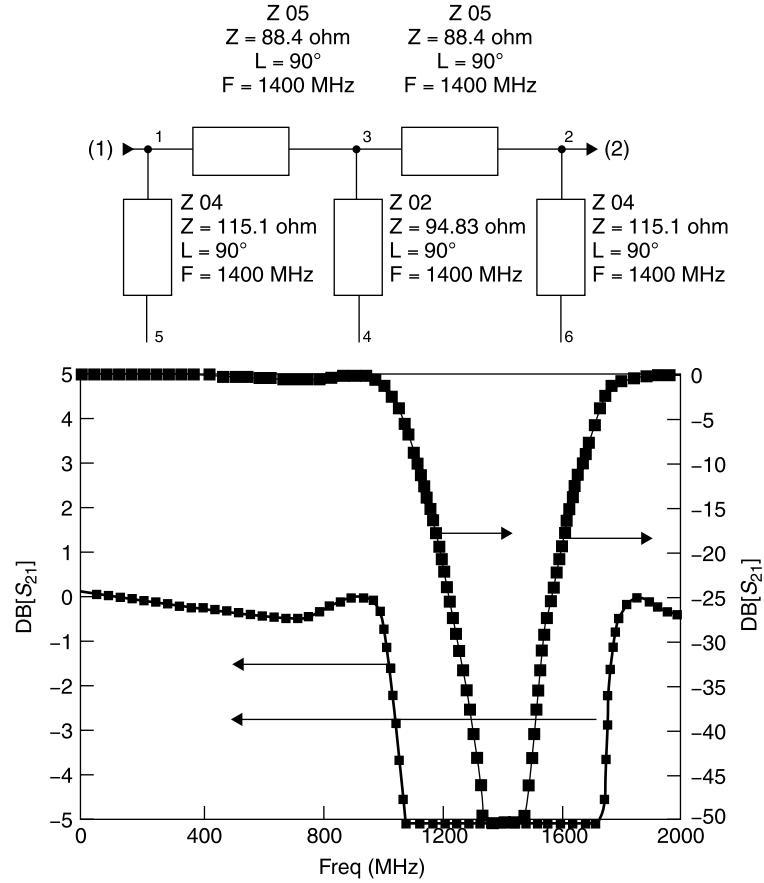

Figure 9.16-2 Circuit and performance of the Chebyshev filter transformed to an all shunt stub format.

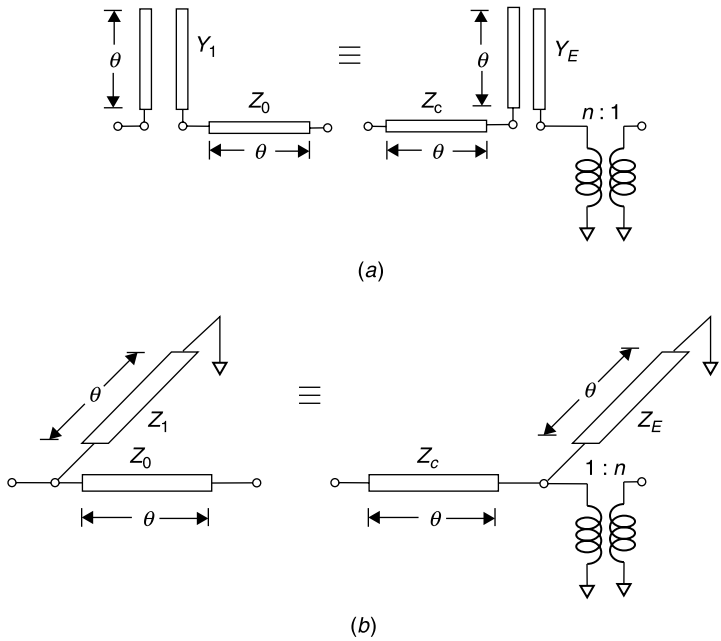

Figure 9.16-3 Kuroda's identities of the second kind: (*a*) $Z_C = nZ_0$ and $Y_E = 1/[n(n-1)Z_0]$ where $n = 1 + 1/Y_1Z_0$. (*b*) $Z_C = Z_0/n$ and $Z_E = Z_0/[n(n-1)]$ where $n = 1 + Z_0/Z_1$.

Then, since $Z_0 = 50\ \Omega$, $n = 1.768$, $Z_C = 88.4\ \Omega$, and $Z_E = 1/Y_E = 115.1\ \Omega$. The transformed filter and its response is shown in Figure 9.16-2, from which it can be seen that the insertion loss is identical to the filter of Figure 9.15-3.

Another pair of equivalences is shown in Figure 9.16-3. These are called *Kuroda's identities of the second kind*. The presence of an ideal transformer in the equivalent circuit can be eliminated by the judicious use of combinations of transformations whose total impedance transformation cancels, eliminating the need for the ideal transformers. With these transformations, for example, a three-stub filter with impedance Z_0 and interconnecting Z_0 line could be transformed into a single stub filter with two cascade lines of impedance different from Z_0.

9.17 MUMFORD'S MAXIMALLY FLAT STUB FILTERS

A simple form of distributed bandpass filter consists of shorted TEM mode stubs that are a quarter-wave long at the center frequency, f_0. They are spaced

TABLE 9.17-1 Normalized Stub Admittances for Mumford's Quarter-Wave Shorted Stub Filters [5]

(a) Three-Stub Filters

$10 \log K_3$	k_1	k_2
−12.728	0.100	0.200
−0.944	0.300	0.600
+5.460	0.500	1.000
+10.138	0.700	1.400
+15.560	1.000	2.000
+21.156	1.400	2.800
+27.604	2.000	4.000
+31.904	2.500	5.000
+35.563	3.000	6.000

(b) Four-Stub Filters

$10 \log K_4$	k_1	k_2
−5.170	0.100	0.292
+3.253	0.200	0.571
+13.329	0.400	1.109
+25.668	0.800	2.141
+35.909	1.300	3.395
+44.873	1.900	4.877
+56.734	3.000	7.568

(c) Five-Stub Filters

$10 \log K_5$	k_1	k_2	k_3
+3.452	0.100	0.366	0.532
+13.577	0.200	0.694	0.989
+20.523	0.300	1.005	1.410
+26.002	0.400	1.304	1.808
+30.601	0.500	1.596	2.193
+38.160	0.700	2.166	2.933
+44.324	0.900	2.724	3.648
+54.172	1.300	3.819	5.038
+66.970	2.000	5.702	7.403
+77.874	2.800	7.829	10.058

Source: From [5].

at quarter-wave intervals along the TEM mode main transmission line path. Mumford [5] analyzed this filter type for the maximally flat (Butterworth) transmission response and created tables of values for the characteristic admittances of the stubs relative to that of the main line. The stub admittances nor-

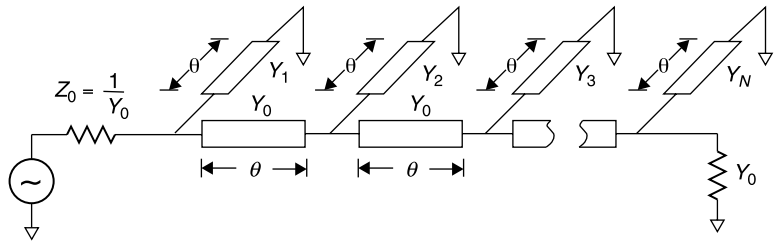

Figure 9.17-1 Schematic of Mumford's quarter-wave stub filters.

malized to Y_0, the characteristic admitttance of the main line and the admittances of the matched generator and load, are listed in Table 9.17-1 for 3, 4 and 5 stub designs. The filters are symmetrical; therefore, only half of the values are listed. The 2-stub design is not listed because, due to symmetry, both stubs are identical. For additional designs using 6 to 10 stubs, refer to Mumford's paper [5] (Fig. 9.17-1). The insertion loss (or isolation) ratio of a filter having N stubs of length l can be computed for any frequency using

$$\mathrm{IL} = 1 + K_N \frac{\cos^{2N} \theta}{\sin^2 \theta} \tag{9.17-1}$$

$$\theta = \frac{2\pi l}{\lambda} \tag{9.17-2}$$

$$K_N = \tfrac{1}{4}\{k_1(k_2+2)\cdots(k_i+2)\cdots(k_N+2)\}^2 \tag{9.17-3}$$

$$k_i = \frac{Y_i}{Y_0} = y_i \tag{9.17-4}$$

where y_i is the normalized characteristic admittance of the ith stub, λ is the wavelength in the TEM mode medium, and K_N is a measure of the steepness of the isolation slope of the filter. For example, the insertion loss of a two-stub filter whose stubs have the same characteristic impedance as the main line is

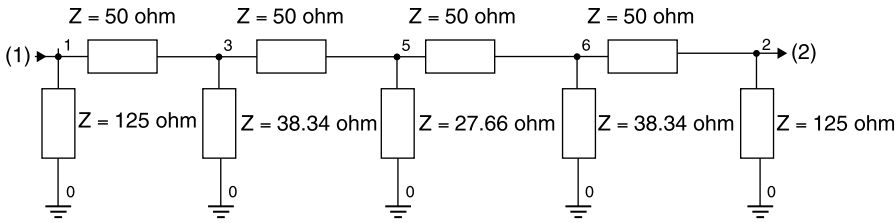

Figure 9.17-2 Five-stub Mumford filter with $K_5 = 26$ dB. For this example, all stubs and interconnecting line lengths are 90° at 1 GHz.

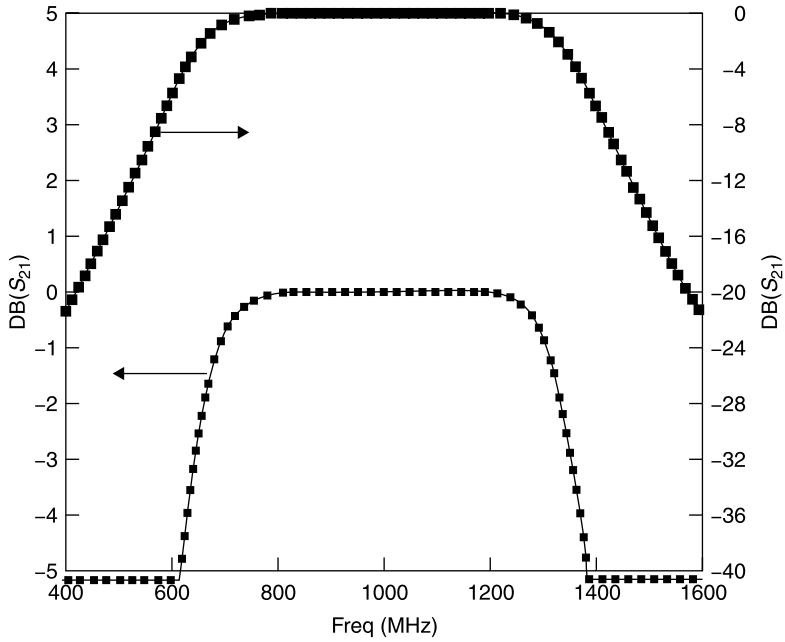

Figure 9.17-3 Calculated insertion loss of the filter in Figure 9.17-2.

$$\text{IL} = 1 + \frac{9}{4}\frac{\cos^4 \theta}{\sin^2 \theta} \tag{9.17-5}$$

As a filter design example, consider the five-stub model for which $K_5 = 26$ dB in Table 9.17-1(c). When this filter is designed for $Z_0 = 50\ \Omega$ the stub impedances are as shown in Figure 9.17-2, and the performance when the stubs and their spacings are 90° at 1 GHz is shown in Figure 9.17-3. The stub impedance values are practical for realization in microstrip or stripline.

9.18 FILTER DESIGN WITH THE OPTIMIZER

Prior to the ready availability of computers, designers were constrained to employ established techniques to design filters and other circuits. Random changing of variables or cut-and-try tuning in the lab could quickly become impractically laborious. Presently, however, even the most basic personal computer can perform thousands of insertion loss evaluations (or other calculations) per second for circuits having 10 or more elements and can be directed through optimizer software to vary the element values to better satisfy a set of performance goals. In principle, any of the filters discussed thus far in this chapter

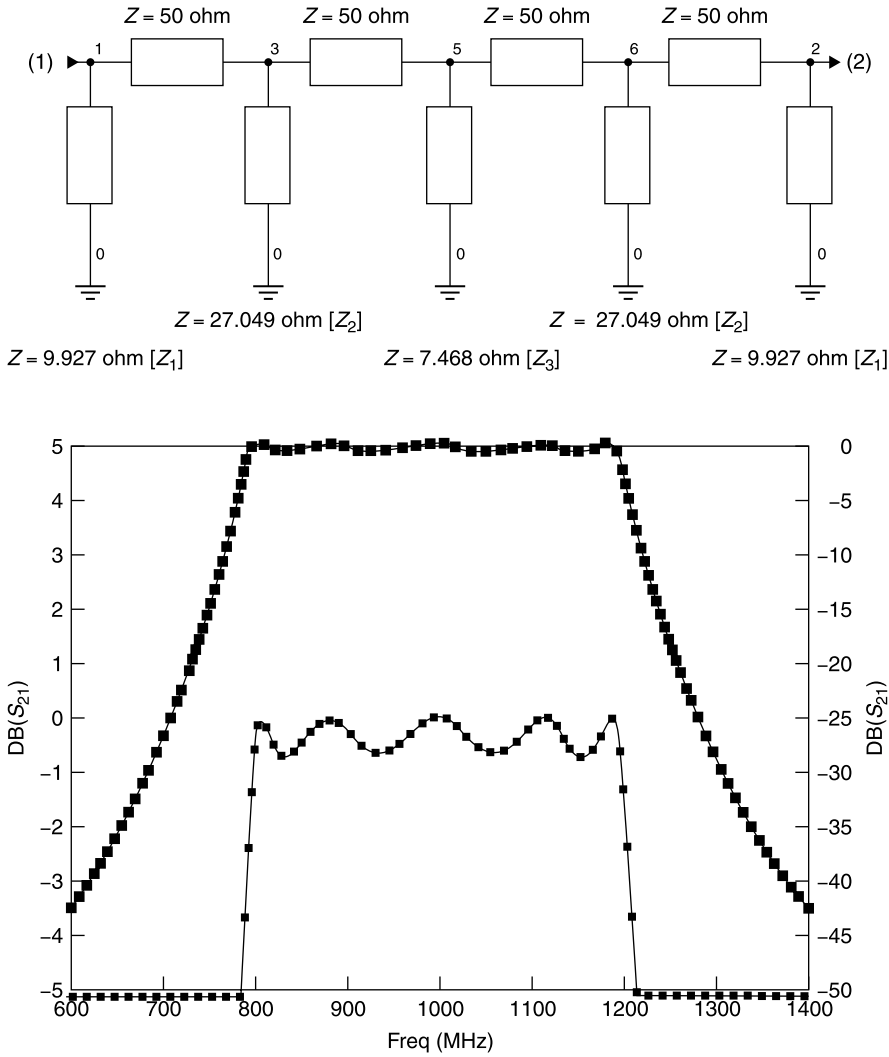

Figure 9.18-1 An 800- to 1200-MHz equal-ripple bandpass filter designed using the network simulator optimizer beginning with the Butterworth filter of Figure 9.18-2.

could have been determined using the optimizer of a network simulator, given an initial circuit of the correct topology.

However, with a completely random search and no good starting point, the optimizer may not converge on the desired solution, and some knowledge of filter performance is required merely to specify an initial circuit topology for the optimization. Furthermore, without prior knowledge of what is achievable,

it is difficult to know what goals are realistic. This is why a study of basic filter designs remains useful. Each different filter type can serve as a starting point from which a design tailored to the application at hand can be optimized.

As an example, consider the five-stub filter described in Figure 9.18-2. Suppose that a passband from 800 to 1200 MHz is required, within which a 0.5-dB maximum insertion loss is acceptable, and that outside of this bandwidth it is desirable to have as much insertion loss (isolation) as possible. Further, suppose that the filter is to be symmetric with respect to input and output, that the main line impedance is to remain 50 Ω, and that the stub lengths and spacings will be 90° at the center frequency of 1 GHz. This leaves only three design variables, the characteristic impedances of the first three stubs.

An optimization was performed with this circuit using as initial goals that $S_{21} > -0.5$ dB from 800 to 1200 MHz and $S_{21} < -20$ dB at 600 and 1400 MHz. This goal was reached by the optimizer almost immediately and therefore was judged to be too easily achieved. After a few additional optimizer executions, it was found that the isolation value could be reduced to <-40 dB at 625 and 1375 MHz. Note that goals must be entered as negative decibels. Optimizers do not recognize that "loss" implies a negative sign.

The resulting circuit and performance are shown in Figure 9.18-1. The isolation is greater than 25 dB only 100 MHz outside of this broad passband of 800 to 1200 MHz. The resulting loss characteristic is a reasonably close approximation to a 0.5-dB equal-ripple Chebyshev filter, even though the circuit optimization began with a Butterworth filter design. The 7- and 10-Ω characteristic impedance stubs required by this design would not be realized in microstrip, but the design might be practical in a coaxial transmission line format.

9.19 STATISTICAL DESIGN AND YIELD ANALYSIS

Using Standard Part Values

In the initial design of a component or system, element values are chosen to provide exactly the performance that is desired. However, in practice, circuits are generally fabricated using standard component values. For example, suppose that a Butterworth low-pass filter with a 3-dB cutoff frequency of 100 MHz is required. The theoretical solution for this filter is shown in Figure 9.19-1.

In checking for the availability of standard parts (Table 9.19-1) that can be provided with a $\pm 10\%$ element value tolerance, it is found that standard values include 47, 56, 150, and 180. Substituting the nearest values to those shown in Figure 9.19-1 leads to the filter shown in Figure 9.19-2.

The adoption of the nearest standard part values to the design has increased the loss at the 100 MHz cutoff frequency from 3.0 to 3.6 dB. The markers on the graph of Figure 9.19-2 indicate that the filter has less than 1 dB of insertion loss up to 86 MHz and greater than 20 dB of isolation above 156 MHz.

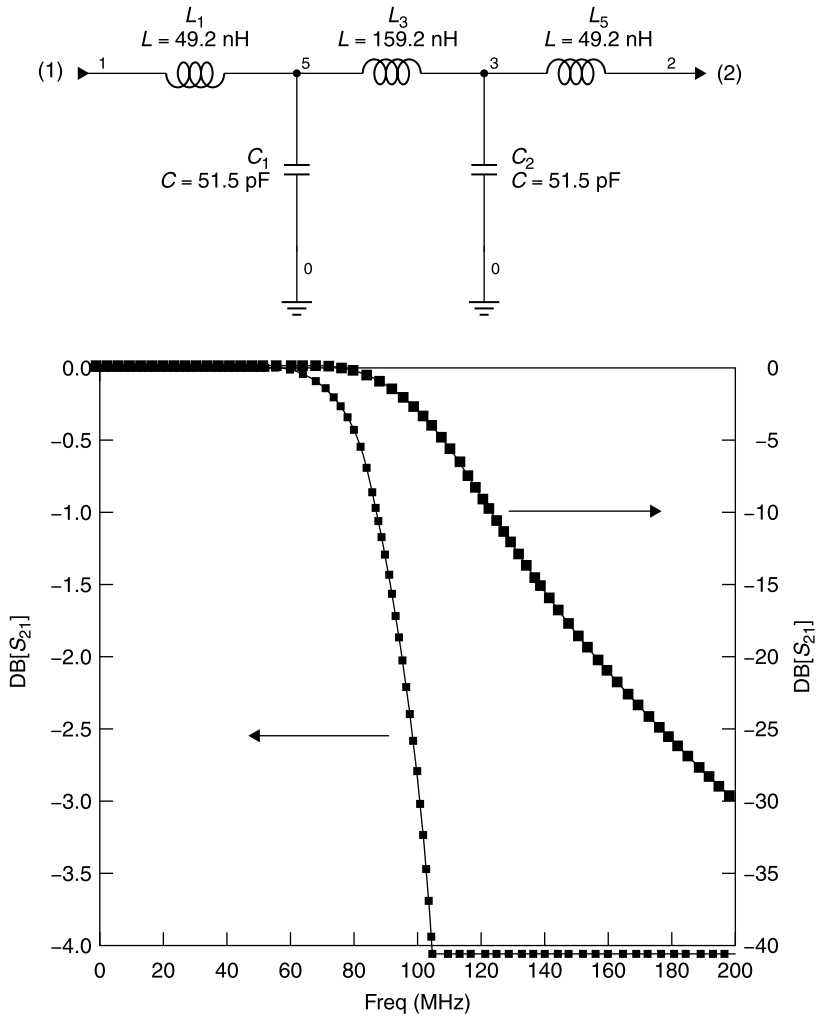

Figure 9.19-1 Insertion loss/isolation of an ideal Butterworth filter with 100 MHz, 3-dB cutoff frequency.

The Normal Distribution

Next, we recognize that even standard value components are not exactly realized but have a distribution of values. When a large quantity of parts are made according to a repetitive process, their distribution usually can be described by a "bell-shaped" curve having the form described by (9.19-1) and sketched in Figure 9.19-3:

$$N(x) = A\, e^{\left[\frac{-1}{2}\left(\frac{x-x_0}{\sigma}\right)^2\right]} \tag{9.19-1}$$

where A and σ are constants.

TABLE 9.19-1 U.S. Standard C83.2[a]

Part Tolerance	±5%	±10%	±20%
Step Multiplier	$10^{1/24} = 1.10$	$10^{1/12} = 1.21$	$10^{1/6} = 1.47$
	10	10	10
	11		
	12	12	
	13		
	15	15	15
	16		
	18	18	
	20		
	22	22	22
	24		
	27	27	
	30		
	33	33	33
	36		
	39	39	
	43		
	47	47	47
	51		
	56	56	
	62		
	68	68	68
	75		
	82	82	
	91		
	100	100	100

[a]Smaller or larger values use decimal multiplication of the values for the separate ±5%, ±10%, and ±20% series values [8].

The distribution in Figure 9.19-3 is so frequently encountered that it is called the *normal distribution*. It describes the likely density of parts, $N(x)$, distributed about a center value x_0. It is also called a *Gaussian distribution* about a nominal value. The expression in (9.19-1) is a continuous quantity; therefore, it can only be applied with good approximation when the quantity of parts is large. The constant σ defines the width of the curve. When $|x - x_0| = \sigma$ the density $N(x)$ is about 60% of its peak value. The constant A is evaluated such that the density of parts integrated over all possible values is equal to N, the total number of parts. That is,

$$N \equiv \int_0^\infty N(x)\,dx = A \int_0^\infty \mathrm{e}^{\left[\frac{-1}{2}\left(\frac{x-x_0}{\sigma}\right)^2\right]} dx \tag{9.19-2}$$

In order to separate this characteristic function from the actual quantity of

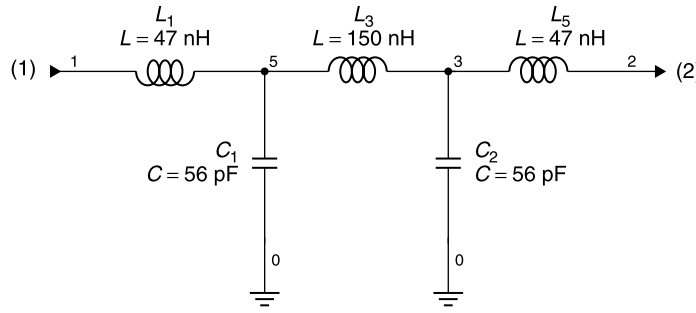

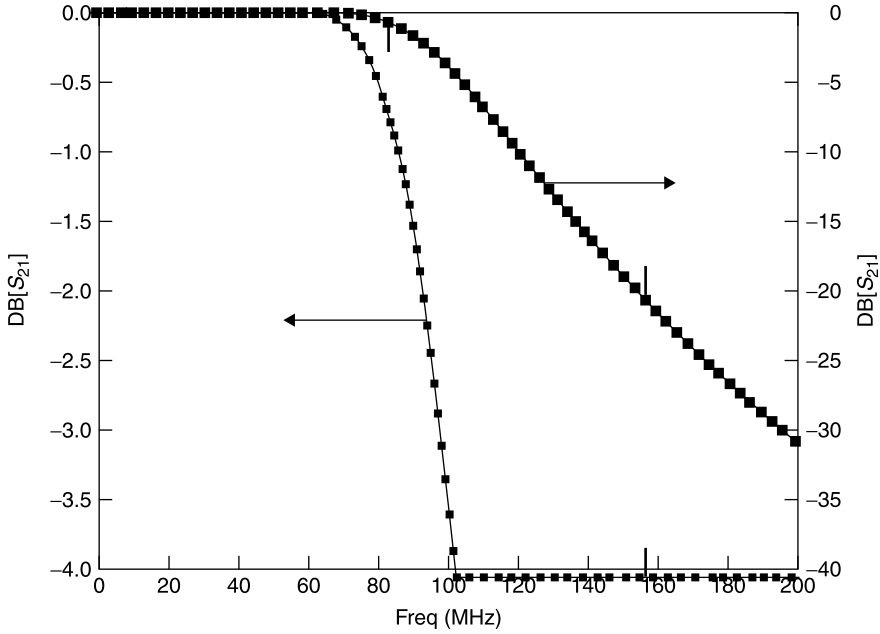

Figure 9.19-2 Low-pass filter realized using standard part values.

parts, the practice is to express $N(x)$ as a product of the total number of parts and the *probability factor*, $\varphi(x)$. With this definition

$$N(x) = N\varphi(x) \tag{9.19-3}$$

where

$$\varphi(x) = C\, e^{\left[\frac{-1}{2}\left(\frac{x-x_0}{\sigma}\right)^2\right]} \tag{9.19-4}$$

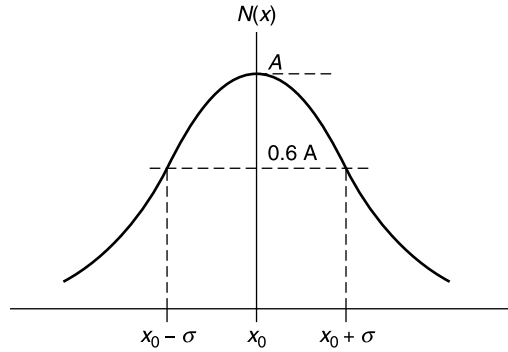

Figure 9.19-3 Normal distribution of parts, also called a Gaussian distribution.

Since $\varphi(x)$ is a probability factor, its value is bounded by

$$0 \leq \varphi(x) \leq 1 \tag{9.19-5}$$

That is, the probability of an event lies somewhere between zero (when the event has no chance of occurring) and unity (when the event is a certainty). Suppose that these statistics are to represent a manufacturing lot of capacitors being made with an intended standard value of 47 pF. Then, theoretically, the range of part values is all positive values for x, and the constant, C, must be defined to satisfy

$$\int_0^\infty \varphi(x)\,dx \equiv 1 = C\int_0^\infty \mathrm{e}^{[\frac{-1}{2}(\frac{x-x_0}{\sigma})^2]}\,dx \tag{9.19-6}$$

Imposition of the condition in (9.19-6) will also satisfy that of (9.19-5). The integration in (9.19-6) required to evaluate C is tricky [7, Chapter 8, Sec. 10]. To perform the integration, express the integral with either of two dummy variables, x and y:

$$I = \int_{-\infty}^{\infty} e^{-x^2/2}\,dx = \int_{-\infty}^{\infty} e^{-y^2/2}\,dy \tag{9.19-7}$$

The integration is carried out from $-\infty$ to $+\infty$ because in general the probability function might have values for both negative and positive values of x. Squaring I and using both the x and y variable forms of (9.19-7) gives

$$I^2 = \int_{-\infty}^{\infty}\int_{-\infty}^{\infty} e^{-(x^2+y^2)/2}\,dx\,dy \tag{9.19-8}$$

The integration in (9.19-8) corresponds to integrating the function $e^{-(x^2+y^2)/2}$ over the entire xy plane. Expressing (9.19-8) in polar coordinates, the same function and area of integration can be rewritten as

$$I^2 = \int_0^{2\pi} \int_0^{\infty} e^{-r^2/2} r\, dr\, d\theta = 2\pi \int_0^{\infty} e^{-r^2/2}\, d\left(\frac{r^2}{2}\right) = 2\pi \tag{9.19-9}$$

Hence,

$$I = \int_{-\infty}^{\infty} e^{-x^2/2}\, dx = \sqrt{2\pi} \tag{9.19-10}$$

and the constant C in (9.19-6) must be equal to $(1/\sigma)\sqrt{1/2\pi}$ so that the normal, or Gaussian, probability function satisfies (9.19-6). The probability function is then defined by (9.19-11) and plotted in Figure 9.19-4:

$$\varphi(x) = \frac{1}{\sigma}\sqrt{\frac{1}{2\pi}}\, e^{\left[\frac{-1}{2}\left(\frac{x-x_0}{\sigma}\right)^2\right]} \tag{9.19-11}$$

and the density of parts $N(x)$ in terms of the total number of parts N is given by

$$N(x) = N\varphi(x) = \frac{N}{\sigma}\sqrt{\frac{1}{2\pi}}\, e^{\left[\frac{-1}{2}\left(\frac{x-x_0}{\sigma}\right)^2\right]} \tag{9.19-12}$$

Given a sufficiently large N for applying statistics (say, a number of capacitors), the number of capacitors N_{SPEC} having a specified value (such as the capacitance value being within $x_1 \le x \le x_2$) is given by

$$N_{\text{SPEC}} = N \int_{x_1}^{x_2} \varphi(x)\, dx = \frac{N}{\sigma}\sqrt{\frac{1}{2\pi}} \int_{x_1}^{x_2} e^{\left[\frac{-1}{2}\left(\frac{x-x_0}{\sigma}\right)^2\right]} dx \tag{9.19-13}$$

The indefinite integral in (9.19-12) does not have a known analytic solution. The number of in-specification parts can be estimated by performing a graphical integration of the curve in Figure 9.19-4, below which the number of squares contained within $-3\sigma \le x \le +3\sigma$ is approximately 240.

For example, suppose that a manufacturer makes 1000 capacitors intended to have a standard value of *47* pF. However, due to an error in the process, the distribution is centered at *52* pF ($x_0 = 52$ pF), with $\sigma = 0.096x_0 = 5$ pF. How many parts will meet a specification of 47 pF $\pm$ 5 pF (*a* $\pm$10.6% *tolerance*)? The distribution is shown in Figure 9.19-5. The shaded area represents the usable parts that meet the capacitance specification, a little less than one half of those produced.

Other Distributions

While the normal distribution is the most common for part manufacture, many factors can influence the distributional outcome. One should not assume that parts obtained with a $\pm$ tolerance can be accurately represented by a normal

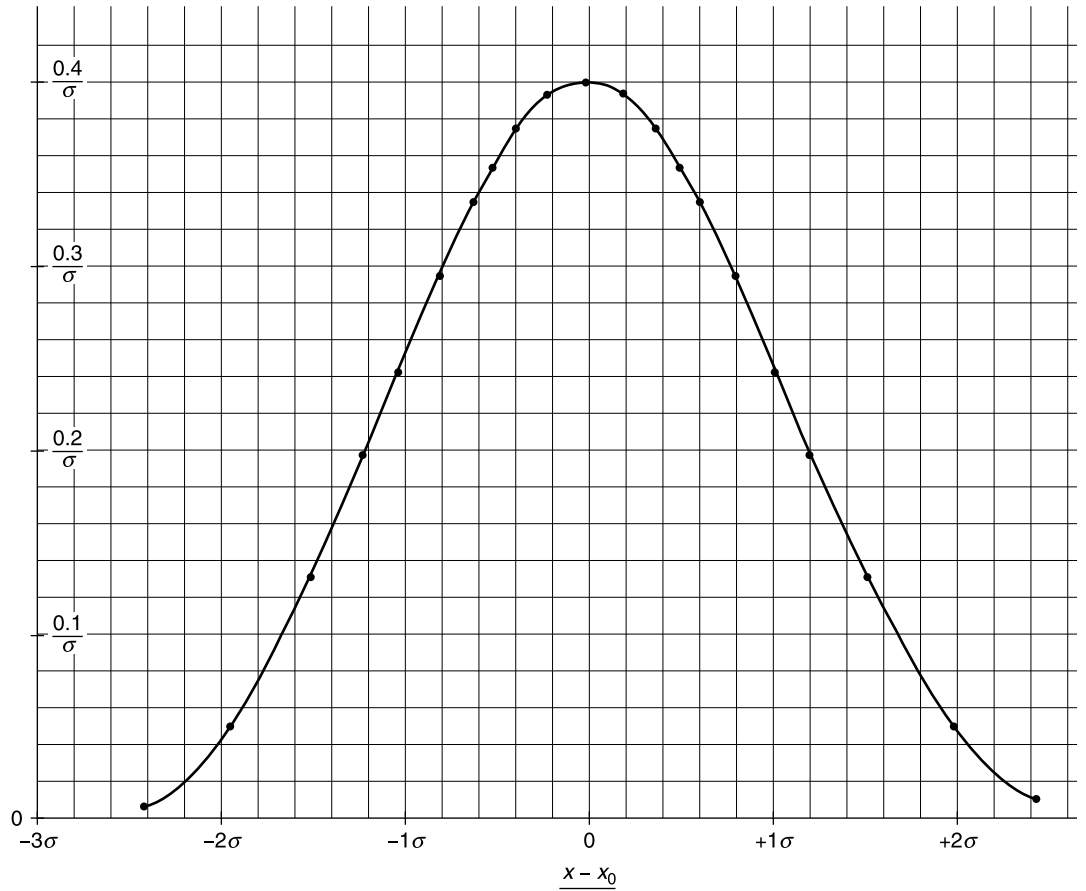

Figure 9.19-4 Normal, or Gaussian, probability function. The area under the curve is approximately 240 squares.

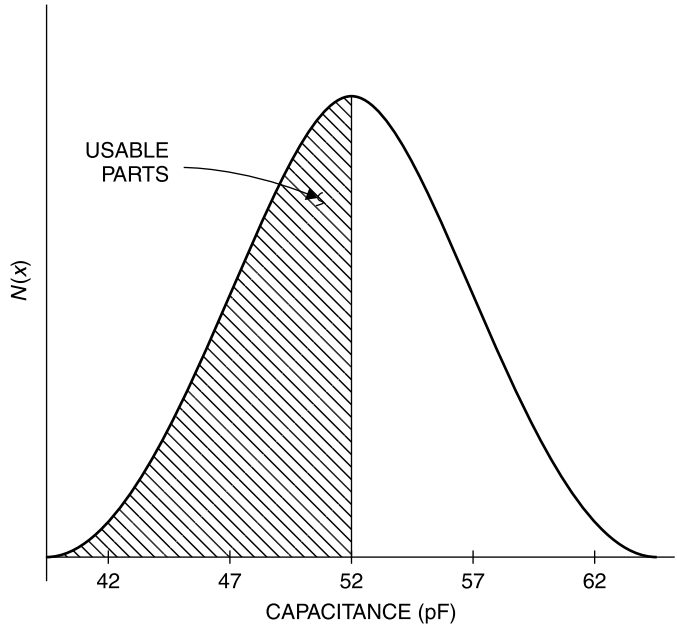

Figure 9.19-5 Normal distribution of capacitors centered at 52 pF with one sigma = 5 pF and the quantity that meet a 47-pF $\pm$ 5 pF specification (shaded area).

distribution centered on their nominal value. As was seen from the previous example, even when the normal distribution does apply, its center value, x_0, may not be the nominal value for that part because the manufacturer's process may not be sufficiently controlled to center the distribution on the part value desired.

Even when the distribution is centered properly on the nominal value, parts delivered to a $\pm$20% tolerance will not necessarily be represented by a normal

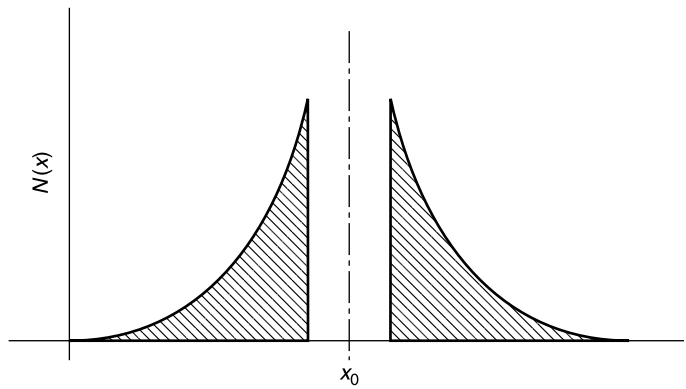

Figure 9.19-6 Gaussian (normal) distribution showing how the center values might be removed to leave a *depleted normal distribution*.

distribution because the supplier may have sold the parts that were within 10% of the nominal value to another customer at a premium price, leaving a *depleted normal distribution* for the parts that will be delivered to a ±20% tolerance (Fig. 9.19-6).

There are numerous other possible distributions for component values. Another common type is the uniform distribution in which all values between the plus and minus component tolerances are equally probable. This might be the approximate distribution if a manufacturer combines parts made from several production runs, each of which has a different x_0. From the uniform distribution, a depleted uniform distribution can result for the same reason as that described for the depleted normal distribution.

To control manufacturing yield, the actual distribution of parts must be controlled, either by first measuring a set of available parts or else procuring parts to a distributional specification (and then verifying on their receipt that they meet that specification). *In manufacture, controlling yield is no less important than designing the circuit.*

Returning to the Butterworth low-pass filter example, the insertion loss does not exceed 1 dB for frequencies up to 86 MHz, and the isolation is greater than 20 dB for frequencies above 156 MHz. Suppose we set a specification for our

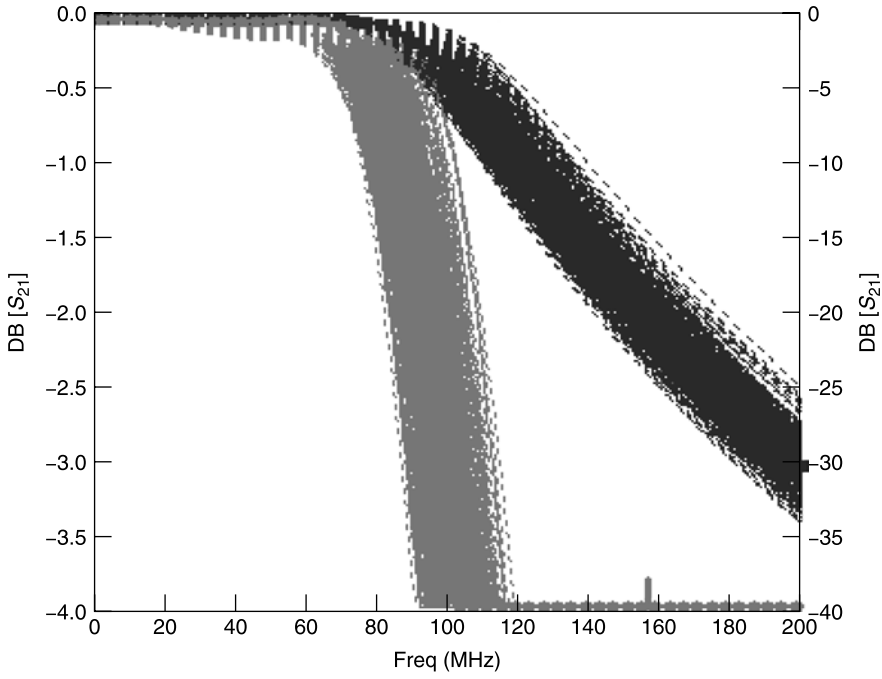

Figure 9.19-7 Calculated performance distribution of 500 filters made using one-sigma values that are 15% of the nominal component value. Only 50 filters passed the 1-dB loss and 20-dB isolation specification for a total yield of 10%.

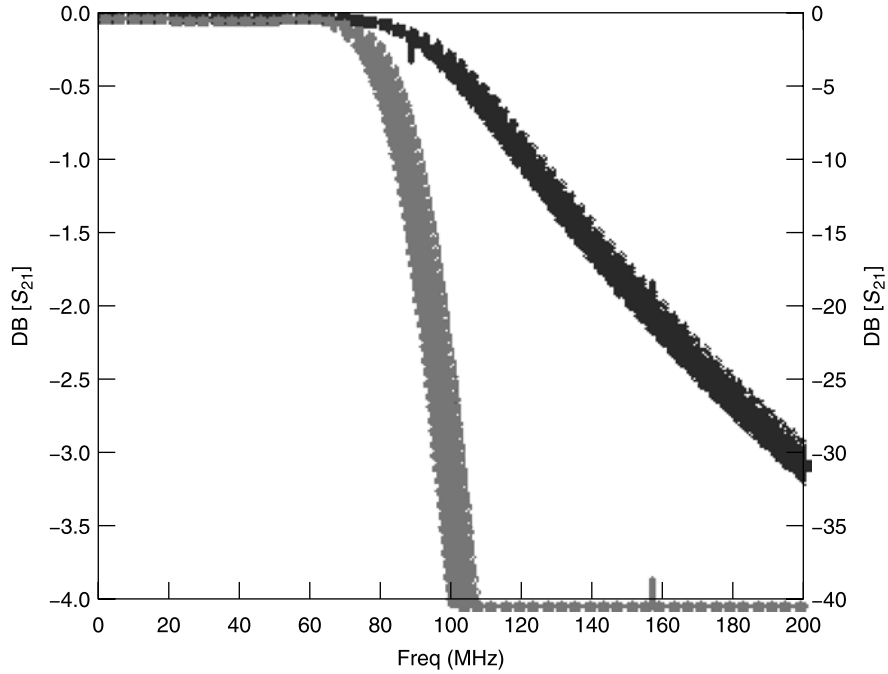

Figure 9.19-8 Distribution of Butterworth filter performance when the components have normal distributions with a one-sigma value that is 5% of the nominal component value. A total of 60 units passed the 1-dB-loss and 20-dB-isolation specification for a yield of 12%.

filter that the loss must be below 1.0 dB up to 86 MHz and the isolation must be greater than 20 dB above 156 MHz.

Further, assume for this example that all components have a normal distribution of values with a one sigma equal to 15% of the nominal value. The resulting performance of 500 filters "built" using these parts is shown in Figure 9.19-7.

Of course, the specifications could be relaxed to allow more filters to pass. Alternatively, components could be procured with a tighter distribution. If the one-sigma value is reduced to 5% of the nominal value, the resulting distribution is that shown in Figure 9.19-8.

While the spread is much tighter than for the 15% one sigma, the yield increased to only 59 units, a 12% yield. If the specification limits are relieved to require less than 1 dB of loss up to 80 MHz and greater than 20 dB of isolation at 170 MHz and above, and if the one-sigma tolerance is made 10%, then 473 units meet the specifications, for a yield of nearly 94.6%. Clearly, both the specifications and the control of parts are crucial to the achievement of high yields.

REFERENCES

1. Randall W. Rhea, *HF Filter Design and Computer Simulation*, Noble Publishing, Atlanta, GA, 1994. *This book is must reading for the filter designer. It contains an excellent introduction to filter theory with numerous examples of both lumped element and distributed filters. It includes practical effects such as coil winding and the element Q's that are practically realizable.*
2. Peter A. Rizzi, *Microwave Engineering, Passive Circuits*, Prentice-Hall, Englewood Cliffs, NJ, 1988. *Excellent microwave engineering textbook covering theory and design of transmission lines, couplers, filters, and numerous other passive devices.*
3. P. I. Richards, "Resistor-Transmission Line Circuits," *Proceedings of the Institute of Radio Engineers (IRE)*, Vol. 36, February, 1948, pp. 217–220.
4. Ralph Levy, "A general equivalent circuit transformation for distributed networks," *IEEE Transactions on Circuit Theory*, CT-12, September 1965, pp. 457–458.
5. W. W. Mumford, "Tables of stub admittances for maximally flat filters using shorted quarter wave stubs," *IEEE Transactions on Microwave Theory and Techniques*, Vol. MTT-13 No. 5, September 1965, pp. 695–696.
6. Matthei, Young, and Jones, *Microwave Filters, Impedance Matching Networks, and Coupling Structures*, McGraw-Hill, New York, 1964 (now also available from Artech House, Norwood, Massachusetts). *Often called the Bible of the filter world.*
7. I. S. Sokolnikoff and R. M. Redheffer, *Mathematics of Physics and Modern Engineering*, McGraw-Hill, New York, 1958.
8. Howard W. Sams & Co., *Reference Data for Radio Engineers*, 5th ed., Howard W. Sams & Co., 1974.

EXERCISES

E9.4-1 **a.** Design a 50-Ω, five-element, lumped-element, Butterworth low-pass filter with a 3-dB cutoff at 1000 MHz to take out the harmonics in a cellular phone transmitter. Use a series L as the first element.

b. How much attenuation would you expect for the second harmonic of an 850-MHz signal?

c. Suppose we need at least 40-dB attenuation of the second harmonic of 850 MHz. What can you do to achieve this and also minimize passband insertion loss?

d. Prove your results using a circuit simulator.

e. If the system bandwidth is 825 to 875 MHz and you wish to eliminate the second harmonic, which could be between 1650 and 1750 MHz, what changes would you make to the filter to minimize its loss in the passband and maximize its isolation to the second-harmonic band?

E9.5-1 **a.** Convert the filter you designed in E9.4-1 into a high-pass filter of the same type and cutoff frequency.

b. Examine your result using a circuit simulator (create a new schematic to analyze this circuit).

c. Are the elements as easy to realize?

E9.8-1 A 50-Ω, 0.0432-dB ripple (20 dB return loss), Chebyshev three-section bandpass filter with 0.0432-dB band edge frequencies of 700 and 1000 MHz is required.

a. What is f_0?

b. What is the fractional bandwidth?

c. What are the low-pass g_i values?

d. What are the actual L and C values of the filter?

e. Plot the loss versus frequency performance using a network simulator.

f. What is the order of the filter?

g. At what rate does the isolation increase in decibels/octave?

h. What is the effect if inductors have a Q of 50 and capacitors have a Q of 100?

i. What would you say is the highest practical frequency at which a filter of this type can be built?

E9.8-2 **a.** Design a Chebyshev 0.0432-dB ripple (20-dB return loss) bandpass filter in the same manner used for E9.8-1 but for a passband of only 800 to 900 MHz.

b. Verify the design using a network simulator.

c. What can you say about the relative practicality of the required components for this filter versus the 700- to 1000-MHz filter designed in E9.8-1? What do you believe causes the added difficulty?

d. Use the circuit simulator to determine the passband insertion loss when the filter is realized using capacitor Q's of 100 and inductor Q's of 50.

E9.14-1 **a.** Repeat the design of the 800- to 900-MHz, 0.0432-dB ripple (20-dB return loss), Chebyshev bandpass filter, but this time realize it as a microstrip end-coupled (half-wavelength resonator) filter with a 0.031-in.-thick substrate of dielectric constant 2.22. *Hint:* Use a filter program if you have one. If not, use a network simulator and begin with three, 50-Ω, half-wavelength resonators end-coupled by capacitors. Use the optimizer to hold loss to 0.0432-dB in the passband. Make the line lengths and capacitor values adjustable in the optimization.

b. Can you get the same loss performance as the lumped-element filter?

c. Can you get the same isolation performance?

d. Compare the practicality of building this filter with the lumped-element filter.

E9.15-1 The Richards transformation is to be used to design a three-stub bandstop filter with $f_R = 1.30$ GHz and a 3-dB bandwidth of 600 MHz (i.e., $f_C = 1$ GHz).

a. Base the design on a three-element tee configuration Butterworth low-pass filter. Determine the characteristic impedances of the series-connected shorted stubs, Z_{SS}, and the shunt-connected open-circuited stub, Z_{OC}. Also calculate the stub lengths l. Assume a 50-Ω system impedance ($Z_0 = 50\ \Omega$) and air dielectric. Make sketches of the equivalent circuit of the lumped-element and stub filters showing element values.

b. Plot the loss/isolation versus frequency response from 1 to 2 GHz. Verify that the 3-dB bandwidth is 600 MHz. What is the 20-dB bandwidth?

E9.16-1 Use the appropriate Kuroda identity to convert the distributed tee filter design of E9.15-1 to a three shunt-connected open-circuit stub filter with the same performance.

a. Calculate the characteristic impedance of the end stubs Z_{ES} and the interconnection lines Z_{01}.

b. Plot the loss versus frequency response of the shunt stub filter and compare it to that of the tee configuration filter of E9.15-1.

E9.16-2 Prove the equivalence of Kuroda's identity in Figure 9.16-1*a*. *Hint:* If two circuits have identical behavior, they must have the same $ABCD$ matrix.

E9.19-1 **a.** Make a scaled sketch of the distribution curve for a manufacturing run of 1000 resistors having a center of distribution value, $x_0 = 68\ \Omega$, and a standard deviation, $\sigma = 5\ \Omega$.

b. Use your drawing to estimate the number of resistors that will meet a $\pm 5\%$ tolerance (say, $\pm 3.5\ \Omega$) about 68 Ω.

CHAPTER 10

Transistor Amplifier Design

10.1 UNILATERAL DESIGN

Evaluating *S* Parameters

The design of a transistor amplifier is the creation of a circuit environment in which a selected transistor performs as closely as possible to a set of design objectives. The circuit designer may have no influence over the transistor's parameters. These are established by its geometry, quality of manufacture, and semiconductor physics. Usually the circuit designer selects a transistor from a catalog, guided by and limited to the properties described by its S parameters.

To the circuit designer the transistor is a two-port network described by a table of S parameters taken over the entire frequency domain over which it has gain. After the bias and heat sinking needs of the transistor have been satisfied, the RF design proceeds using the S parameters. At this point it is of no consequence whether the device is a bipolar or field-effect transistor (FET) or any other device whose S parameters suggest the prospect of gain.

As was shown in Chapter 6, when the source and load impedances are the same as those used to determine the S parameters, the magnitude of S_{21} is the ratio of the outgoing wave b_2 to the incoming wave a_1. Hence it is equivalent to the *voltage or current gain* of the amplifier. Similarly, the magnitude of the square of S_{21} is equal to the power gain.

As an example, suppose it is desired to design an amplifier to operate at 1 GHz with 50-Ω source and load impedances, and that it is desirable to obtain as much gain as practical at 1 GHz. On reviewing tables of S parameters provided in a catalog or in an electronic file within a circuit simulator, suppose that the Motorola 2N6679A bipolar transistor is selected for the amplifier design. Its S parameters are shown in the standard format in Table 10.1-1.

We see that the magnitude of S_{21} is *6.6 at 1 GHz*. Then the basic gain, without tuning, in a *50*-Ω system is

$$G = 20 \log|S_{21}| = 20 \log 6.6 = 16.4 \text{ dB} \qquad (10.1\text{-}1)$$

High Frequency Techniques: An Introduction to RF and Microwave Engineering, By Joseph F. White.
ISBN 0-471-45591-1

TABLE 10.1-1 The *S* Parameter File for the Motorola 2N667A Bipolar Transistor[a]

```
! 2N6679A.S2P
! 2N6679
! VCE = 15 V; IC = 25 mA
# GHZ S MA R 50
! S-PARAMETER DATA
```

0.1	0.60	−76	38.6	141	0.01	55	0.83	−20
0.5	0.67	−158	12.7	95	0.02	40	0.50	−27
1	0.68	−178	6.6	77	0.03	53	0.46	−32
1.5	0.68	170	4.4	64	0.04	54	0.47	−41
2	0.69	162	3.4	54	0.05	54	0.47	−50
2.5	0.69	154	2.7	42	0.06	55	0.49	−59
3	0.69	146	1.3	31	0.07	55	0.53	−70
3.5	0.69	138	1.9	21	0.08	54	0.55	−79
4	0.69	131	1.7	11	0.09	51	0.57	−89
4.5	0.69	123	1.5	1	0.10	49	0.59	−97
5	0.69	114	1.4	−9	0.12	44	0.62	−106
5.5	0.69	106	1.2	−19	0.14	39	0.64	−113
6	0.69	98	1.1	−28	0.15	33	0.68	−122
6.5	0.69	90	1.0	−37	0.17	31	0.69	−130

Source: From the *Genesys S* parameter directory.

[a] By convention the columns contain left to right: freq (in GHz), $S_{11}, S_{21}, S_{12}, S_{22}$, where each S parameter is contained in two columns, the first is the magnitude (numeric, not decibel) and the second is the phase angle in degrees.

Transistor Biasing

At this point suppose that we consider this to be desirable performance. It is necessary to design a bias circuit [1, pp. 273–283]. For the bias a 20-V source is selected, since the S parameter file indicates the performance was obtained with a 15-V bias between collector and emitter. From the transistor data, we see that the performance was obtained with $V_{CE} = 15$ V and $I_C = 25$ mA. The DC current gain $\beta = I_C/I_B$ is not listed in the S parameter file, but on contacting the manufacturer, suppose that at room temperature $\beta = 40$. Then a suitable biasing network is as shown in Figure 10.1-1.

The resistor values are calculated as follows. A base current of 0.63 mA is required (25 mA/40). But we want a shunt path to carry about 5 times this value, say 3 mA, so that when the 15-V level falls, the base current will fall nearly proportionately. Since the transistor is a silicon NPN, the base emitter junction is a silicon diode. Hence it will have a voltage drop at turn-on of about 0.75 V. The emitter-base shunting resistor is calculated as:

$$R_3 = \frac{0.75 \text{ V}}{3 \text{ mA}} = 250 \ \Omega \tag{10.1-2}$$

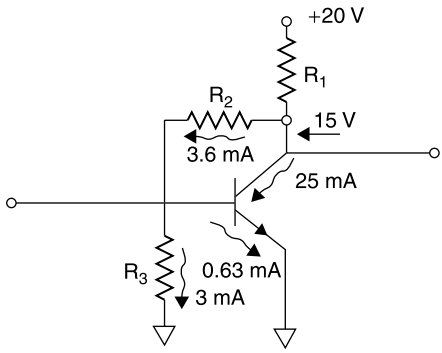

Figure 10.1-1 Bias circuit for the 2N6679A transistor.

Next,

$$R_2 = \frac{15\text{ V} - 0.75\text{ V}}{3.63\text{ mA}} = 3925\ \Omega \tag{10.1-3}$$

Finally,

$$R_1 = \frac{20\text{ V} - 15\text{ V}}{28.6\text{ mA}} = 175\ \Omega \tag{10.1-4}$$

In practice, the closest values of standard resistors may be used. This bias circuit tends to self-compensate. As temperature increases, the base current increases for a given V_{BE}. However, this causes an increase in I_C, causing a larger voltage drop in R_1, reducing V_{BE}.

By themselves, the resistors R_2 and R_3 are large compared to the 50-Ω RF impedance level at the input. However, their parasitics may cause them to place an excessive load on the RF circuit. Furthermore, it is undesirable to have RF signals present in the bias circuit since this may cause undesired RF radiation. Therefore, circuitry to isolate the bias from the RF signals is employed, as, for example, that shown in Figure 10.1-2.

Basically the bias isolation circuitry presents a high RF impedance from the transistor terminals to those of the bias circuitry. This can be accomplished using discrete components (Fig. 10.1-2*a*). For the present 1 GHz, 50-Ω amplifier example isolating elements of $L = 100$ nH and $C = 100$ pF might be employed. When space permits, the isolating elements can be "printed" as distributed elements along with the RF circuit. The transmission lines shown are made a quarter wavelength long at the RF center frequency of the amplifier. For the *50* Ω amplifier example, the high impedance lines made $Z_H = 150\ \Omega$, and the low impedance lines made $Z_L = 25\ \Omega$.

The bias isolating networks are crucially important in amplifier design and should not be given short shrift in the design effort. As we shall later discuss, transistors may have gain well above the design bandwidth. In the present

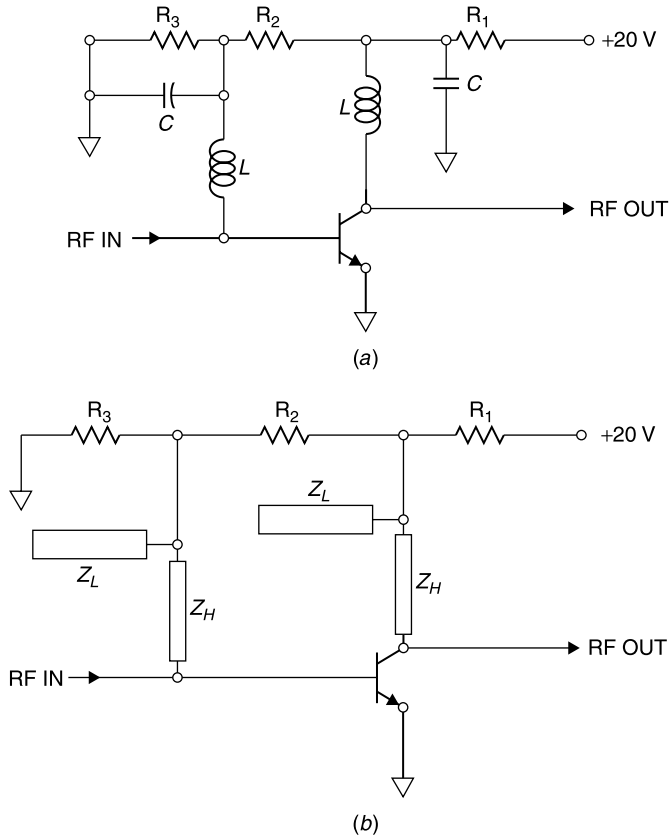

Figure 10.1-2 Transistor with bias isolation components: (*a*) discrete bias isolation and (*b*) distributed bias isolation.

1-GHz amplifier example, it can be seen from Table 10.1-1 that the transistor has gain above 5 GHz. Therefore, it could break into oscillation given certain out-of-band impedance loading.

The *single-stage* bias circuits shown in Figure 10.1-2 have only single high impedance and low impedance elements for isolation. They are shown for illustration of the bias isolating methods and are not presented as adequate designs for all applications. Where practical, *multistage* bias isolation is preferable as shown in Figure 10.1-3.

An informal measure of the effectiveness of the distributed bias structure is to bring a screwdriver tip near the open-circuit ends of the *bias flags* (the open-circuited ends of the low-impedance line sections) while measuring the output power of the amplifier. A significant power change experienced when so probing the end of the second bias flag, Z_{L2}, indicates the bias circuit may be resonant at the wrong frequency or that more isolating stages are required.

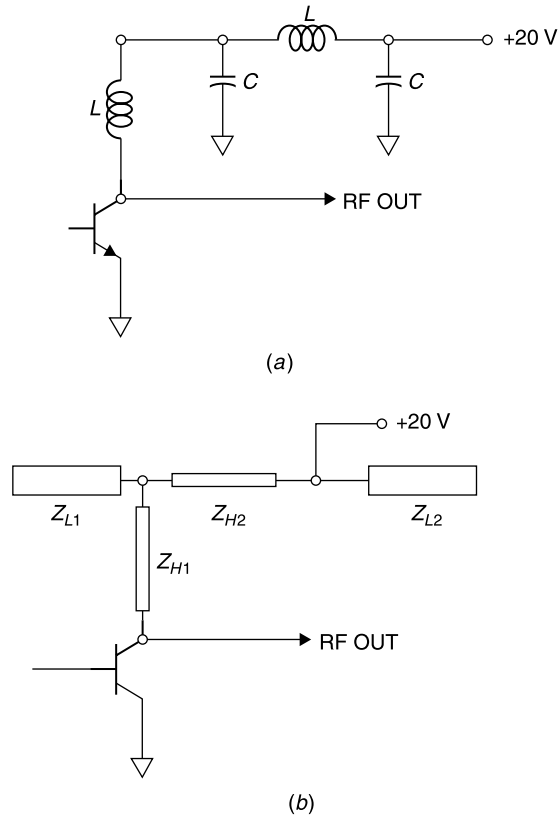

Figure 10.1-3 Two-stage bias isolating circuits: (*a*) discrete and (*b*) distributed.

Evaluating RF Performance

Most circuit simulators can accept the S parameter table to provide an analysis over frequency, interpolating the data to calculate the circuit behavior between frequencies for which S parameter data are available. The circuit evaluation could be performed with bias elements, but we will assume in this text that sufficient bias isolation is achieved, and only the RF circuit will be shown for purposes of illustration. However, when the amplifier design is critical, as for an integrated circuit, it is wise to include the bias circuit and any peripheral circuit elements on the broadband simulation of the amplifier. The gain of the present example, using the 2N6679A transistor, is shown in Figure 10.1-4. As will be common in this text, the impedance of the input and output ports is 50 Ω unless otherwise noted.

At this point, *if this performance is satisfactory*, the electrical portion of the amplifier design is complete. On the other hand, on examining the input and output reflection coefficients, S_{11} and S_{22}, respectively, in Table 10.1-1, it can

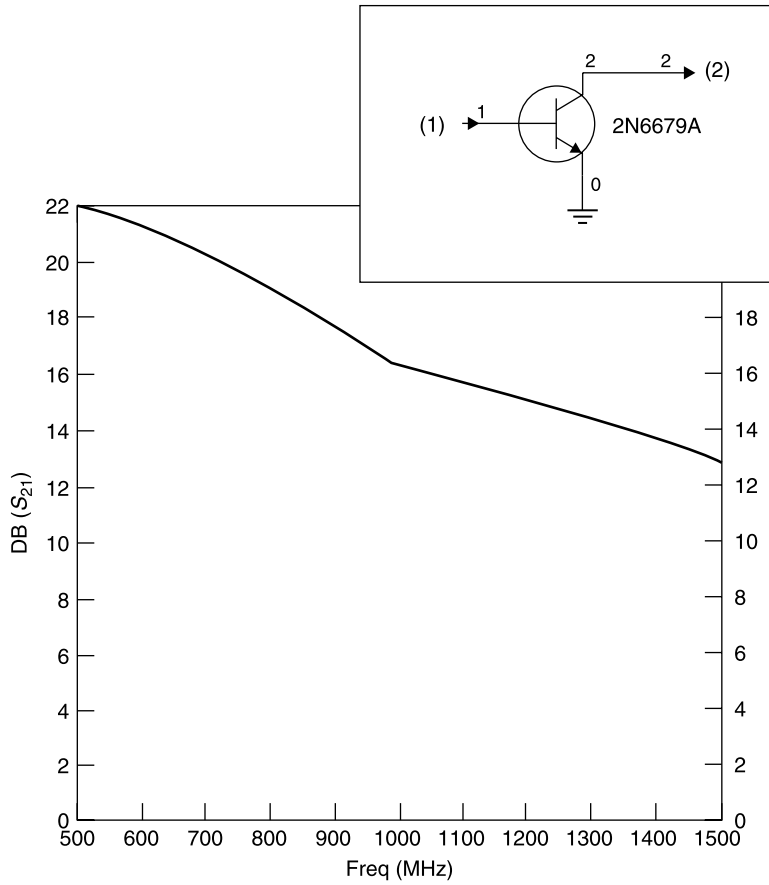

Figure 10.1-4 Amplifier consisting of a biased Motorola 2N6679A silicon bipolar transistor with 50-Ω source and load terminations.

be seen that a good amount of power is lost to reflection at the input and mismatch at the output. At 1 GHz

$$|S_{11}| = 0.68$$

$$\text{Input mismatch loss} = 1 - |S_{11}|^2 = 1 - 0.68^2 = 0.54 \qquad (10.1\text{-}5)$$

$$= 10 \log(1 - |S_{11}|^2) = -2.7 \text{ dB}$$

$$|S_{22}| = 0.46$$

$$\text{Output mismatch loss} = 1 - |S_{22}|^2 = 1 - 0.46^2 = 0.79 \qquad (10.1\text{-}6)$$

$$= 10 \log(1 - |S_{22}|^2) = -1.0 \text{ dB}$$

These mismatch losses correspond to 46% power loss at the input and 21% at the output. Therefore, by matching input and output, we could have up to 3.7 dB of additional gain and have a matched circuit at input and output as well.

10.2 AMPLIFIER STABILITY

Thus far, even if we are satisfied with the performance obtained by installing a transistor in the same impedances in which it was measured, there is a point that we have not considered. We have treated the transistor as if it were a *unilateral device*. Put in other words, we have assumed that signals pass from the input to the output, but not in the reverse direction.

Making the *unilateral assumption is equivalent to assuming that* S_{12} *is zero*. The S_{12} parameter provides the feedback term by which power from the output circuit (which is relatively high due to the transistor's amplification) can feed back to the input. When it does so, it may combine with reflections already present at the input to produce an effective S_{11} whose magnitude exceeds unity.

This corresponds to *reflection gain*, and a transistor amplifier that can experience this gain, is termed *conditionally unstable*, the condition being certain combination(s) of load impedance, S_{12} and S_{11}, that could produce self-oscillation (instability).

In the current 2N6679A example, the magnitudes of S_{11} and S_{22} of the transistor are less than one for all frequencies. This means that the transistor is *stable when embedded between 50-Ω source and load* (Fig. 10.2-1). That is, it will not oscillate in the 50-Ω input/output environment. However, this would not be generally considered sufficient within the industry. Rather, the expectation is that *a properly designed (stabilized) amplifier will not oscillate no matter*

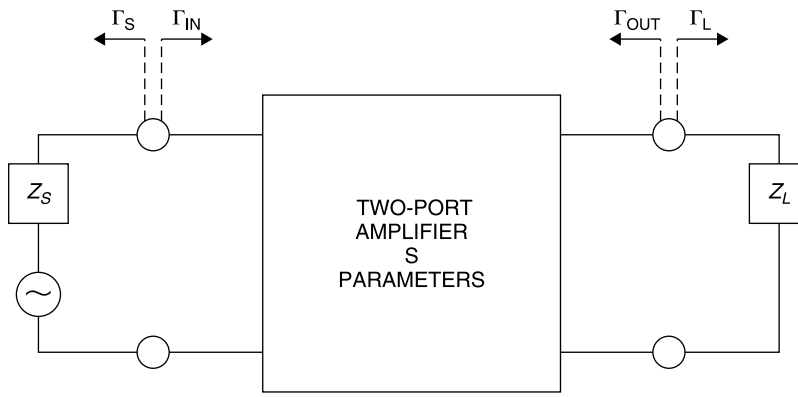

Figure 10.2-1 An *S* parameter represented network embedded between source and load of general complex reflection coefficients.

what passive source and load impedances are presented to it, including short or open circuits of any phase.

Because the S_{12} of practical transistors is not zero, a signal path exists from the output (where power levels are higher due to the device's gain) to the input. It is possible that for certain values of load Γ_L, Γ_{IN} can exceed unity, turning the circuit into a reflection amplifier at the input. Similarly, certain values of Γ_S at the input might cause Γ_{OUT} to exceed unity magnitude. When either or both of these conditions can occur, at any frequency, the circuit is said to be only *conditionally stable* or equivalently, *potentially unstable*.

The boundary line between stable and unstable operation at the input is the $|\Gamma_{IN}| = 1$ circle centered at the origin of the Smith chart. The contour of values for Γ_L (also a circle) that produces a unity magnitude reflection coefficient at the input is called the *input stability circle*. This is shown in Figure 10.2-2 for the 2N6679A transistor. Keep in mind that *the input stability circle represents a set of load reflection coefficients* that cause the input reflection coefficient to have a unity magnitude. Also note that the *input stability circle* represents a *boundary*, on one side of which $|\Gamma_{IN}| < 1$ resulting in load impedances that

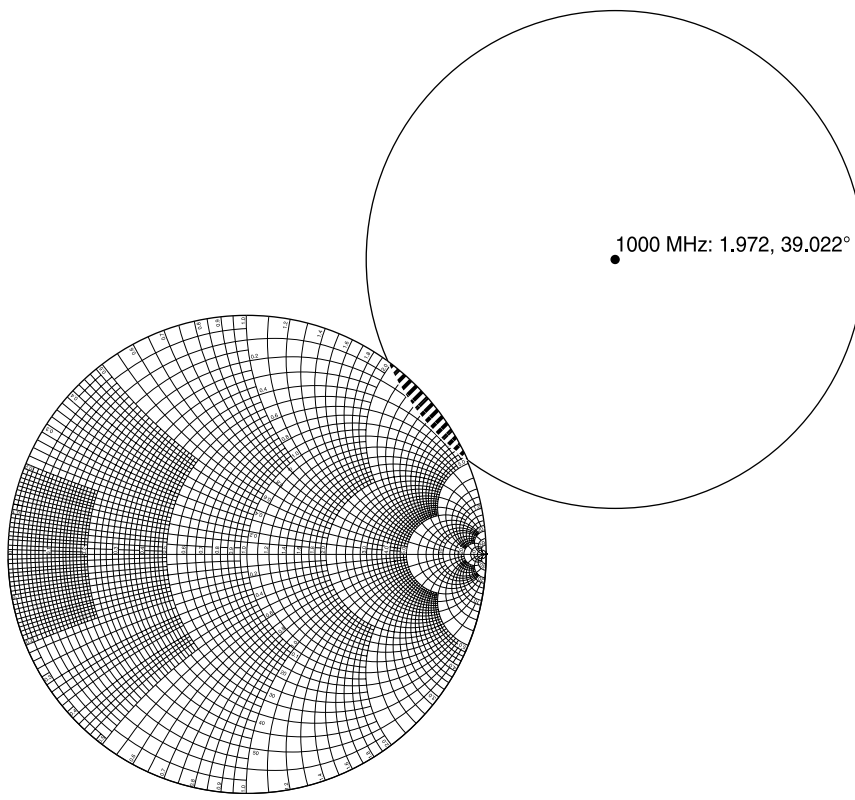

Figure 10.2-2 Load instability circle for the Motorola 2N6679A transistor at 1 GHz.

result in stable operation and on the other side of which $|\Gamma_{IN}| > 1$, corresponding to load impedances that produce potential instability.

The Γ_L values are related to the Γ_{IN} values according to (10.2-1), called a mapping function because it maps a Γ_{IN} contour into a Γ_L contour [2, pp. 140–145]. This function maps the $|\Gamma_{IN}| = 1$ into a Γ_L contour, in this case a circle, to a circle:

$$\Gamma_L = \frac{\Gamma_{IN} - S_{11}}{S_{22}\Gamma_{IN} - \Delta} \quad \text{where } \Delta = S_{11}S_{22} - S_{12}S_{21} \tag{10.2-1}$$

Inserting the condition $|\Gamma_{IN}| = 1$ into the above equation creates a mapping of the $|\Gamma_{IN}| = 1$ circle into the input stability circle in the Γ_L plane with center at

$$C_L = \frac{S_{22}^* - \Delta^* S_{11}}{|S_{22}|^2 - |\Delta|^2} \tag{10.2-2}$$

and a radius of

$$R_L = \left| \frac{S_{12}S_{21}}{|S_{22}|^2 - |\Delta|^2} \right| \tag{10.2-3}$$

The input stability circle for the 2N6679A untuned amplifier at 1 GHz, is shown in Figure 10.2-2.

The *input stability circle* is also called the *load instability circle* because it describes the Γ_L values that border on causing instability, that is, which result in $|\Gamma_{IN}| = 1$. *Henceforth, we will refer to the input stability circle as the load instability circle* because this places the focus on the load impedances that cause instability.

The circle intersects and intrudes into the unity radius area of the Smith chart. This means that the transistor is *potentially unstable* for certain passive load impedances bounded by the circle. Note, again, that the circle is the *boundary* of the unstable impedances. Since it is only the boundary, when we first plot the circle we do not know whether the unstable load impedances are those inside the circle or outside of the circle. Of course, in the example in Figure 10.2-2 it would seem highly likely that the unstable points are inside the circle since most of the circle is in the negative resistance domain of the Smith chart. However, there are instances in which the entire circle may lie within the unity radius, passive impedance portion of the Smith chart. Therefore, some means for determining which side of the boundary represents the unstable impedances is needed. The determination is facilitated by the availability of the S parameters, which apply with a known load, usually 50 Ω. *To determine whether the unstable load impedances are inside or outside the circle, consider the "easy point" S_{11}.*

We know from the S parameter file for the 2N5579A transistor that when the transistor is loaded with 50 Ω, the center of the Smith chart, $|S_{11}| < 1$.

Therefore, the center of the Smith chart is a stable load point. Since the center of the Smith chart is outside the load instability circle, it follows that in this case all points outside the circle are stable, and that the points inside the circle in Figure 10.2-2 are the unstable loads.

From Figure 10.2-2 it can be seen that high inductive load impedances at the output can cause instability (at the input). Also, notice that points outside the $\Gamma = 1$ circle correspond to loads with negative resistance. These do not concern us because any amplifier can be made unstable by subjecting it to an appropriate source or load impedance with a negative real part. *Amplifier stability only requires that the circuit be stable with passive input and output reflection coefficients, that is, passive source and load impedances.*

Next consider the source reflection coefficients that cause $|\Gamma_{OUT}| = 1$. The relation of Γ_S to Γ_{OUT} is given by [2, p. 142]

$$\Gamma_S = \frac{S_{22} - \Delta\Gamma_{OUT}}{1 - S_{11}\Gamma_{OUT}} \tag{10.2-4}$$

In a similar fashion, this can be used to map the $|\Gamma_{OUT}| = 1$ circle onto the Γ_S plane. This maps as a circle with center at

$$C_S = \frac{S_{11}^* - \Delta^* S_{22}}{|S_{11}|^2 - |\Delta|^2} \tag{10.2-5}$$

and radius

$$R_S = \left| \frac{S_{12}S_{21}}{|S_{11}|^2 - |\Delta|^2} \right| \tag{10.2-6}$$

Plotting this for our transistor at 1 GHz gives the left circle outside the Smith chart in Figure 10.2-3.

The *output stability circle* is also called the *source instability circle* because it represents Γ_S values that cause instability in the input circuit. *Henceforth we will call it the source instability circle*. Once again, we know that the points within the output stability circle are the unstable ones because, from the S parameters of the transistor, $|S_{22}| < 1$ with a 50-Ω termination on the input. Notice that the output circuit may become unstable ($|\Gamma_{OUT}| > 1$) when the input sees low source impedances.

What do these circles mean? If we attempt to get more gain from the transistor by adding matching circuits to the input and output, they must not present those impedances which would cause instability. In fact, even if we accept the transistor as it is and specify that only 50-Ω loads should be applied, if the source or load is removed and there is a transmission line whose length transforms an open circuit to one of the unstable impedances, the circuit may oscillate. In other words, the circuit will be *potentially unstable*.

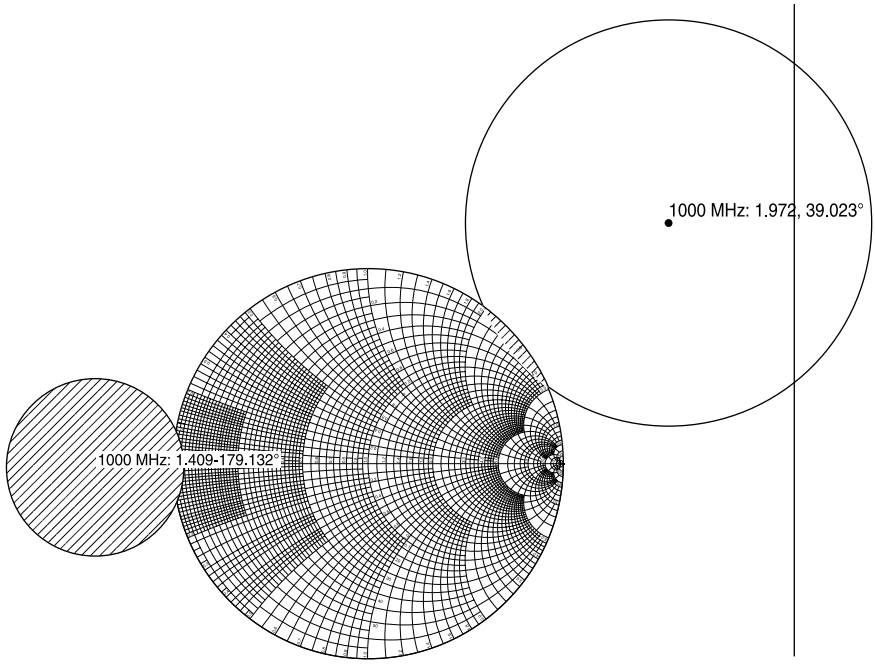

Figure 10.2-3 Source instability circle (at left) and load instability circle (at right) for the 2N6679A transistor at 1 GHz.

Thus far, in our examples of stability circles, we have only examined the transistor's behavior at 1 GHz. But, for an amplifier to be unconditionally stable, it must be so at all frequencies. To assure this requires that it be found to be unconditionally stable at all frequencies for which the transistor has more than unity gain. The resulting *source and load instability circles are two separate families of circles* (Fig. 10.2-4).

10.3 *K* FACTOR

Since the stability circles can be calculated directly from the S parameters, it would seem possible that stability could be determined from the S parameters themselves, without need for the elaborate graphical construction of the stability circles, and this is so. We define the *stability factor* K as [2, p. 145]

$$K = \frac{1 - |S_{11}|^2 - |S_{22}|^2 + |\Delta|^2}{2|S_{12}S_{21}|} \tag{10.3-1}$$

where